

Aus der Klinik für Strahlentherapie und Radioonkologie
der Medizinischen Fakultät Mannheim
(Direktor: Prof. Dr. med. Frederik Wenz)

Regulation of glioblastoma cell proliferation in dependence of cell density
and growth factors *in vitro*

Inauguraldissertation
zur Erlangung des Doctor scientiarum humanarum (Dr. sc. hum.)
der
Medizinischen Fakultät Mannheim
der Ruprecht-Karls-Universität
zu
Heidelberg

vorgelegt von
Yun Liu

aus
Henan, China
2018

Dekan: Prof. Dr. med. Sergij Goerd
Referent: Prof. Dr. med. Frederik Wenz

CONTENTS

	Pages
LIST OF ABRREVIATIONS.....	1
1 INTRODUCTION	3
1.1 Glioblastoma	3
1.2 GBM cell biology.....	4
1.2.1 Loss of cell cycle control.....	4
1.2.2 Resistance to apoptosis.....	6
1.2.3 Invasion and migration.....	6
1.3 Growth factors and kinases in GBM	7
1.3.1 Growth factor	7
1.3.2 Receptor tyrosine kinase	8
1.4 Major oncogenic pathways in GBM	10
1.4.1 PI3K/AKT signaling pathway	11
1.4.2 MAPK signaling pathway	12
1.5 Influence of cell density on GBM proliferation <i>in vitro</i>	15
1.5.1 Focal adhesion kinase	15
1.5.2 Contact inhibition	16
1.6 Aim of the study.....	18
2 MATERIALS AND METHODS	19
2.1 Materials.....	19
2.1.1 Chemicals and reagents	19
2.1.2 Growth factors	21
2.1.3 Inhibitors	21
2.1.4 Buffer preparation	21
2.1.5 Antibodies.....	23
2.1.6 Cell culture materials	24
2.1.7 Apparatus and software.....	24
2.2 Methods.....	25

2.2.1	Cell culture.....	25
2.2.2	Proliferation assay	26
2.2.3	Detachment assay	28
2.2.4	Western blotting.....	29
2.2.5	Caspase 3 activity.....	30
2.2.6	Colony forming assay	31
2.2.7	Flow cytometry.....	31
2.2.8	Immunofluorescence	32
2.2.9	Statistics	33
3	RESULTS.....	34
3.1	Effect of culture conditions on cell proliferation	34
3.1.1	GBM cells undergo apoptosis under certain conditions	34
3.1.2	EH cells have G2 arrest and downregulation of cell cycle proteins....	38
3.1.3	Effect of FAK on EH cell apoptosis	41
3.1.4	Effect of upregulation of p27 on EH cell apoptosis	43
3.2	The balance between ERK1/2 and JNK activation in parent cultures.....	45
3.2.1	ERK1/2 activation in parent cultures.....	45
3.2.2	The regulation of ERK1/2 and JNK activation.....	47
3.3	Radiation response of U251 cells from different parent cultures	52
3.3.1	Clonogenic survival of U251 cells from different parent cultures	52
3.3.2	Induction and decay of DSBs after irradiation.....	54
3.4	Effect of different growth factors on proliferation of GBM cells <i>in vitro</i>	56
3.5	Contact inhibition retained in glioblastoma cells <i>in vitro</i>	60
4	DISCUSSION	67
4.1	Role of FAK in regulating apoptosis	67
4.2	Role of ERK1/2 and JNK activation in GBM	68
4.2.1	Regulation of ERK1/2 and JNK	68
4.2.2	Effect of ERK1/2 on radiation response.....	71
4.3	Role of cyclin-dependent kinase inhibitor p27	73
4.4	Role of exogenous growth factors	75

5 SUMMARY	77
6 REFERENCE	79
7 LIST OF FIGURES AND TABLES	91
7.1 List of figures	91
7.2 List of tables	93
8 CURRICULUM VITAE	94
9 ACKNOWLEDGEMENT	95

LIST OF ABRREVIATIONS

°C	grad Celsius
μ	Micro (10^{-6})
APS	Ammonium persulfate
BSA	Bovine serum albumin
CDK	Cyclin-dependent kinase
CDKI	Cyclin-dependent kinase inhibitor
DAPI	4',6-diamidino-2-phenylindole
DMEM	Dulbecco's modified eagle medium
DMSO	Dimethyl sulfoxide
ECM	Extracellular matrix
EDTA	Ethylenediaminetetraacetic acid
EGF	Epidermal growth factor
EGFR	Epidermal growth factor receptor
ERK1/2	Extracellular signal-regulated kinase1/2
FAK	Focal adhesion kinase
FBS	Fetal bovine serum
FGF-2	Fibroblast growth factor-2
GAPDH	Glyceraldehyde 3-phosphate dehydrogenase
GBM	Glioblastoma multiforme
GSC	Glioma stem cell
HCl	Hydrogen chloride
HRP	Horseradish peroxidase
IGF-1	Insulin-like growth factor-1
IGF-1R	Insulin-like growth factor-1 receptor
JNK	c-Jun N-terminal kinase
kg	kilo gram
m	Milli (10^{-3})
min	Minute
M	molar (mol/l)
MAPK	Mitogen-activated protein kinase
MGMT	O(6)-methyl-guanine DNA methyl transferase

LIST OF ABRREVIATIONS

mTOR	Mammalian target of rapamycin
NF-1	Neurofibromatosis type I
NSC	Neural stem cell
PAGE	Polyacrylamide-Gel-electrophoresis
PBS	Phosphate buffered saline
PFA	Paraformaldehyde
PDL	Poly-D-lysine hydrobromide
PI	Propidium Iodide
PI3K	Phosphatidylinositol-3-kinase
PIP3	Phosphatidylinositol 3, 4, 5-triphosphate
PLO	Poly-L-ornithin hydrobromide
PTEN	Phosphatase and tensin homolog deleted on chromosome 10
rpm	Revolutions per minute
RTK	Receptor tyrosine kinase
SD	Standard deviation
SDS	Sodium dodecyl sulfate
SE	Standard error
TBS	Tris buffered saline
TBS-T	Tris buffered saline with Tween20
TEMED	N,N,N',N'-Tetramethylethylenediamine
TGF- β	Transforming growth factor β
Tris	Tris(hydroxymethyl)-aminoethane
TMZ	Temozolomide

1 INTRODUCTION

1.1 Glioblastoma

According to the World Health Organization (WHO) grading scale, gliomas are categorized based on histological characteristics as low-grade astrocytoma (WHO grade I and II), anaplastic astrocytoma (WHO grade III) and glioblastoma multiforme (WHO grade IV) [1]. Glioblastoma multiforme (GBM) is the most common primary malignant tumor of the central nerve system, with an average incidence of 3-4 in 100,000 people newly diagnosed per year in the United States [2]. GBM can occur at any age, but is more frequently diagnosed in elder population with the median age of 64 years [3].

The current standard treatment for newly diagnosed GBM comprises of maximal safe surgery, followed by radiotherapy with temozolomide (TMZ) [4]. Despite the improvements in treatment modalities, the clinical outcome in GBM still remains disappointing, and the median survival time hardly reaches 15 months [5]. Several variables have been regarded as prognostic factors, including age, tumor size and location, and extent of surgery [6, 7]. Surgical resection plays a critical part in the management of GBM. The importance of aggressive tumor removal has been emphasized due to the association between greater extents of surgical resection and better outcome for patients with GBM [8]. However, GBM cells show aggressive behavior with high invasion and diffuse infiltration into surrounding brain parenchyma, making it impossible to completely remove tumor cells [9]. The goal of radiotherapy coupled with chemotherapeutic agents is to eliminate residual tumor cells. The standard of care is the concomitant use of TMZ and radiotherapy up to 60Gy over 30 days followed by 6 cycles of adjuvant TMZ treatment [5]. TMZ is an alkylating agent that induces DNA damage and thus causes cell death [10]. However, the effect of such alkylating agents can be impaired by O6-methylguanine DNA methyltransferase (MGMT) which is a DNA repair enzyme. MGMT expression is suppressed by methylation of the promoter region of the *MGMT* gene [11]. Therefore, methylation of the *MGMT* promoter has been shown as a strong predictive factor of patients undergoing chemotherapy with TMZ [12, 13].

Radiotherapy is a powerful tool in cancer treatment and has yielded significant survival benefit for patients with GBM [14]. The standard protocol of postoperative radiotherapy is to deliver a total dose of 60Gy in 2Gy per fraction using external-beam radiation. However, the effectiveness of radiotherapy is limited by resistance to tumor cell death after exposure to ionizing irradiation, which is referred as radio-resistance. GBM is one of the most radio-resistant malignancies because 90% of GBM patients experience local recurrence despite aggressive treatment [15]. It has been recognized that radio-resistance is mediated by both intrinsic and extrinsic factors. These factors include DNA damage repair, accelerated tumor repopulation after fractionated RT, tumor heterogeneity, as well as radiation-induced microenvironment changes which provide suitable conditions for tumor survival [16, 17]. Notably, Glioma stem cells (GSC) contribute to GBM radio- and chemo-resistance due to their unique characteristics of quiescent cell cycle, enhanced expression of drug-resistant protein, DNA repair capacity as well as resistance to apoptosis [18, 19]. To a better integrative overview, it is important to gain insights into the biology and molecular pathogenesis of GBM.

1.2 GBM cell biology

GBM arises from a number of genetic alterations, oncogene activation, and tumor suppressor gene inactivation [20]. The initiation and progression of GBM is complex, and is driven by multiple intracellular events, which promotes cell proliferation, survival, invasion and angiogenesis. The hallmarks of GBM include loss of cell cycle control, resistance to apoptosis, invasion and migration, which leads to aggressive behavior of this dismal tumor and even resistance to therapies [21, 22]. Understanding the distinct molecular biology of GBM will enable further effects to specifically interfere with its inherent alterations to achieve a more effective therapy.

1.2.1 Loss of cell cycle control

The cell cycle is the process by which a eukaryotic cell is duplicated and segregated into daughter cells. It is comprised of four phases: G1 (gap1) phase when cells synthesize mRNA and protein for DNA synthesis; S (synthetic) phase when DNA replicates; G2 (gap2) phase when cells synthesize protein; M (mitotic) phase when duplicated chromosomes are divided into two daughter cells [23]. In normal cells, cell cycle progression is under strict control by the coordinated activities of cyclin/cyclin-dependent kinases (CDK) complexes, which act as master regulators to govern cell

cycle progression by phosphorylating downstream substrates [23, 24]. It is well known that cyclin D-CDK4/6, cyclin E-CDK2, cyclin B-CDK1 and cyclin A-CDK1/2 are critical for cell cycle progression through G1/S transition, S phase and G2/M transition, respectively [25]. On the other hand, cyclin-dependent kinase inhibitors (CDKIs) are able to control cell cycle progression by binding to CDKs [26]. For instance, the cell cycle inhibitor p16 belongs to the INK4 family of CDKIs and negatively regulates cell cycle transition by binding to CDK4. The cell cycle inhibitor p27 and p21 are members of the Cip/Kip family and exhibit broad CDK inhibitory activity, including interacting with cyclin D-CDK4/6 to negatively control the G1/S transition [27, 28]. Several signaling pathways have been involved in the regulation of cell cycle progression, including the retinoblastoma pathway (RB) and p53 pathways. In quiescent cells, RB associates with the transcription factor E2F to prevent cell progression into S phase. Upon stimulation, activated cyclin D-CDK4/6 phosphorylates and inactivates RB, enabling the release of E2F that activates genes required for the G1/S transition [27]. The p53 pathway is well known to be involved in cell cycle arrest, apoptosis, senescence and DNA damage repair [29]. In response to DNA damage, p53 is activated and acts as a transcription factor. One of the well characterized effectors is p21 that functions as a critical regulator of cell cycle progression in G1 phase [30]. P53 is stabilized by binding to p14 and degraded by murine double minute 2 (MDM2). Loss of cell cycle control due to genetic alterations in these cell cycle regulators has been proposed to be associated with tumorigenesis of several tumors, including GBM [31, 32].

Dysregulation of RB signaling has been reported in about 80% of GBM and is implicated in the progression of astrocytoma [33]. Alterations of this pathway include genetic loss of RB, CDK4/6 amplification as well as deletion of *CDKN2A* coding for p16, causing uncontrolled cell cycle [34]. P53 mutation has been documented in primary GBM with a low frequency of 28-35%, and loss of p53 is frequently observed in the pathological progression of secondary GBM [35, 36]. Alterations of p53 pathway are associated with inactivation of cell cycle inhibitor p14 and amplification of MDM2 [33]. Dysregulated p53 pathways impair cell cycle progression by affecting both G1/S and G2/M transition [37]. It has also been reported that p53 is associated with G2/M arrest induced by TMZ, and altered p53 expression affects the response of GBM cells to TMZ [38, 39].

1.2.2 Resistance to apoptosis

Apoptosis is a highly regulated process whereby cells undergo programmed cell death. The process can be achieved either through the intrinsic pathway or the extrinsic pathway [40]. The intrinsic pathway is initiated by signals inside the cell, such as DNA damage and growth factor deprivation, and is regulated by pro- and anti-apoptotic proteins of the B-cell lymphoma 2 (BCL-2) family. The extrinsic pathway is triggered from outside the cell by binding of death inducing ligands to cell surface receptors [41].

Evasion of apoptosis is a hallmark of tumors, including GBM [42]. GBM cells exhibit intrinsic deregulation in apoptosis signaling pathways and develop complex mechanisms to evade its accompanying cell death, thereby promoting cell survival [43]. For instance, the anti-apoptotic BCL-2 family members BCL-2 and BCL-XL have been reported to be up-regulated in initial and recurrent GBM, while the pro-apoptotic BCL-2 protein BAX was down-regulated. This indicated that the dysregulated BCL-2 proteins contributed to enhanced anti-apoptotic capacity of GBM cells [44]. On the other hand, as a notable regulator in apoptotic response, p53 is found to regulate the expression of the pro-apoptotic proteins [45]. 87% of GBM harbor impaired p53 pathways, which leads to deregulation of apoptosis signaling and increased resistance to treatment-induced apoptosis [46].

1.2.3 Invasion and migration

The rapid progression of GBM is related to their ability to infiltrate into surrounding brain parenchyma, by way of invasion and migration. Invasive GBM cells escape complete surgical removal and hide from lethal radiation exposure, which is responsible for disease progression or even recurrence [47, 48]. Tumor cell invasion requires several steps, including detachment from the primary tumor mass, adhesion to extracellular matrix (ECM), degradation and remodeling of ECM, and cell motility through brain parenchyma [49]. Infiltration of GBM cells into brain tissue is determined by the interactions between tumor cells and extracellular microenvironment [50]. A multitude of molecules are involved, including adhesion molecules, cytoskeletal proteins, ECM components and proteases [48]. Integrins are the most common adhesion molecules that allow cell to adhere to ECM proteins such as laminin, collagens, matrigel and fibronectin [51]. In GBM, the binding of ECM to cell integrins mediates various intracellular signals interaction with growth factors and

receptors, leading to enhanced GBM cell adhesion, proliferation and migration [52]. Focal adhesion kinase (FAK) has been proposed as a key component of integrin-mediated signal transduction pathways, which is overexpressed in invasive GBM cells [53]. In addition to cell adhesion, GBM expresses elevated levels of matrix metalloproteases (MMPs), by which tumor cells are able to degrade and remodel ECM proteins, favoring cell invasion [54].

1.3 Growth factors and kinases in GBM

GBM produces various kinds of growth factors and expresses the corresponding membrane receptor kinases, which overall confers growth advantage to tumor cells. Upon the binding of diffusible growth factors to transmembrane receptors, mitogenic signaling pathways are activated and subsequently transduce intracellular signals required for cell growth, proliferation, and survival [55]. Tumor cells acquire the ability to decrease their dependence on exogenous growth factors by altering receptor kinases and downstream signaling pathways [56].

1.3.1 Growth factor

Growth factors are major regulators in tumor progression and GBM is enriched in a variety of growth factors, including IGF-1, FGF-2, EGF, PDGF, VEGF and others [57]. Three key growth factors in GBM are described below.

The epidermal growth factor (EGF): EGF and its epidermal growth factor receptor (EGFR) are important in mediating the proliferative and transforming responses via autocrine or paracrine mechanisms [58]. The significant roles of EGF/EGFR have been well established in GBM [59]. As a potent mitogen, the primary function of EGF is to promote the growth of GBM cells by stimulating DNA synthesis and cell division via EGF/EGFR signaling pathway [60]. It has been shown that EGF expression level was upregulated in the GBM tumor region, but reduced in the cerebrospinal fluid after surgical resection of the tumor, indicating a crucial role of EGF in the course of GBM progression [61]. In addition to its mitogenic effects, EGF has been reported to participate in the key processes of GBM cell invasion and angiogenesis [62-64]. Notably, EGF is essential for the maintenance of neural stem cells (NSC) as well as glioma stem cells (GSC), by promoting sphere formation and self-renewal capacity [65].

Fibroblast growth factor family (FGFs): FGFs play crucial roles in a wide range of cellular processes, such as cell proliferation, differentiation, migration and angiogenesis [66]. Of all the members in this family, FGF-1 and FGF-2 have been implicated in GBM, and alterations of FGF/FGFR signaling pathways play a critical role in the malignant progression of this tumor type [67-69]. GBM is characterized by high vascularization and FGF-2 has been observed to contribute to the process of angiogenesis [62]. FGF-2 can enhance the proliferation of endothelial cells and cooperate with VEGF to promote angiogenesis [70]. Besides, it is demonstrated that FGF-2 derived from GBM cells was able to increase the blood brain barrier function of endothelial cells, leading to drug resistance in GBM [71]. Specifically for GSC, FGF-2 is considered as an essential supplement for self-renewal and maintenance GSC pool [72]. Moreover, FGF-2 is the most effective inducer of Nestin expression, a stem cell marker [73]. Withdraw of FGF-2 induces more differentiation of GSCs through asymmetric cell division [74]. However, the necessity of adding FGF-2 as a component in culture medium is still debatable. It has been reported that GSC can sustain their self-renewal independent of exogenous growth factors, mainly in an autocrine fashion due to secretion of FGF-2 by GSCs [75, 76]. Thus, to avoid undesired alterations in cell culture, it is critical to maintain GSC *in vitro* similar to their original tumor cells [77].

Insulin-like growth factor (IGF) axis: The IGF signaling axis notably regulates cellular processes in normal cells as well as malignant cells [78]. The system is made up of ligands IGF-1 and IGF-2, transmembrane receptors IGF-1R and IGF-2R, as well as binding proteins IGFBP1-6. IGF-1 is a powerful mitogenic and anti-apoptotic factor involved in the control of cell proliferation, differentiation and apoptosis. The elevated levels of IGF-1 expression have been observed in GBM, suggesting the crucial role of IGF-1 in gliomagenesis [79]. Recently, Ho et al. showed that IGF-1 regulated GBM cell invasion by mediating cytokine secretions [80]. Since the important role of IGF-1 is proposed in NCS proliferation [81], it might provide a growth benefit for the addition of IGF-1 as a supplement for GSC culture *in vitro*.

1.3.2 Receptor tyrosine kinase

Cellular receptors with tyrosine kinase function as key mediators of signal transduction. Once activated, receptor tyrosine kinases (RTK) initiate a stream of signals that regulate multiply of cell possesses. RTKs are transmembrane

glycoproteins that contain an amino-terminal extracellular ligand-binding domain, a single anchoring transmembrane domain, and a cytosolic carboxy-terminal domain with tyrosine kinase enzymatic activity [55]. Activation of RTK is initiated by a cognate ligand binding to extracellular domain of receptor, leading to receptor homo/hetero-dimerization and other conformational changes. Juxtaposition of tyrosine kinase domain of both receptors stabilizes the active state of kinase and enables trans-phosphorylation of tyrosine residues in kinase activation loop. The phosphorylated residues serve as docking sites for cytoplasmic proteins which contain Src homology or phosphor-tyrosine binding domains, such as PI3K, phospholipase C, growth factor receptor-binding protein, or the kinase Src [82].

Alterations of RTK through protein overexpression, genetic amplification or mutations are identified in most GBMs and considered to be an essential component of vital oncogenic pathways [22]. In the followings, two crucial RTKs are described in detail.

Epidermal growth factor receptor (EGFR): EGFR, also referred to ERBB1 and HER1, is a transmembrane protein belonging to ERBB family of RTKs. Other members with shared structure and function are ERBB2 (HER2), ERBB3 (HER3) and ERBB4 (HER4) [83]. Dysregulated EGFR activation is considered the most common abnormality, occurring in about 57% of primary GBM patients [35]. EGFR activity is frequently upregulated due to amplification of the *EGFR* gene, overexpression of EGFR protein, or constitutively activation of oncogenic mutations [84]. The variant III EGFR deletion mutant (EGFRvIII) is the most common type of EGFR mutations expressed in about half of GBMs with EGFR amplification [85]. Due to the lack of binding domain, this truncated EGFR is constitutively activated and sustains a low level of autophosphorylation with decreased internalization and reduced degradation. This weak but continuous signal mediated by overexpression of EGFRvIII contributes to enhanced dysregulation of downstream pathways involved in amplified oncogenic effects, including increased proliferation, angiogenesis, invasion, tumorigenicity and resistant to therapy [85, 86].

EGFR dysregulation is associated with poor prognosis and decreased survival time in GBM patients [87]. However, a conflicting result was found by Quan et al. who showed no association of EGFR amplification with survival in patients with GBM [88]. Nevertheless, as a hallmark of high-grade GBM, alterations of EGFR are rare in low-grade gliomas, indicating these alterations play a crucial role in the late event of

gliomagenesis and aggressive behavior [59]. Half of EGFR can translocate to the nucleus and interact with gene transcriptions that modulate radio- and chemo-resistance [89]. In spite of high levels of EGFR expression, cells with amplified EGFR are prone to lose amplification *in vitro* [90]. In the commonly used glioblastoma cell line U251, Wang et al. found activation of EGFR was low under standard culture, implying EGFR activation may be not required for the transmission of mitogenic stimuli in U251 cells [91].

Insulin-like growth factor-1 receptor (IGF-1R): Activation of IGF system is mediated by ligand-receptor binding and further modulated by IGFBP, leading to signal transduction via PI3K/AKT pathway or MAPK pathway [92]. The aberrant signaling pathways mediated by overexpression of IGF-1R contribute to the growth, migration, angiogenesis and survival of malignant cells, including tumorigenesis of GBM [93]. Currently, IGF-1R expression has been considered as an independent prognostic factor associated with poor survival of patients with GBM. In addition, overexpression of IGF-1R was associated with resistance to TMZ in GBM patients [94]. With regard to radio-resistance, Osuka et al. showed that upregulation of IGF-1R induced by fractionated radiation had a radio-protective effect on GSCs via PI3K/AKT signaling pathway [95]. Besides, it has been reported that blockage of IGF-1R inhibited GBM growth mediated either by a direct effect on tumor cell proliferation or an effect on tumor vascularization [96]. Interestingly, IGF-1R was responsible for serum-induced activation of ERK1/2 *in vitro*, highlighting the mitogenic effect of IGF-1R signaling [91].

1.4 Major oncogenic pathways in GBM

Multiple cellular processes regulate cell proliferation and survival, with several signaling pathways playing pivotal roles in these contexts. The molecular pathogenesis of GBM is a complex interconnected network involved in the alterations of key signaling pathways, which drives tumor cells with features of uncontrolled proliferation and defective apoptosis [22]. In addition to alterations in tumor suppressive pathways such as RB and p53 pathways, activation of oncogenic pathways contributes to growth, survival and invasion of GBM [97]. The major oncogenic pathways involving RTKs in GBM are PI3K-AKT-mTOR and MAPK/RAS-RAF-ERK1/2 signaling pathways.

1.4.1 PI3K/AKT signaling pathway

PI3K/AKT/mTOR signaling pathway is one of the crucial signaling pathways regulating cell cycle, cell survival and growth (Figure 1) [98]. Its signal transduction is initiated by membrane-bound RTK phosphorylation followed by activation of phosphoinositide 3-kinases (PI3K) [99]. PI3K then phosphorylates phosphatidylinositol 4, 5-bisphosphate (PIP2) to generate phosphatidylinositol 3, 4, 5-triphosphate (PIP3). This process can be reversed by phosphatase and tension homolog deleted on chromosome ten (PTEN) which dephosphorylates PIP3 [100]. The main function of PIP3 is to serve as docking sites for intracellular signaling proteins containing pleckstrin-homology domains and recruit serine/threonine kinase 3'-phosphoinositide-dependent kinase1 (PDK1) and protein kinase B (PKB) known as AKT to plasma membrane. Once translocated to the membrane, AKT is phosphorylated by PDK1 via its activation loop at threonine 308 as well as by DNA-dependent protein kinase or mammalian target of rapamycin (mTOR) at Serine 473 [101]. AKT activation mediates diverse cellular functions by further activating multiple downstream substrates. Specifically, AKT promotes cell survival by targeting apoptosis-related genes such as Bad, forkhead transcription factors, apoptosis signal-regulating kinase 1, glycogen synthase kinase-3 and caspase 9 [102]. Besides, AKT has been shown to regulate the cell cycle through cyclin D1, cyclin E and p21 [103]. mTOR is also a crucial target of AKT by phosphorylation of tuberous sclerosis complex-2 (TSC2) and disruption with TSC1-TSC2 complex. Activation of mTOR results in protein synthesis by phosphorylation of p70 S6 kinase and deactivation of eukaryotic initiation factor 4E binding protein 1[101].

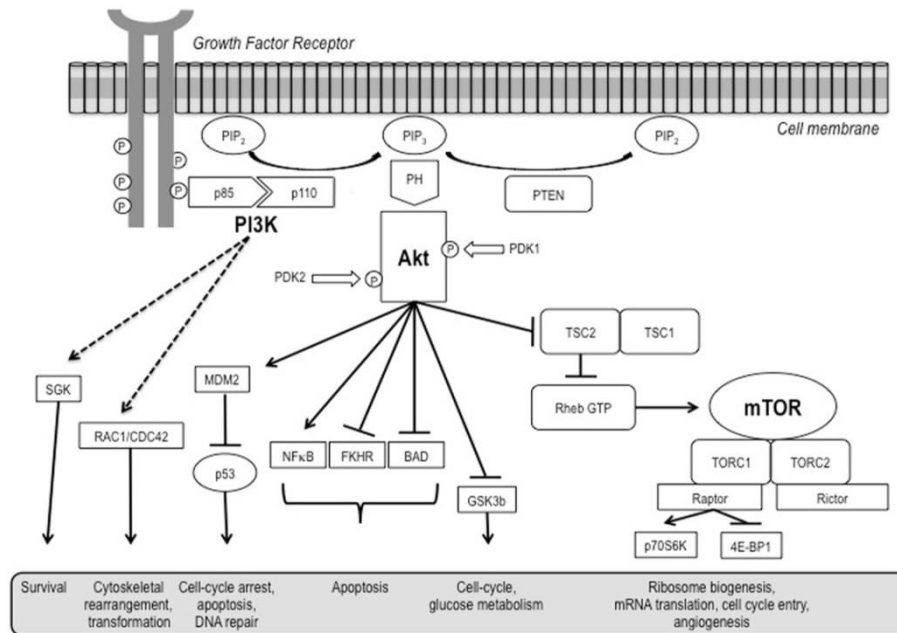


Figure 1. **Schematic illustration of PI3K/AKT/mTOR pathway** [98].

Dysregulation of PI3K/AKT signaling pathways is frequently induced by loss-of-function mutations in negative regulators, or gain-of-function alterations in RTK, and plays a significant role in driving gliomagenesis [104].

Constitutive activation of AKT has been observed in 80% GBM, which contributes to altered PI3K/AKT pathway in nearly 90% of GBM [35]. However, mutation of *AKT* is rarely detected in human GBM. AKT activity is elevated by loss of PTEN in GBM and also mutation in *PI3K* regulatory subunit [105, 106]. As a negative regulator of AKT, loss of PTEN leads to constitutive activation of PI3K/AKT pathway, which is also associated with tumorigenesis [107]. About 50% of GBM patients harbor tumors with genetic loss, mutation or epigenetic inactivation of *PTEN* [104, 108]. Also in commonly used glioblastoma cell lines including U251, AKT is constitutively activated due to the absence of PTEN [91, 109]. Elevated expression of phosphorylated AKT is associated with poor prognosis in patients with GBM [110]. It has been documented that irradiation can induce AKT activation which modulates radio-resistance in GBM [111]. Therefore, targeting AKT is a potential option for increase of radiation sensitivity in GBM, including primary glioma stem cells [112, 113].

1.4.2 MAPK signaling pathway

Mitogen-activated protein kinase (MAPK) is the main mitogenic signaling initiated by RTKs in both normal cells and tumor cells [114]. The pathway is activated by ligands binding to RTKs, leading to receptor dimerization and trans-phosphorylation.

Phosphorylated residues serve as binding sites containing Src homology 2 (SH2) or phosphotyrosine binding (PTB) domains like SHC. SHC then recruits growth factor receptor-bound protein 2 (Grb2) and guanine exchange factor son of sevenless (SOS) as adaptor proteins, allowing release of GDP and binding of GTP on RAS. Activated RAS can then lead to translocation of serine/threonine kinase RAF to plasma membrane where RAF is phosphorylated and activated. RAF further activates MEK, which phosphorylates ERK. Upon activation, ERK translocate to the nucleus to interact with transcription factors involved in diverse cellular functions such as cell proliferation, differentiation, cell cycle progression, protein synthesis and migration [115, 116]. Neurofibromin is the product of tumor suppressor gene Neurofibromatosis type I (*NF-1*) and functions as a negative regulator of RAS [117].

Regulated MAPK signaling is important for normal cell growth and proliferation, whereas a constitutive activation of this pathway plays a critical role in tumor formation and progression [118]. MAPK cascades facilitate excessive proliferative phenotype – a key characteristic of GBM. Approximately 88% of GBM possess at least one alteration that contributes to aberrant activation of MAPK signaling pathways, including RTK overexpression, activating ligands via sustained autocrine or paracrine, *B-RAF* gene mutation or *NF-1* gene deletion [35]. It is reported that enhanced p-MAPK was associated with increased radiation resistance in patients with GBM [119]. Moreover, activated MAPK expression is considered as a strong independent prognostic marker for a poor clinical outcome [120].

MAPKs are a family of serine/threonine kinases and conventional MAPKs contain three members: extracellular signal-regulated kinase1/2 (ERK1/2), c-Jun N-terminal kinase (JNK) and p38 MAPK. ERK5 now is considered an additional MAPK. Despite sharing structural homology, different members are activated via different stimuli and initiate individual MAPK cascades (Figure 2) [118]. The critical roles of ERK1/2 and JNK are emphasized below.

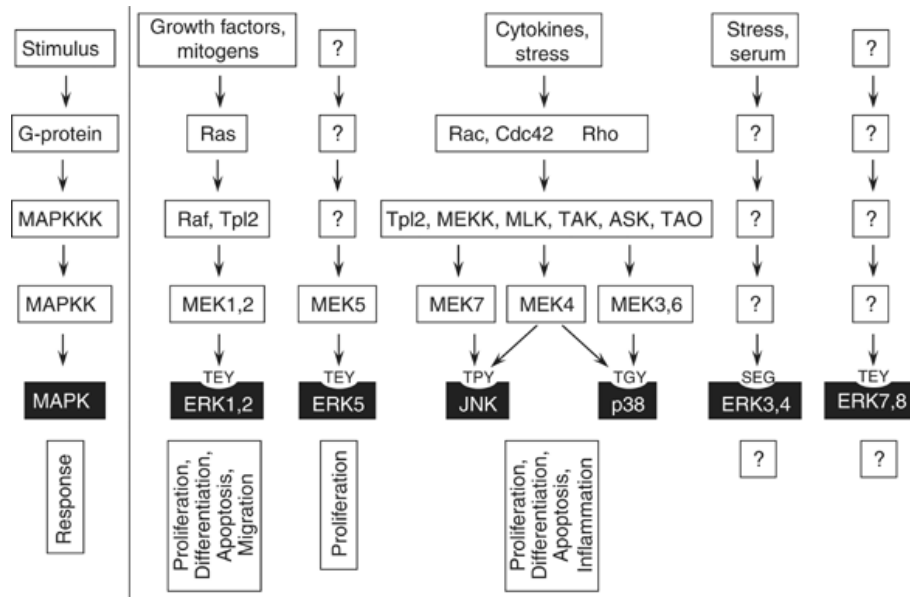


Figure 2. **Schematic illustrations of MAPK pathways** [118].

Extracellular signal-regulated kinase 1/2 (ERK1/2): ERK1/2 is the best characterized MAPK family. RAS/RAF/MEK/ERK1/2 cascade is the classical signal transduction required for cell survival and proliferation. Enhanced ERK1/2 activity has been found in tumor tissue of GBM patients, suggesting that ERK1/2 activation contributes to gliomagenesis [121]. Besides, the presence of constitutive ERK1/2 activation has been illustrated in glioma cell lines as well as primary culture of GBM [122]. In a recent study, ERK1/2 has been shown to be involved in the dispersal and growth of human primary GBM cells [123]. As a downstream effector of RTK, the relationship between ERK1/2 activation and RTK overexpression remains controversial in GBM. Lopez-Gines et al. demonstrated that 50% of GBM tissues with ERK1/2 expression had EGFR amplification [124]. However, Antonelli et al. showed that EGFR was not expressed in pediatric high-grade astrocytoma and was not related to ERK1/2 activation [125]. A possible explanation may be the involvement of other RTKs in ERK1/2 activation. Wang et al. found ERK1/2 activation under normal cell culture with FBS was mediated via IGF-1R signaling but not EGFR in U251 cells [91]. It is also suggested that PDGFRA expression controlled growth of GBM cells via regulation of ERK1/2 activity [126].

C-Jun N-terminal kinases (JNKs): JNKs also belong to MAPK family but are considered as stress-activated protein kinases, due to their activation predominantly by environmental and genotoxic stresses and to a lesser extent by growth factors [127]. JNKs have three isoforms: JNK1, JNK2 and JNK3 and activation of JNKs

requires phosphorylation of tyrosine and threonine residues in a reaction catalyzed by the dual-specificity kinase MKK4 and MKK7 [128]. JNKs pathway can sense and process stress signals and participate in a spectrum of cellular functions regarding inflammation, DNA damage response, transformation and apoptosis [129]. A well-known substrate for JNKs is a transcription factor c-Jun leading to elevated activity of activator protein-1 [128]. JNKs have been identified to play context-dependent roles in both cell proliferation and apoptosis [130]. As an oncogene, JNK signaling pathway is critical for cell proliferation, survival and inflammation in cancers, including GBM [131]. It has been reported that constitutive activation of JNK contributes to enhanced transformation and resistance to apoptosis in GBM [132, 133]. Consistent with its role as a tumor suppressor, several studies have found significant activation of JNK in apoptosis mediated by several agents in GBM [134-136]. Furthermore, JNK activation is involved in radiation-induced apoptosis [137]. Therefore, further investigation is needed to find out more details regarding the role of ERK1/2 and JNK activation in GBM cell proliferation and survival.

1.5 Influence of cell density on GBM proliferation *in vitro*

In a previous study, Wang et al. have found that ERK1/2 activity was strongly influenced by manipulating growth conditions in U251 cells *in vitro*. Specifically, passage of exponentially growing cells followed by re-seeding at high density resulted in complete downregulation of ERK1/2 phosphorylation compared with re-seeding at low cell density. By contrast, cells released from plateau phase showed upregulation of ERK1/2 activation irrespective of cell density upon re-seeding [91]. Taken together, these data indicate an important role of cell density-dependent regulation in ERK1/2 activity, which mediates mitogenic signaling in GBM. However, the impacts of the dysregulated ERK1/2 activation on GBM cell proliferation have not been elucidated yet. The detailed underlying mechanisms remain to be explored. To date, several studies have demonstrated that cell density induced biological effects on cell proliferation might be mediated via FAK signaling pathway and related to cell contact inhibition [138-140].

1.5.1 Focal adhesion kinase

FAK is a non-receptor tyrosine kinase and resides at the sites of integrin clustering. FAK can be activated by interactions with integrin as well as growth factor receptors, thus transmitting cell adhesion-dependent or growth factor-dependent signals to cell

interior [141]. Phosphorylation of FAK at Y397 results in its association with tyrosine kinase Src, which leads to phosphorylation of other tyrosine residues including tyrosine 925 and then full activation of FAK. Activated FAK recruits Grb2 adaptor protein, leading to activation of MAPK signaling pathway. FAK phosphorylation can also induce activation of PI3K/AKT signaling pathway [142]. Therefore, as a key mediator in cell signaling involving cell matrix interaction, FAK participates in multiple cell functions and promotes cell proliferation, migration and adhesion [143]. A handful of studies have shown that GBM cells express upregulated FAK activity both *in vitro* and *in vivo*. In human GBM tumor biopsy samples, the expression of FAK was elevated compared to normal brain [53, 144]. Overexpression of FAK enhances the activity of RAS and subsequently ERK1/2 signaling, which contributes to GBM proliferation and invasion [145-147].

FAK signaling pathway may mediate ERK1/2 activity in response to the changes in cell density. First, the relationship between FAK and cell density has been documented. FAK phosphorylation is associated with cell density, and tyrosine phosphorylation of focal adhesion components is altered in a density-dependent manner [140, 148]. In human glioblastoma cells, cell density can modulate survival signaling via activation of FAK [149]. Second, as a potential downstream effector of FAK, ERK1/2 activation upon cell adhesion to ECM is dependent on FAK signaling [150, 151]. It has been proposed that FAK interacts with IGF-1R and these two signaling pathways converge [152]. Since Wang et al. showed that IGF-1R was responsible for ERK1/2 activation under serum-culture condition [91], it is possible that the crosstalk between these two pathways coordinately mediate ERK1/2 activation. Therefore, the possible involvement of FAK signaling needs further investigation.

1.5.2 Contact inhibition

The proliferation of normal cells stops when they reach high densities and come in contact with each other even in the presence of extracellular nutrients. This process is termed contact inhibition or density-dependent inhibition of cell division [153]. Normal cells stop proliferation when they form monolayer in culture vessel. Unlike normal cells, lack of contact inhibition is a hallmark of tumor cells. They continue to proliferate when confluency and pile up upon each other [21]. Contact inhibition is mediated by elevated levels of CDKIs including p16 and p27, which can arrest cell

proliferation in G1 phase of the cell cycle by binding of cyclin-CDK complexes [154]. Tumor cells are refractory to contact inhibition due to the absence of p27 induction [155]. A number of signaling pathways have been implicated in the process of cell contact inhibition, including FAK, Hippo, p38/MAPK and Merlin/EGFR [140, 156-158].

Previously, Wang et al. observed that ERK1/2 downregulation was inversely related to upregulated p27 expression when exponential growth cells are re-seeded at high density, indicating a certain degree of contact inhibition is preserved in U251 cells. Contact inhibition is rarely described in aberrant tumor cells. Therefore, it would be of interest to further explore this phenomenon in GBM.

1.6 Aim of the study

Based on the previous findings that ERK1/2 activation was strongly influenced by culture conditions including cell density in U251 cells, the objective of the study was to investigate the impact of cell density as well as growth factors on glioblastoma cell proliferation and the underlying mechanisms. Specifically, the aims were to:

- I. study the effect of changes in cell culture conditions including cell density on proliferation of U251 cells
- II. study the effect of FAK on ERK1/2 activity induced by changes in culture conditions
- III. investigate ERK1/2 regulation in different culture conditions and study the effect of ERK1/2 activity on radiation response in U251 cells
- IV. explore the effect of different growth factors on glioblastoma cell proliferation

2 MATERIALS AND METHODS

2.1 Materials

2.1.1 Chemicals and reagents

Table 1. Chemicals and reagents

Chemicals and reagents	Product No.	Company
AC-DEVD-AFC (substrate)	13401	AAT Bioquest, Sunnyvale, USA
Advanced DMEM/F-12	12634010	Life Technologies, Bleiswijk, Netherlands
Albumin fraction V (BSA)	80764	Carl Roth, Karlsruhe, Germany
Ammonium persulfate (APS)	A3678	Sigma-Aldrich, Steinheim, Germany
BIT 9500 serum substitute	09500	Stem cell, Vancouver, Canada
Bradford Quick Start™ Bradford	5000205	Bio-Rad, Munich, Germany
Bovine Serum Albumin Standard Quick Start™	5000206	Bio-Rad, Munich, Germany
Protease Inhibitor Cocktail Tablet	17325200	Carl Roth, Karlsruhe, Germany
Collagenase IV	17104019	Life Technologies, Bleiswijk, Netherlands
4',6-diamidino-2-phenylindole (DAPI)	D21490	Life Technologies, Bleiswijk, Netherlands
Dulbecco's MEM	FG445	Biochrom AG, Berlin, Germany
Dulbecco's MEM/F12	11320-074	Life Technologies, Bleiswijk, Netherlands
Dimethyl sulfoxide (DMSO)	4720.1	Carl Roth, Karlsruhe, Germany
DRAQ5	4084S	Cell signaling Technology, Frankfurt am Main, Germany
EDTA	112K0765	Sigma-Aldrich, Steinheim, Germany
Ethanol 100%	5054.2	Carl Roth, Karlsruhe, Germany
Fetal bovine serum (FBS)	S0115	Biochrom AG, Berlin, Germany
Fibronectin	356008	BD Bioscience, Heidelberg, Germany
Glutamine	K0302	Biochrom AG, Berlin, Germany
Glycine	3908.3	Carl Roth, Karlsruhe, Germany

Hydrochloric acid fuming 37%	4625	Germany Carl Roth, Karlsruhe, Germany
2x Laemmli sample buffer	161-0737	Bio-Rad, Munich, Germany
PageRuler™ Plus Prestained Protein Ladder	26619	Life Technologies, Bleiswijk, Netherlands
β-Mercaptoethanol	4227.1	Carl Roth, Karlsruhe, Germany
Methanol	1627.6	Carl Roth, Karlsruhe, Germany
Dulbecco' Phosphate-Buffered Saline (PBS)	L1825	Biochrom AG, Berlin, Germany
Paraformaldehyde 37%	P733.2	Carl Roth, Karlsruhe, Germany
Penicillin/streptomycin	3029	Sigma-Aldrich, Steinheim, Germany
Phosphatase Inhibitor Cocktail 2	P5726	Sigma-Aldrich, Steinheim, Germany
Rotiphorese® Gel30	3029	Carl Roth, Karlsruhe, Germany
RPMI 1640 Medium	FG1215	Biochrom AG, Berlin, Germany
Poly-D-lysine hydrobromide (PDL)	P7280	Sigma-Aldrich, Steinheim, Germany
Poly-L-ornithine hydrobromide (PLO)	P3655	Sigma-Aldrich, Steinheim, Germany
Sodium chloride (NaCl)	3957.2	Carl Roth, Karlsruhe, Germany
Sodium dodecyl sulfate (SDS)	L3771	Sigma-Aldrich, Steinheim, Germany
TEMED	T9281	Sigma-Aldrich, Steinheim, Germany
Tris	AE15.3	Carl Roth, Karlsruhe, Germany
Triton® X-100	T8787	Sigma-Aldrich, Steinheim, Germany
10% Tween® 20	1610781	Bio-Rad, Munich, Germany
Trypsin	L2133	Biochrom AG, Berlin, Germany
Vectashield® mounting medium with DAPI	H-1200	Vector Laboratories, Burlingame, USA
Western Lightning PLUS	275-15021	Perkin Elmer, Shelton, USA
Propidium Iodide (PI)	P-1470	Sigma-Aldrich, Steinheim, Germany
RNase A	19101	Qiagen, Hilden, Germany

2.1.2 Growth factors

Table 2. Growth factors

Growth factors	Product No.	Company
Epidermal growth factor (EGF)	GRF-10326	Immunological Sciences, Rome, Italy
Basic fibroblast growth factor (FGF-2)	GRF-15595	Immunological Sciences, Rome, Italy
Insulin-like growth factor 1(IGF-1)	50356	Biomol, Hamburg, Germany
Transforming growth factor (TGF- β)	100-21C	PeptoTech Inc., Rocky Hill, USA

2.1.3 Inhibitors

Table 3. Inhibitors

Inhibitor	Product No.	Company
U0126	662005-5MG	Merck KGaA, Darmstadt, Germany
Erlotinib	CDS022564	Sigma-Aldrich, Steinheim, Germany
AG1024	121767	Merck KGaA, Darmstadt, Germany

2.1.4 Buffer preparation

Table 4. Buffer

Chemicals	Ingredient
APS (for WB)	1g APS add to 10ml ddH ₂ O
Assay buffer	50mM HEPES 100 mM NaCl 0.1% CHAPS 10mM DTT 100 μ M EDTA 10% Glycerol PH 7.4
1% BSA	20mg BSA 20ml 0.3% PBST
Ladder (for WB)	950 μ l Laemmli buffer 50 μ l β - Mercaptoethanol
RIPA buffer, stock	50 mM Tris-HCl pH 7.2-7.6 150 mM NaCl 2 mM EDTA

	0.1 % SDS
	0.5 % Sodium-Deoxycholate
	1% Nonidet P-40
	10% v/v Glycerol
Lysis buffer (ready to use for WB)	90 µl RIPA buffer
	1 µl Phosphatase Inhibitor
	15 µl Protease Inhibitor
Lysis buffer (for caspase 3 activity)	50 mM HEPES
	100 mM NaCl
	0.1% CHAPS
	1 mM DTT
	0.1 mM EDTA pH 7.4
0.3% PBST	PBS, 1x
	0.3 % Triton-X
TBS, 10x	24.23g 0.2M Tris PH7.5,
	58.44g 1M NaCl,
	add to 1L ddH ₂ O
	adjust pH value to 8.0
TG, 10x	30.27 g 0.2M Tris,
	144g Glycine,
	add to 1L ddH ₂ O
	adjust pH value to 8.3
Transfer buffer 1x	100ml TG 10x,
	200ml methanol,
	add to 1L ddH ₂ O
Running buffer 1x	100ml TG 10x
	10ml 10%SDS
	add to 1L ddH ₂ O
TBST	100ml TBS 10x
	10ml 10%Tween 20
	add to 1L ddH ₂ O
3x TE (Trypsin and EDTA)	0.15% trypsin
	0.06% EDTA

2.1.5 Antibodies

Table 5. Antibodies

Chemicals	Product No.	Company
Phospho-p44/42 MAPK (ERK1/2)	#9101	Cell signaling Technology, Frankfurt am Rhein, Germany
p44/42 MAPK (ERK1/2)	#9102	Cell signaling Technology, Frankfurt am Rhein, Germany
p27 Kip1	#2552	Cell signaling Technology, Frankfurt am Rhein, Germany
Cyclin D1(92G2)	#2978	Cell signaling Technology, Frankfurt am Rhein, Germany
Cleave caspase 3 (Aps175)	#9664S	Cell signaling Technology, Frankfurt am Rhein, Germany
Cleaved caspase 8 (Asp391)	#9496	Cell signaling Technology, Frankfurt am Rhein, Germany
Caspase 8 (1C12)	#9746	Cell signaling Technology, Frankfurt am Rhein, Germany
Phospho-PLK1 (Thr210)	#9062	Cell signaling Technology, Frankfurt am Rhein, Germany
Phospho-FAK Tyr397	sc-11765R	Santa Cruz Biotechnology, Heidelberg, Germany
Phospho-FAK Tyr925	Sc-11766	Santa Cruz Biotechnology, Heidelberg, Germany
Phospho-SAPK/JNK (Thr183/Tyr185)	#9251	Cell signaling Technology, Frankfurt am Rhein, Germany
SAPK/JNK	#9252	Cell signaling Technology, Frankfurt am Rhein, Germany
CD133/2 (293C3)	130-090-851	Miltenyi Biotec, Teterow, Germany
Ki67	ab15580	Abcam, Cambridge, U.K.
Ki67 Alexa Fluor® 647	558615	BD Pharmingen™, Heidelberg, Germany
SOX2 (E4)	sc-365823	Santa Cruz Biotechnology, Heidelberg, Germany
Gamma-H2AX(phospho S139)	Ab26350	Abcam, Cambridge, U.K.
GAPDH	sc25778	Santa Cruz Biotechnology, Heidelberg, Germany
Goat anti-rabbit IgG-HRP	Sc-2004	Santa Cruz Biotechnology, Heidelberg, Germany
Goat anti-mouse IgG-HRP	Sc-2005	Santa Cruz Biotechnology, Heidelberg, Germany
Goat anti-rabbit IgG-Rhodamin	AP187R	Merck KGaA, Darmstadt, Germany
Goat anti-rabbit IgG-Fluorescein	AP307F	Merck KGaA, Darmstadt, Germany

Goat anti-mouse IgG-FITC AP181F Merck KGaA, Darmstadt, Germany

2.1.6 Cell culture materials

Table 6. Cell culture materials

Type	Company
Cell culture flask T25 T75	Falcon, BD Bioscience, Heidelberg, Germany
Cell culture 6 well, 12well, 96 well plate	Falcon, BD Bioscience, Heidelberg, Germany
Cell culture 96 well plate (white)	Thermo Scientific, Denmark
Cell culture 60mm ² dish	Sarstedt, Nuembrecht, Germany
Cell scraper	Falcon, BD Bioscience, Heidelberg, Germany
8-well chamber slides	Falcon, BD Bioscience, Heidelberg, Germany
Tubes 1.5ml or 0.5ml	Eppendorf, Hamburg, Germany
Pipette tips	Eppendorf, Hamburg, Germany
Polypropylene conical tube 15 ml, 50ml	Falcon, BD Bioscience, Heidelberg, Germany
Nitrocellulose Blotting Membrane	GE Healthcare Life science, Freiburg, Germany
Flow cytometry tube	Falcon, BD Bioscience, Heidelberg, Germany
Sterile pipettes	Falcon, BD Bioscience, Heidelberg, Germany
Syringe Filter	Merck Millipore, Darmstadt, Germany
Microscope slide	Carl Roth, Karlsruhe, Germany

2.1.7 Apparatus and software

Table 7. Apparatus and software

Apparatus or software	Company
BD FACS Canto II	BD Becton Dickinson, Heidelberg, Germany
Centrifugation	Eppendorf, Hamburg, Germany
CO ₂ incubator	Heraeus GmbH, Hanau, Germany
TCS SP2 Confocal microscope	Leica, Wetzlar, Germany
FlowJo software 10.1	Tree Star, Ashland, USA
Fusion SL	Vilber Lourmat, Eberhardzell, Germany
GraphPad Prism 5.0	GraphPad Software, USA
Immunofluorescence optical microscopy	Olympus, Hamburg, Germany
Infinite M200	Tecan, Crailsheim, Germany
Image J	National Institutes of Health, Maryland, USA
Inverted microscopy	Zeiss, Oberkochen, Germany

Light microscope	Leica, Wetzlar, Germany
Linear accelerator	ELEKTA, Crawley, U.K.

2.2 Methods

2.2.1 Cell culture

The human glioblastoma cell line U251 cells (ATCC, LGC Promochem, Wesel, Germany) were cultured in RPMI1640 with 10% fetal bovine serum (FBS) and 1% penicillin-streptomycin. U87 cells (ATCC, LGC Promochem, Wesel, Germany) were cultured in Dulbecco's modified Eagle's medium (DMEM) with 10% FBS and 1% penicillin-streptomycin. Cell cultures were incubated at 37°C in humidified 5% CO₂ incubators. Cells were trypsinized with 3xTrypsin/EDTA and passaged every 3 to 4 days. Cells used in all experiments were within 12 passages.

Floating U251 cells were collected from supernatant of U251 cells cultured as monolayer in serum-containing medium [159]. After centrifugation at 1200rpm for 5 minutes, cells were washed with phosphate buffered saline (PBS). Then pellets were re-suspended in serum-free advanced DMEM/F12 medium containing 10% BIT 9500 and 2mM L-glutamine supplied with 10ng/ml human recombinant epidermal growth factor (EGF), 10ng/ml human recombinant basic fibroblast growth factor (FGF-2) and 1% penicillin-streptomycin, which was referred as defined serum-free medium. Sphere-like structures were formed 2-5 days of culture.

The glioma stem-like cell line NCH644 was grown as neurospheres in defined serum-free medium. Neurospheres were mechanically dissociated by pipetting to single cell suspension when they reached to around 200µm in diameter and split 1:5 to 1:9. In order to enrich for spheres, the entire content of culture flask was collected in conical tubes which were left at room temperature to allow spheres to settle down to the bottom of tube by gravity for 10 min. Then 1/2 to 3/4 of medium was removed and replaced with fresh complete medium. Medium was refreshed every 3-4 days by the method described above.

Patient-derived glioma cells GBM46 and GBM48 were established from tumor tissues of patients with GBM (GBM46 glioblastoma WHO grade IV; GBM48 gliosarcoma WHO grade IV) after surgical resection at Medical Faculty Mannheim. Informed consent was obtained from both patients. Tumor cells were grown as monolayer in defined serum-free medium in plates pre-coated with poly-l-ornithine

(PLO)/fibronectin. Due to the different volumes of tissues obtained from surgery, growth rates of cells from each tumor were variable. Fresh medium was replaced every 4 days and cells were passaged when reaching confluent monolayer culture.

2.2.2 Proliferation assay

To explore the growth of U251 cells in different culture conditions, cells were harvested from exponential growth (U251-E) or plateau phase (U251-P) respectively, and re-seeded at high (8×10^4 cells/cm²) or low (2.4×10^4 cells/cm²) seeding density, defined relative to the standard cell culture density (4×10^4 cells/cm²) according to the previous study [91]. The schemes of parent culture and re-seeding culture were described in Table 8 and Table 9. Cells were detached by 3x Trypsin/EDTA at different time points. Cell numbers were counted by hemocytometer under microscope. The experiments were repeated in triplicate and the error bar represented standard error (SE).

Table 8. Parent culture of U251 cells in exponential growth and plateau phase

Parent culture	Exponential growth phase (U251-E)	Plateau phase (U251-P)
Initial seeding number	5x10 ⁵ /flask T75 flasks	1x10 ⁶ /flask in T25 flasks
	4x10 ⁴ /well in 6-well plates	2x10 ⁵ /well in 12-well plates
	1x10 ⁵ /dish in 60mm ² dishes	
Culture time (day)	2	4

Table 9. Re-seeding culture of U251 cells in 12-well plates

Parent culture Reseeding density (12-well plates: 4cm ²)	Exponential growth phase	Plateau phase
High density (8×10^4 cells/cm ²)	EH (3.2×10^5 cells/well)	PH (3.2×10^5 cells/well)
Low density (2.4×10^4 cells/cm ²)	EL (9.6×10^4 cells/well)	PL (9.6×10^4 cells/well)

To analyze the growth factor-stimulated proliferation of U251 cells, 2×10^4 per well of cells were seeded in 12-well plate for 12-18h and starved in basal RPMI1640 medium for 16-24h before different growth factors were added (shown in Figure 3). U251 cells from different days were fixed with 4% paraformaldehyde (PFA) for 15min at room temperature and stained with DAPI (1:1000 diluted in 1xPBS) for 5 min. Then DAPI solution was removed and PBS was added. The plates were covered by aluminum foil. Hereafter images were taken for different days by inversed fluorescence microscope. Ten bright field and DAPI staining images were captured from one side to the other along the diameter. Cell numbers were counted. All data were obtained by three independent experiments.

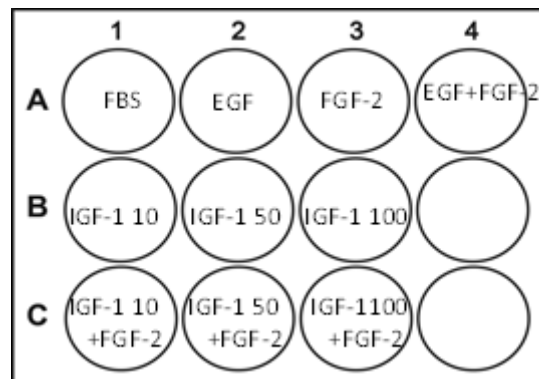


Figure 3. **Culture of U251 cells with different growth factors in 12 well plates.** (FBS: 10%; EGF: 20ng/ml; FGF-2: 20ng/ml; IGF-1 10: 10ng/ml; IGF-1 50: 50ng/ml; IGF-1 100: 100ng/ml)

To further test the optimal cell culture for proliferation of NCH644 cells, NCH644 cells were plated in serum-free DMEM/F12 medium as single cell suspension by mechanical segregation. After 16-24h starvation, different growth factors were added on day 0. Growth factors were added on day 3 and day 5 (shown in Figure 4). Images of NCH644 cells were taken from day 0 to day 6 and continually cultured at 37°C in humidified 5% CO₂ incubator. Images were captured by inversed fluorescence microscope. For each well, 10 bright field images were taken from one side to the other along the diameter. The number of spheres and area were analyzed by Image J software. The volume of spheres was calculated according to the formula: $\text{volume} = (4/3) \times \pi \times (\text{area}/\pi)^{3/2}$. All data were obtained by three independent experiments.

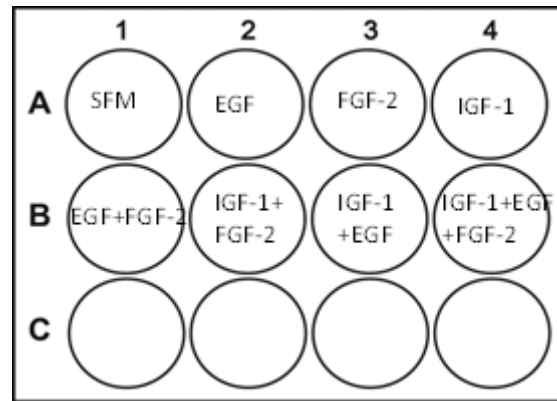


Figure 4. **Culture of NCH644 cells with different growth factors.** (SFM: serum-free DMEM/F12 medium, 20ng/ml EGF, 20ng/ml FGF-2, 100ng/ml IGF-1)

2.2.3 Detachment assay

2.2.3.1 Harvest from attached monolayer culture

Adherent U251 cells were washed with cold PBS twice and incubated with cold lysis buffer on ice. Lysates were directly harvested by scraping from cell culture plates with cell scraper referred as no-TE.

2.2.3.2 Cell detachment with agents

U251 cells were detached by different agents, including 3x Trypsin/EDTA, 0.25%Trypsin, 0.06%EDTA and 200U/ml collagenase IV. Cells were incubated with trypsin or EDTA for 3min and collagenase IV for 2h with gentle pipetting at 37°C in humidified 5% CO₂ incubator. After cell detachment, fresh medium was added and cells were re-suspended in 15ml conical tubes in incubator for indicated time. Thereafter, cells were washed with PBS once and harvested by centrifugation. The pellets were lysed with cold lysis buffer.

2.2.3.3 Collection of conditioned medium

U251 cells were detached by 3x Trypsin/EDTA. U251-E were re-suspended in RPMI1640 medium with 10% FBS. U251-P cells were re-suspended in basal RPMI1640 medium containing 1% BSA. Suspended cells were cultured at 37°C in humidified 5% CO₂ incubators for 1h. Then conditioned medium (CM) was harvested by centrifugation followed by passing through a 0.2µm-pore-diameter Millipore filter, referred to CM-detached. Supernatant collected from attached cells was filtered and referred to CM-attached.

2.2.3.4 Inhibitor assay

For U251-E cells, cells were incubated with inhibitors and CM. Inhibitors were applied as followed: 10 μ M AG1024 and 10 μ M Erlotinib and 0.1%DMSO used as control. Cells were harvested at the indicated time points. For U251-P cells, cells were incubated with 10 μ M U0126, 10 μ M AG1024 and 10 μ M Erlotinib for 1h with and without CM.

2.2.4 Western blotting

Table 10. Separating and stacking gels

Ingredient	Separate gel (12%)	Stack gel
ddH ₂ O	3.3 ml	1.4 ml
30% acrylamide-bisacrylamide	4.0 ml	0.33 ml
1.5M Tris (PH 8.8)	5.0 ml	
1.5M Tris (PH 6.8)		0.25 ml
10 % SDS	0.1 ml	0.02 ml
10 % APS	0.1 ml	0.02 ml
TEMED	0.004 ml	0.002 ml

Cells were harvested at different time points and placed on ice. Cells were rinsed with cold PBS three times and lysed in cold RIPA buffer together with phosphatase inhibitor and protease inhibitor. Adherent cells were scraped using a cold cell scraper and lysates were transferred to 1.5 ml Eppendorf tube. For suspended U251 cells, lysates were harvested by centrifugation at 1200rpm for 5min and then washed with cold PBS once. Lysates were centrifuged at 14000rpm for 10min at 4°C and supernatants were transferred to new 1.5ml tubes. Thereafter protein concentration was determined by Bradford assay. Briefly, samples were diluted to 1:10 in aqua bidest (2 μ l sample added into 18 μ l aqua bidest) and 5 μ l of the mixture were loaded in a 96-well plate. Then 250 μ l 1x Bradford dye reagent was added into each well. Each sample was repeated in three wells. Binding of Coomassie Brilliant Blue G-250 dye to proteins converts the red-brown dye to blue. After incubation at room temperature for 10 min, the blue dye was detected at 595 nm by microplate reader (Tecan). Bovine serum albumin standard were used for the standard curve (0.125, 0.25, 0.5, 1, 1.5, 2mg/ml).

Cell lysates (15-20µg of total protein) were mixed with the same volume of 2x Laemmli buffer with 5% β-mercaptoethanol. All samples were boiled for 5min at 95°C and cooled down on ice for at least 5min before loading on a 12% SDS-PAGE gel (Table 10). 2µl of protein standard marker was also loaded. SDS-PAGE run at 75V for 40min, and 120V for 100min. Hereafter proteins were electroblotted to the nitrocellulose blotting membrane at 300mA for 1 hour. The membrane was later blocked in 5% BSA in 1% TBS-T for 1 hour at room temperature, and subsequently in the following primary antibody at 4°C: anti-phospho-ERK1/2, anti-ERK1/2, anti-p27, anti-phospho-FAK Tyr397, anti-phospho-FAK Tyr925, anti-cleaved caspase 3, anti-cleaved caspase 8, anti-caspase 8, anti-cyclin D1, anti-phospho-PLK1, anti-phospho-JNK, anti-JNK and GADPH (1:1000 diluted in 5% BSA). After overnight incubation at 4°C, membranes were washed with TBS-T three times for 10min and incubated for 1 hour at room temperature with an appropriate goat anti-rabbit or goat anti-mouse IgG-HRP conjugates (1:20000 diluted in 1% TBS-T). The membranes were incubated with enhanced chemiluminescence (ECL) reagent (1:1 mixture of solution A and B in Western Lightning Plus ECL detection kit) for 1-2min in the dark at room temperature. Subsequently, immunoreactive bands were detected and visualized by chemiluminescence system (Fusion SL). Protein bands from western blot films were quantified using Image J. The intensity of each protein was normalized by dividing the corresponding loading control. The relative level of normalized protein was calculated as a ratio relative to the normalized control group.

2.2.5 Caspase 3 activity

Caspase-3 activity was tested using a colorimetric activity assay kit according to manufacturer's instructions. Briefly, cells were washed with PBS and lysed in cold lysis buffer containing 50mM HEPES, 100mM NaCl, 0,1% CHAPS, 100µM EDTA, 1mM DTT on ice. As shown in Table 11 below, 20µl cell extracts were added to 70µl assay buffer, followed by applying 10µl fluorimetric substrate Ac-DEVD-AFC (50µg/ml diluted in assay buffer). Each sample was repeated in triplicate. After 1h incubation at room temperature in the dark, fluorescence was measured at 405 nm excitation and 505 nm emission. Meanwhile, protein concentrations of cell extracts were measured by Bradford assay. The caspase3 activity was normalized with the absorbance intensity dividing the protein concentration and expressed as relative fluorescent units (RFU) per minute per mg protein for each condition.

Table 11. Reaction scheme for 96-well plate microassay method

	Assay buffer	Cell lysate	Caspase 3 substrate Ac-DEVD-AFC
Control	90µl	-	10 µl
Sample	70 µl	20 µl	10 µl

2.2.6 Colony forming assay

Cellular radiosensitivity was determined by clonogenic cell survival using the colony forming assay. U251 cells were harvested and sequentially diluted into desired concentrations in the concentrations 10 times higher than the number of cells seeded per flask (if 100 cells were seeded per T25, suspension of 1000cells/ml was prepared). The cell number and doses were shown in Table 12. Immediately before irradiation, 400µl suspensions of cells were centrifuged at 300g for 5min into a pellet at the tip of 0.5 ml Eppendorf tube. After irradiation, cells were re-suspended and 100µl of suspensions were plated into T25 flask with 5ml fresh culture medium in triplicate. After incubation for 11 days, colonies were washed with PBS and fixed with 1:3 methanol/acetic acid solution for 10 min followed by staining with crystal violet solution (1 g/l in aqua bidest). Colonies containing more than 50 cells were scored. The survival curve was analyzed with Linear-Quadratic (LQ) model using the SigmaPlot8.0 regression tool: $SF(D)=\exp[-(\alpha D+\beta D^2)]$. Three independent experiments were performed.

Table 12. The cell number seeded in T25 flask with different doses

U251 cells irradiated with 6MV X-rays					
Dose (Gy)	0	2	4	6	8
Cell number	100	100	300	1000	3000

2.2.7 Flow cytometry

The nuclear antigen Ki67 is a proliferation marker present in proliferating cells throughout G1, S, G2 and M phase but absent in non-proliferating cells in G0 phase [160]. Propidium Iodide (PI) is a DNA binding dye most commonly used for cell cycle distribution based on the DNA content [161].

In order to explore cell cycle distribution and Ki67 expression of U251 cells in different conditions, 1×10^6 U251 cells were collected by trypsinization and transferred to 15 ml conical tubes followed by wash once with PBS. Then the pellet was re-

suspended in 500 µl ice cold PBS and the suspension was slowly added drop wisely to 500 µl ice cold 2%PFA. After incubation on ice for 5min, cells were washed with 1% BSA /PBS once and re-suspended in 500 µl of permeabilizing solution 0.25% Triton X-100 in PBS for 5min at room temperature. Cells were then washed with 1% BSA /PBS again and centrifuged at 1500rpm for 5min. The pellet was re-suspended in 100 µl PBS and cell mixture was transferred to 1.5ml Eppendorf tubes (at this step the cells can be stored at 4°C fridge until antibody staining). 5µl of anti-Ki67 antibody (Alexa Fluor® 647) was added, mixed and the mixture was incubated at room temperature for 1h in the dark. Afterwards, 1ml 1% BSA /PBS was added to tube and cells were centrifuged at 1500rpm for 5min. The supernatant was discarded carefully and cells were washed once with PBS. The pellet was re-suspended in 500µl PBS. Cell nuclei were stained with 2µg/ml PI following pretreatment with 50µg/ml RNase and kept at room temperature for 30min in the dark. Flow cytometry was performed on a FACS Calibur and data analysis was performed using Flowjo version10 software.

2.2.8 Immunofluorescence

Anti-Ki67 antibody was used to detect proliferating cells when U251 cells and NCH644 cells were grown as colonies or spheres. The plasma membrane protein CD133 and transcription factor SOX2 are markers associated with stemness.

U251 and U87 cells were plated at 200 cells per well in 6-well plates. After 10-14 days, colonies were formed and fixed with 4% PFA for 15min at room temperature. Then cells were blocked with 1% BSA in PBS with 0.3% Triton-X (PBST) for 20 min. Anti-Ki67 antibody (1:200 diluted in PBST) was applied for 1h at room temperature. Then cells were washed 3 times and incubated in the dark with second antibodies (Goat anti-rabbit IgG-HRP1:200 diluted in PBST). After 1h incubation, cells were washed with PBS three times. Then nuclei were counterstained with DAPI. Images were captured by inversed fluorescence microscope.

Floating U251 cells and NCH644 spheres were seeded as single cells at the number of 1×10^4 in 12-well plates. Medium was refreshed by removing 250µl old medium and adding 250µl fresh medium every 2 days. On indicated days, cell suspension was plated on the slide pre-coated with poly-D-lysine for 3-4h to attach at room temperature and fixed with 4% PFA for 15 min. After blocking with 1% BSA in PBST

for 20min, cells were incubated with first antibodies (1:500 anti-CD133, 1:200 anti-Ki67, 1:200 anti-SOX2) for 1h at room temperature. Then cells were washed three times with PBST and incubated in the dark with second antibodies (Goat anti-rabbit conjugated with Rhodamine 1:200 diluted in PBST; Goat anti-mouse conjugated with FITC 1:200 diluted in PBST) for 1h at room temperature. After three times washing with PBS, nuclei were counterstained with Draq5. Then mounting medium was added and a coverslip was put on the top. Images were captured by confocal microscope (Leica SP8).

γ H2AX was used to examine radiation-induced DNA double-strand breaks (DSBs) repair foci. After irradiation of U251 cells in pellets, 1×10^4 cells were seeded in 8-well chamber slides and incubated at 37°C for attachment. At different time points after the end of irradiation, cells were washed, fixed and blocked as above. Thereafter, cells were incubated with primary antibodies (1:200 anti- γ H2AX) and then second antibodies (Goat anti-mouse conjugated with FITC 1:200 diluted in PBST). Finally, cells were sealed with Vectashield® mounting medium with DAPI and covered with coverslip. Cells were observed under fluorescence microscope and photographed. Foci were counted in each cell and 100 cells per well were analyzed.

2.2.9 Statistics

Results were shown as mean values \pm standard errors (SE) or mean values \pm standard deviation (SD). *P* values were calculated using Student's t test for differences between different groups. Statistical significance was taken as *P* < 0.05.

3 RESULTS

3.1 Effect of culture conditions on cell proliferation

3.1.1 GBM cells undergo apoptosis under certain conditions

In the previous work, Wang et al. showed that passage of exponentially growing U251 cells and re-seeding at high density resulted in complete downregulation of ERK1/2 phosphorylation at 12–36 h, whereas ERK1/2 activation was more strongly upregulated when U251 cells were harvested from plateau phase [91]. The results suggested that cell culture conditions including cell density have strong influences on ERK1/2 activity. In order to further investigate the functional implications of this paradox, cell proliferation in different re-seeding cultures was determined. U251 cells from exponential growth (U251-E) and plateau phase (U251-P) were re-seeded at high density (3.2×10^5 cells/well) and low density (9.6×10^4 cells/well) in 12-well plates and cultured for 3 days (Figure 5A). Cells were trypsinized and the numbers were counted by hemocytometer at different time points. As shown in Figure 5B, proliferation occurred when cells were re-plated at low density irrespective of the growth state of parent culture. Surprisingly, re-plating of U251-P cells at high density also resulted in further proliferation, consistent with the finding that releasing density-arrest plateau phase cells provided upregulated mitogenic signaling, whereas re-plating of U251-E cells at high density showed limited proliferation.

To exclude the potential influence of growth factor depletion on this observation, the experiment was repeated with media change on day 2. This led to an enhanced proliferation of cells re-seeded at low density as well as U251-P cells at high density on day 2-4, further implying that ERK1/2 activity affected by changes in culture conditions has a profound mitogenic impact on U251 cell proliferation (Figure 5C).

However, refreshing of the medium did not change the limited proliferation of U251-E cells when re-plated at high density (Figure 5C). The limited proliferation in EH cells was associated with cell detachment on day 3-4 as quantified by the number of floating cells in the medium, corresponding to approx. 2-7% of the attached cells (Figure 5D).

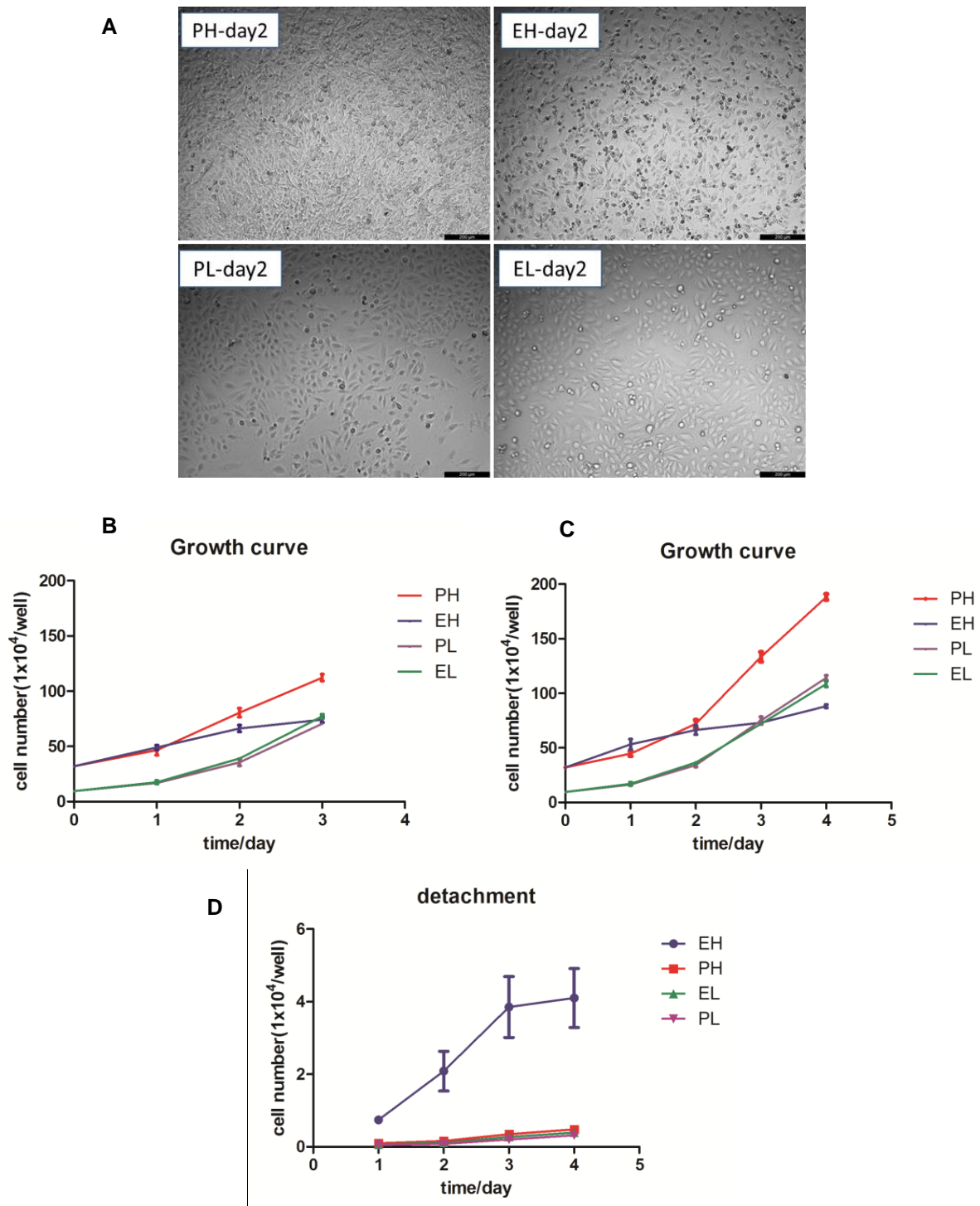


Figure 5. Proliferation of U251 cells from different culture conditions. U251-E cells and U251-P cells were re-seeded at the density of 3.2×10^5 cells/well and 9.6×10^4 cells/well in 12-well plates. Cell numbers were counted by hemocytometer at different time points. A. Images of U251 cells under different conditions on day 2. Scale bar=200 μ m. B. Growth curve in four different groups without medium refreshed. C. Growth curve in four different groups with medium refreshed on the second day. D. The number of detached cells in four different groups. PH: cells harvested from U251-P and re-seeded at high density; EH: cells harvested from U251-E and re-seeded at high density; PL: cells harvested from U251-P and re-seeded at low density; EL: cells harvested from U251-E and re-seeded at low density. Results are shown as means \pm SE from three independent experiments.

In order to test if the limited proliferation with detachment was associated with apoptosis, expression of cleaved caspase 3 and cleaved caspase 8 was analyzed by western blotting. Caspase activation was observed, as indicated by detectable cleavage of caspases 3 and 8 on day 2, suggesting that passage of exponentially growing cultures followed by re-seeding at high cell density resulted in programmed cell death (Figure 6A). The results were also confirmed by caspase 3 assay, which showed the increased activity of caspase 3 in EH cells compared with other groups (Figure 6B).

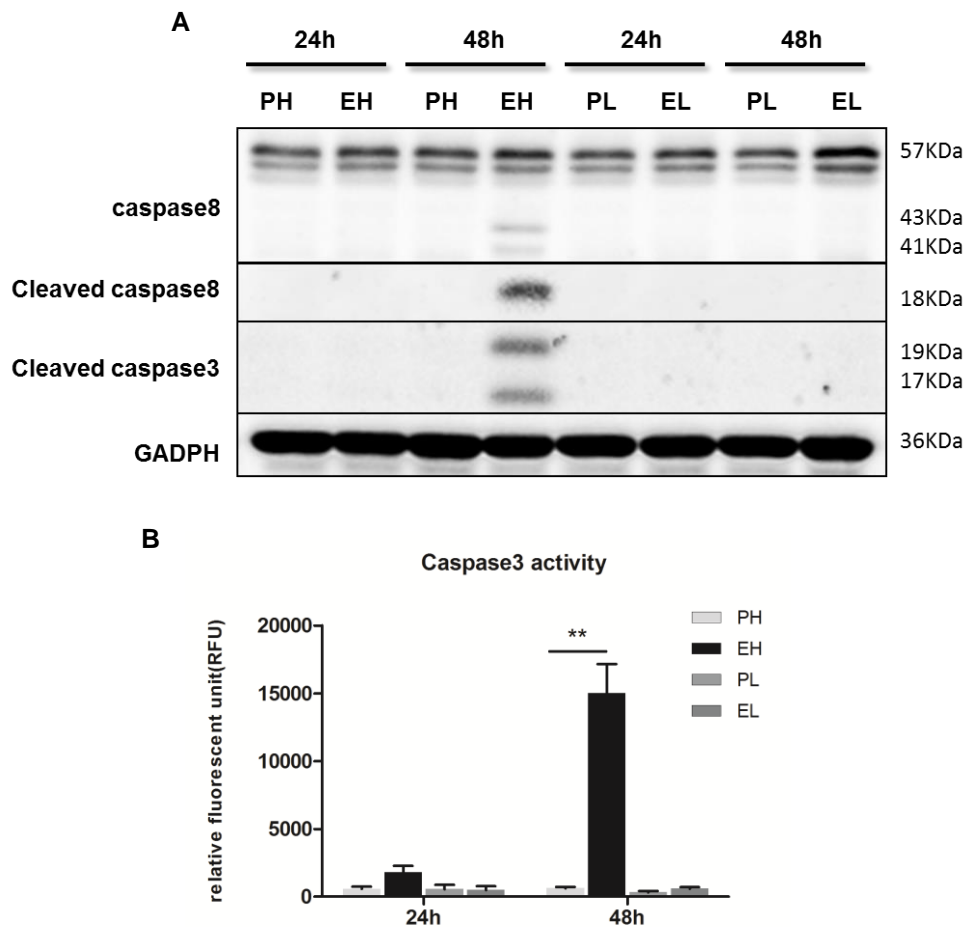


Figure 6. **Caspase assay in U251 cells from different culture conditions.** A. Western blot analysis of apoptosis proteins, including caspase 8, cleaved caspase 8 and cleaved caspase 3 with GAPDH as control. B. Activity levels for caspase 3 in the four groups. Activity is expressed as RFU. PH: cells harvested from U251-P and re-seeded at high density; EH: cells harvested from U251-E and re-seeded at high density; PL: cells harvested from U251-P and re-seeded at low density; EL: cells harvested from U251-E and re-seeded at low density. ** represents $P < 0.01$. Results are shown as means \pm SE from three independent experiments.

To further test if this was a general phenomenon or limited to the U251 cell line, the same experiment was conducted with the patient-derived glioblastoma cells GBM46 and GBM48. Similar to U251 cells, GBM46 and GBM48 cells from exponentially growing phase that were re-plated at high density showed an increased expression of cleaved caspase activation at 72h as confirmed by western blots and caspase 3 assay (Figure 7A-D).

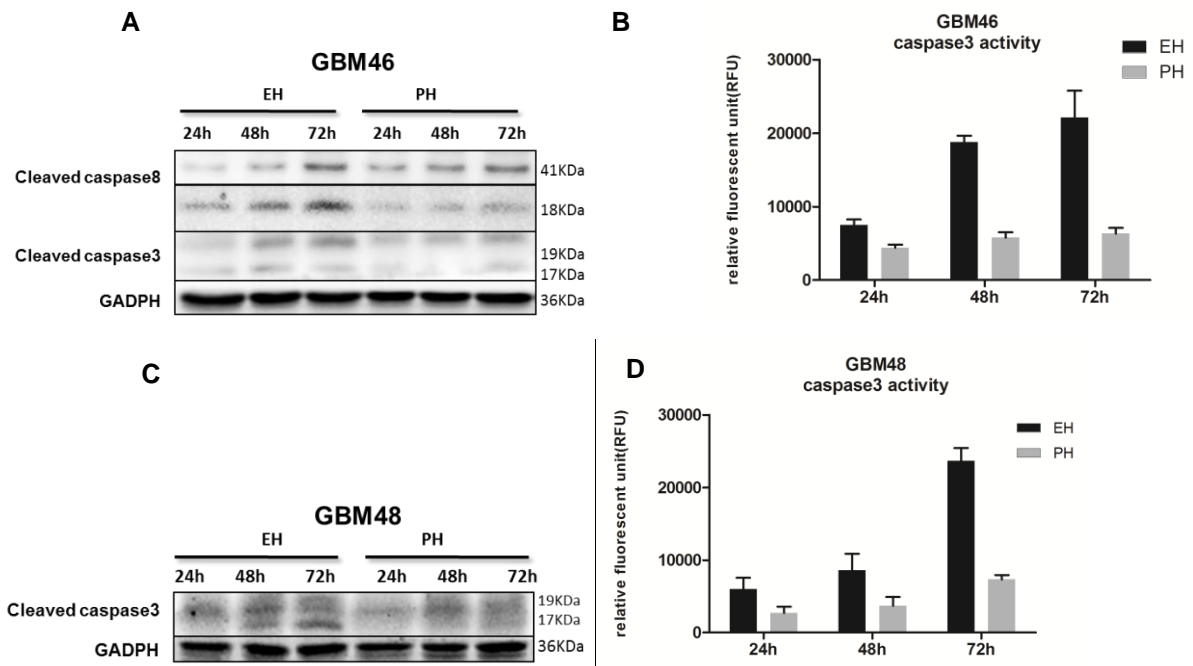
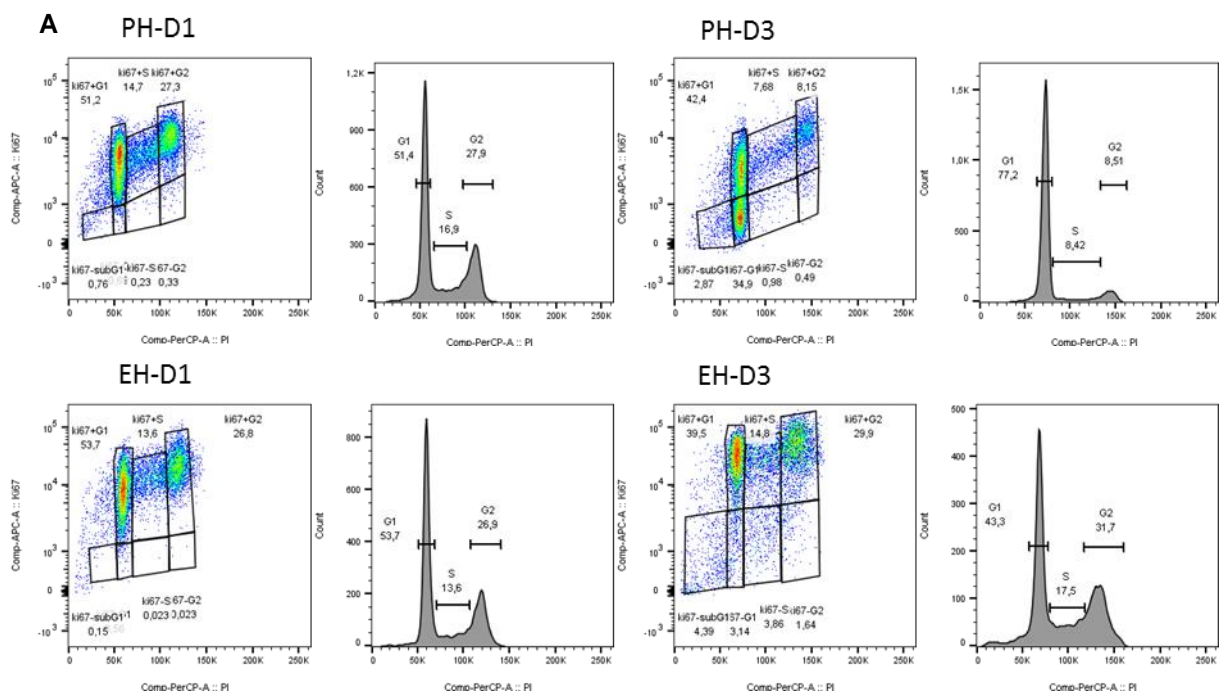


Figure 7. **Caspase assay in GBM46 and GBM48 cells from different culture conditions.** A. Western blot analysis of apoptosis protein cleaved caspase 8 and cleaved caspase 3 in GBM46 cells. PH: cells harvested from plateau phase and re-seeded at high density; EH: cells harvested from exponential growth phase and re-seeded at high density. B. Activity levels for caspase 3 of of GBM46 cells at the indicated time points. Results of caspase 3 activity for GBM46 shown as means \pm SD from one experiment. PH: cells harvested from plateau phase and re-seeded at high density; EH: cells harvested from exponential growth phase and re-seeded at high density. C. Western blot analysis of cleaved caspase 3 in GBM48 cells. D. Activity levels for caspase 3 of GBM48 cells at indicated time points. Results are shown as means \pm SE from three independent experiments.

3.1.2 EH cells have G2 arrest and downregulation of cell cycle proteins

To better understand the different phenotypic responses of exponentially growing and plateau phase cells, flow cytometry was performed to assess the cell cycle distribution and proliferation of U251 cells. DNA content was quantified by propidium iodide, while proliferating cells were detected with antibodies against proliferation marker Ki-67. Cell cycle histograms with G1, S and G2/M distributions characteristic of proliferating cells were seen on day 1 for all cultures, approximately 50-60% of the cells in G1, 15-20% in S, and 20-30% in G2. On day 3, however, plateau phase cells re-plated at high density were predominantly distributed in G1 (about 70%) and 15% in G2 phase with a significant fraction of non-proliferating (Ki67-low) cells in both phases. In contrast, Ki67-high EH cells accumulated in G2 (35%) while the G1 fraction was reduced to 40% with only a small minority being Ki67-low. Although Ki67-low cells with sub-G1 DNA content were observed in both cultures, the fraction was high in EH cells. Furthermore, cells re-plated at low density showed slightly increased G1 fractions on day 3, but were all Ki-67 positive (Figure 8A, B).



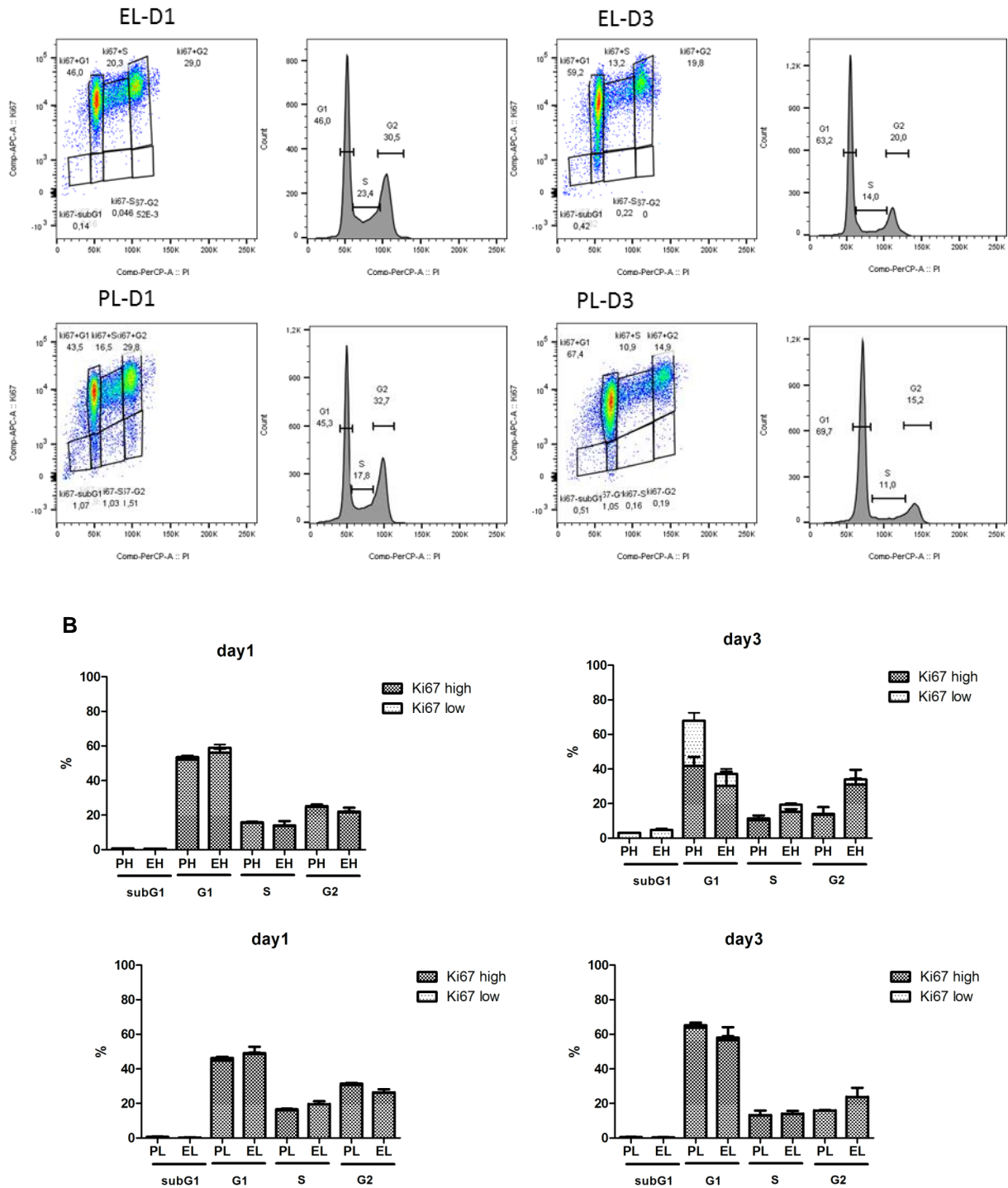


Figure 8. **Effect of different culture conditions on cell cycle distribution of U251 cells.** A. Dot-Plot analysis of PI and Ki-67 staining in different groups on day 1 and day 3. B. Proportion of cells in different cell cycles and Ki67 expression. Results are shown as means \pm SE from three independent experiments.

Since re-seeding exponentially growing cells at high density resulted in G2 accumulation, the expression of cell cycle regulating proteins was investigated by western blotting. Phosphorylation of ERK1/2 showed strong, transient downregulation in EH cells 24h after re-plating (Figure 9A), similar to the previous study [91]. Expression of cyclin D1 was lower in EH than in PH cells at all time points and was increasingly downregulated in EH cells at 24h and 48h, consistent with the observed inhibition of cell proliferation from day 2 (Figure 5B, C). Phosphorylation of PLK-1 which is required for entry into mitosis was strongly down-regulated in EH cells at 48h (Figure 9A, B). This was consistent with the accumulation of cells in G2 phase (Figure 8B). Furthermore, the expression of p27 was upregulated in EH cells at 24h compared with PH cells (Figure 9A, B).

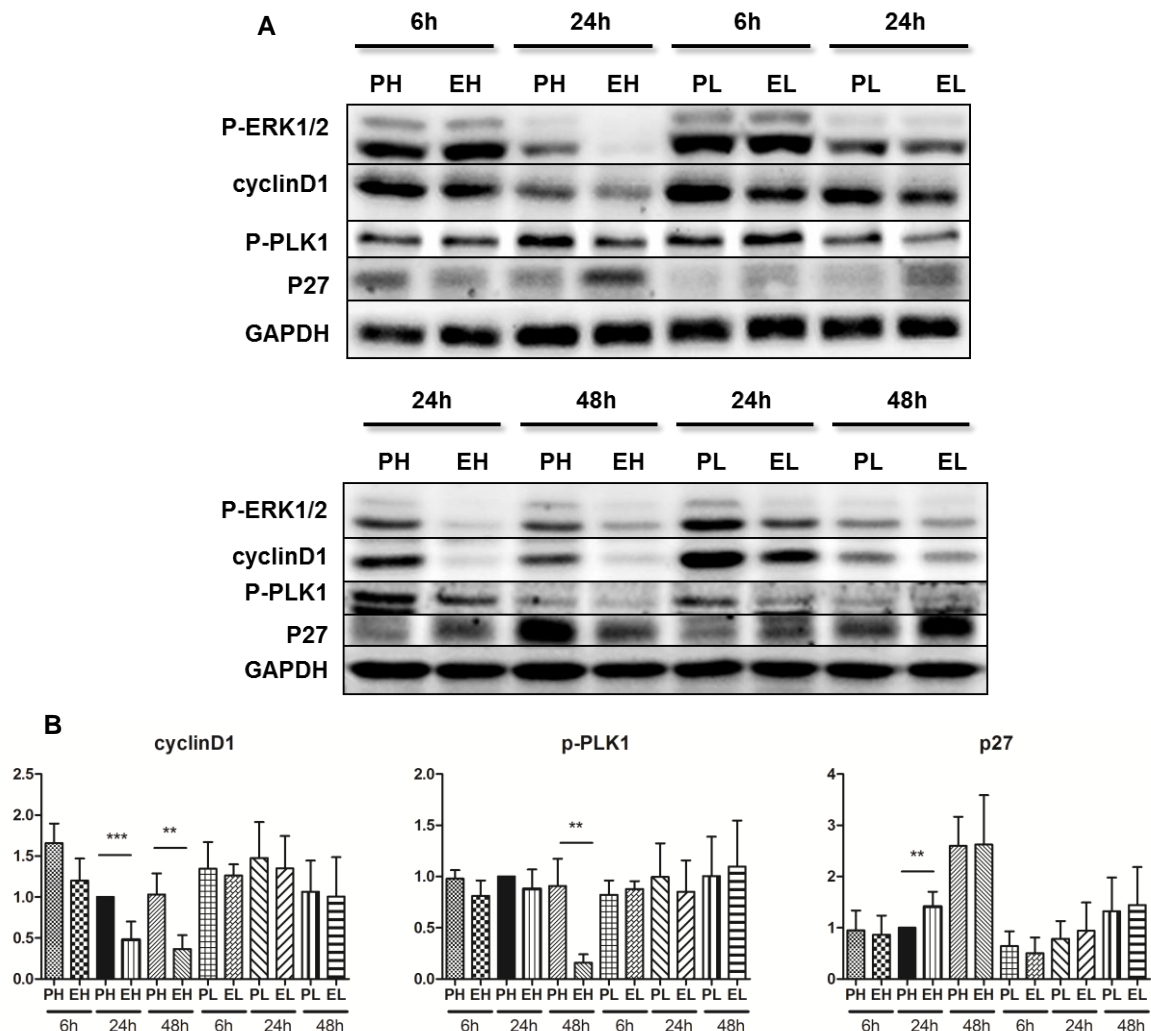


Figure 9. **Western blot analysis of cell cycle proteins of U251 cells.** A. Western blot analysis of expression of p-ERK, cyclin D1, p-PLK1 and p27 with GAPDH as control. B. Densitometric analysis of the western blot intensity of the indicated proteins shown in Fig.9A, normalized to GAPDH. PH at 24h was used as reference. Results are shown as means \pm SE from at least three independent experiments. * represents $P < 0.05$; ** represents $P < 0.01$; *** represents $P < 0.001$.

Moreover, in the patient-derived GBM46 and GBM48 cells, expression of cyclin D1 was decreased in EH cells compared with PH cells, accompanied by decreased ERK1/2 activation. In contrast, upregulation of p27 was seen on day 3 in EH cells (Figure 10).

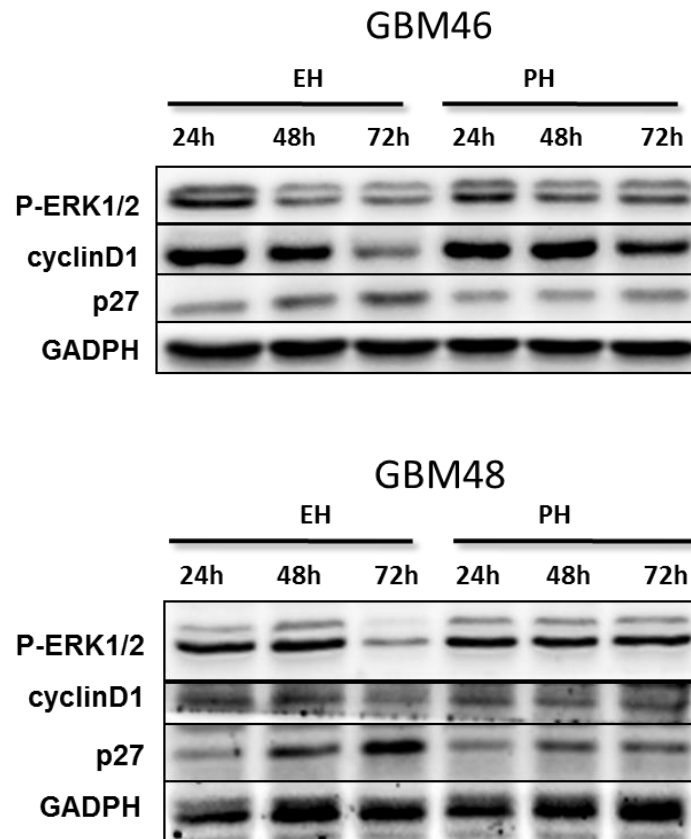


Figure 10. **Western blot analysis of cell cycle proteins of GBM46 and GBM48 cells.** Western blot analysis of expression of p-ERK, cyclin D1 and p27. GAPDH as control.

3.1.3 Effect of FAK on EH cell apoptosis

To test if FAK activation is altered with respect to changes in culture conditions, the expression of FAK phosphorylation was detected by western blotting. The best-characterized FAK phosphorylation event is the autophosphorylation at Y397, further leading to phosphorylation of other tyrosine residues including Y925 [162]. Western blots showed that FAK phosphorylation at Y397 was significantly lower in EH cells at 6h compared with PH cells and remained reduced at 24h and 48h. In contrast, FAK phosphorylation at Y925 was only moderately reduced in EH at 6-24h compared with PH but markedly reduced at 48h (Figure 11A, B).

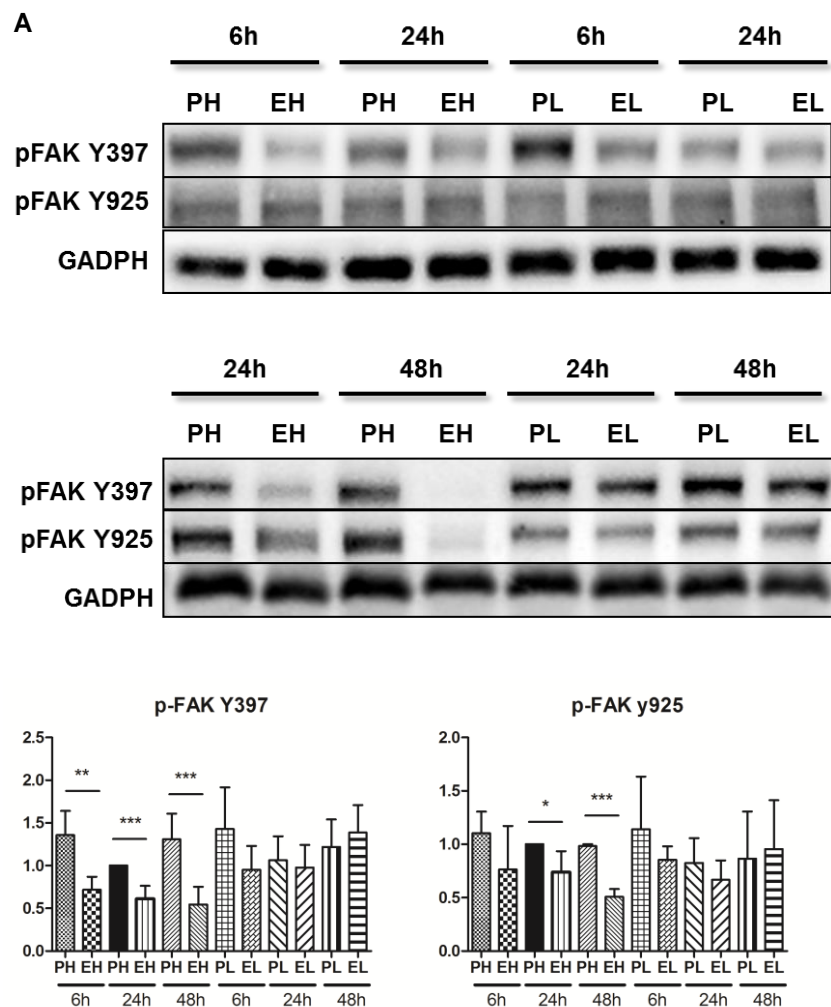


Figure 11. **FAK expression in different culture conditions in U251 cells.** A. Western blots analysis of p-FAK-397 and p-FAK-925 with GAPDH as control. B. Densitometric analysis of the western blot intensity of the indicated proteins shown in Fig.11A, normalized to GAPDH. PH at 24h was used as reference. Results are shown as means \pm SE from at least three independent experiments.* represents $P < 0.05$; ** represents $P < 0.01$; *** represents $P < 0.001$.

Because activated FAK expression was decreased and loss of attachment might downregulate this pathway, it was assumed that increasing FAK expression might rescue apoptosis when exponentially growing cells were re-plated at high density. It has been documented that growth factors as well as EMC can increase the expression of FAK [163]. Thus, U251 cells were seeded in plates coated with 0.83mg/ml collagen I or 10 μ g/ml fibronectin and supplied with growth factors 100ng/ml IGF-1 and 10ng/ml TGF β . However, EH cells were not rescued from apoptosis as shown by western blots (Figure 12A, B). The results indicated that

downregulation of FAK signaling pathways is not responsible for the decreased p-ERK1/2 and that anoikis in this case does not depend on FAK.

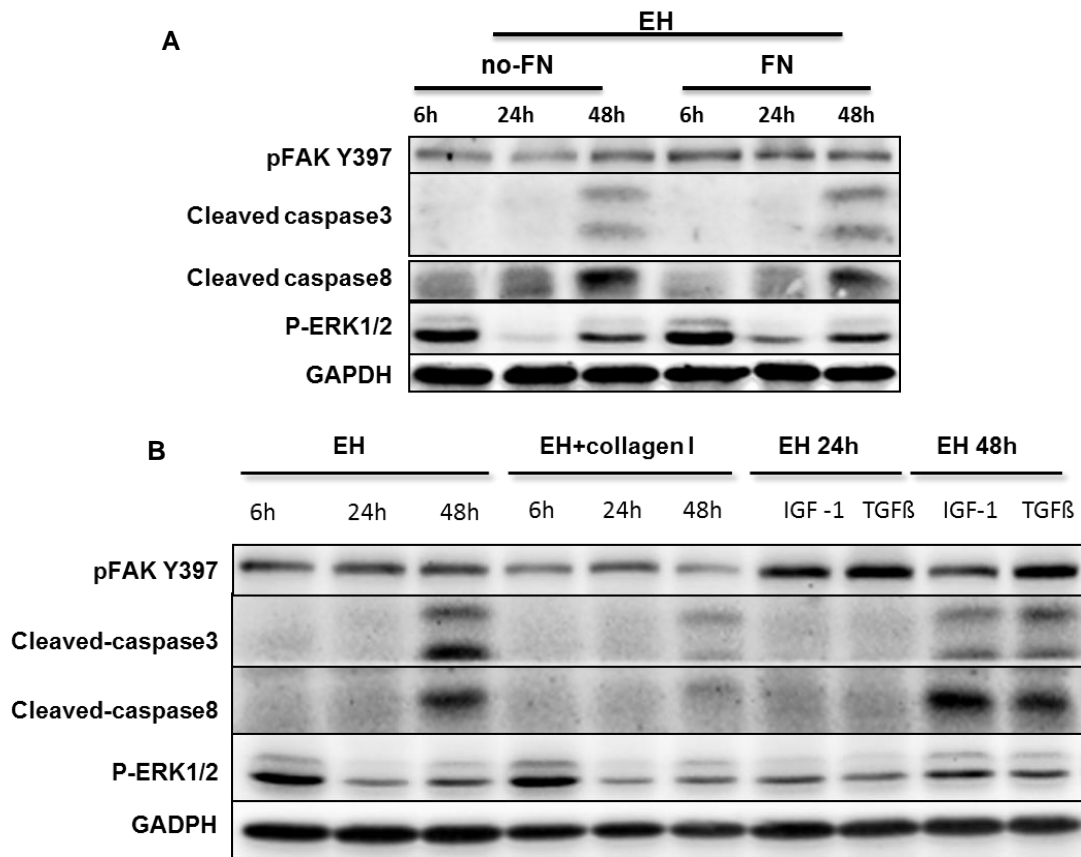


Figure 12. **Effect of increasing FAK on cell apoptosis.** U251-E cells were re-plated at high density in fibronectin pre-coated plates. Protein lysates were harvested at the indicated time points. Western blot analysis of p-FAK-397, cleaved caspase 3, cleave caspase 8 and p-ERK1/2 with GAPDH as control. FN: plates pre-coated with fibronectin. B. U251-E cells were re-plated at high density in collagen I pre-coated plates or adding growth factors. Western blot analysis of p-FAK-397, cleaved caspase 3, cleave caspase 8 and p-ERK. GAPDH as control. Collagen I: plates pre-coated with 0.83mg/ml collagen I. IGF-1 100ng/ml; TGF-β: 10ng/ml.

3.1.4 Effect of upregulation of p27 on EH cell apoptosis

To test the possible involvement of cell cycle progression, p27 in exponentially growing cells was induced to upregulate by starvation before the re-seeding experiment. As shown in Figure 13A, U251-E cells had increased expression of p27 after 24h starvation, resulting in cell cycle arrest. Then, U251-E were incubated with 0.5% FBS medium for 12h and re-seeded at high density in the same low FBS medium referred as 0h. After another 12h incubated in 0.5% FBS medium, medium was refreshed with 10% FBS medium and cells were collected at the indicated time points. No evidence of apoptosis was observed, as shown by the absence of cleaved

caspase by western blot (Figure 13B). Moreover, starved U251-E cells survived and continued to proliferate with no obvious detachment after re-plating at high density (Figure 13C). The results demonstrated that upregulation of p27 prevents cells from undergoing apoptosis, suggesting that uncontrolled cell cycle progression plays a vital role in inducing apoptosis.

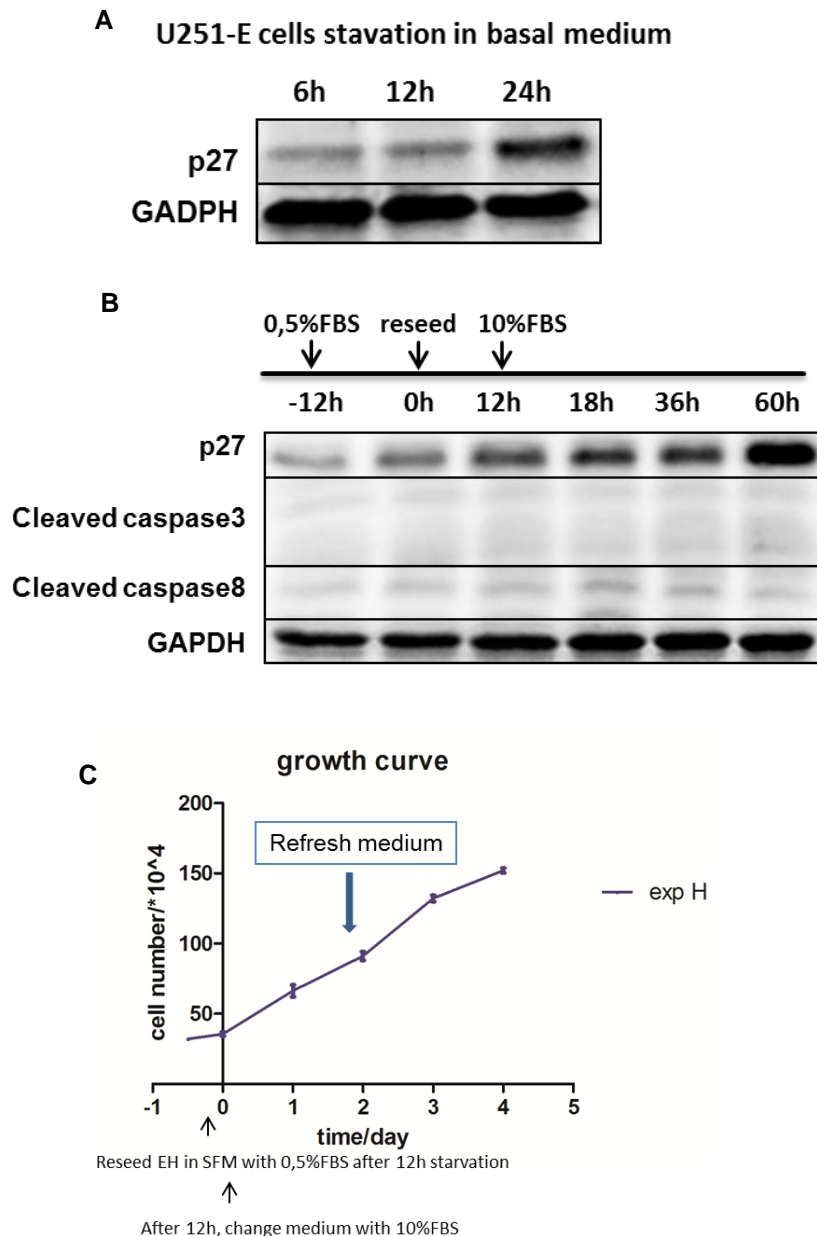


Figure 13. **Effect of P27 upregulation on cell apoptosis.** A. Western blot analysis of p27 and p-ERK with GAPDH as control. U251-E cells were cultured in basal RPMI medium for 6h, 12h and 24h. B. Western blot analysis of p27, cleaved caspase 3 and cleaved caspase 8 with GAPDH as control. U251-E cells in basal medium with 0.5% FBS were starved for 12h and re-seeded at high density. After 12h, medium was changed with 10% FBS as 0h and cells were collected at the indicated time points. C. Growth curve of EH cells after starvation. Results are shown as means \pm SE from three independent experiments.

3.2 The balance between ERK1/2 and JNK activation in parent cultures

3.2.1 ERK1/2 activation in parent cultures

Since downregulation of activated ERK1/2 preceded caspase activation at 48h, the assumption was made that programmed cell death after exponentially growing cells reseeded at high cell density might be induced by downregulation of p-ERK1/2, causing blockage of cell entry into mitosis. In order to explore the underlying mechanisms of downregulation of activated ERK1/2 after re-plating of exponential growth cells at high density, ERK1/2 activation in U251-P and U251-E cells was detected by western blots.

Firstly, parent cell cultures were tested by harvesting from attached monolayer culture or cell lysis after cell detachment. Western blots showed low activation of ERK1/2 and upregulated expression of p27 in U251-P cells by directly scraping cells from substrate (Figure 14). Interestingly, cells in U251-P had a robust activation of ERK1/2 immediately after loss of cell adhesion while the high level of p27 expression was not affected. When cells were treated with different incubation time of trypsin/EDTA, the strong activation of ERK1/2 was still observed in U251-P cells (Figure 14). On the other hand, U251-E cells showed a higher basal level of ERK1/2 activation and low p27 expression when directly scraping cells from substrate, indicating the mitogenic signature of proliferating cells. However, the levels of activated ERK1/2 remained unchanged after cell detachment using different incubation time or concentrations of trypsin/EDTA (Figure 14).

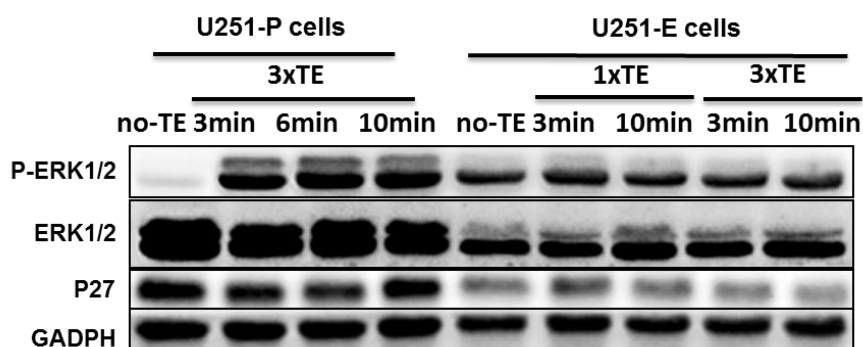


Figure 14. **ERK1/2 activation after cell detachment by trypsinization in parent cell cultures of U251 cells.** U251-P and U251-E cells were directly scraped from substrate (no-TE) or trypsinized with different incubation time or concentrations of trypsin/EDTA (TE). The expression of p-ERK1/2, ERK1/2 and p27 was detected by western blots with GAPDH as control.

Next, the effect of cell detachment in a long time course on ERK1/2 activation was tested. U251 cells in both phases were detached by trypsinization and kept re-suspended in fresh medium. Lysate collected immediately after trypsinization was referred as 0h. Cells in suspension were incubated for indicated time points when lysates were harvested. In U251-P cells, upregulation of ERK1/2 activation was seen immediately after cell detachment and sustained for at least 6h in suspension. The activation of ERK1/2 in U251-E cells remained high after cell detachment but decreased in cell suspension incubated for 1h (Figure 15). To be noted, FAK phosphorylation at Y397 was undetectable after loss of adhesion in both parent cultures (Figure 15). This result was consistent with other findings that phosphorylation of FAK at Y397 required cell attachment [164], further suggesting that activation of ERK1/2 is FAK independent.

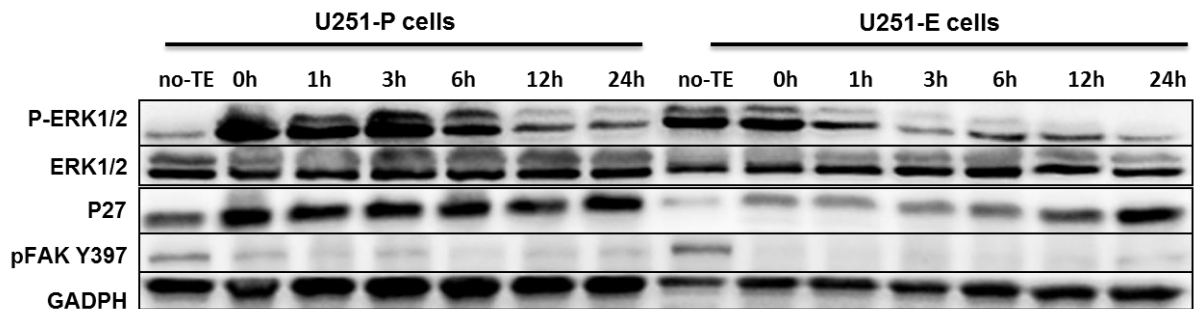


Figure 15. **ERK1/2 activation in suspension after detachment in parent cell cultures of U251 cells.** U251-P and U251-E cells were directly scraped from substrate (no-TE) or trypsinized and incubated in suspension for indicated time points. The expression of p-ERK1/2, ERK1/2, p27 and p-FAK was detected by western blots with GAPDH as control.

Finally, in order to test whether upregulation of ERK1/2 activation was an artifact of trypsinization, different agents were used for cell detachment. Collagenase IV is believed to be relatively gentle to preserve the integrity of cell membrane receptors [165]. Different agents were used for cell detachment, including 3xTE, 0.25% trypsin, 0.06% EDTA and 200U/ml collagenase IV. As shown in Figure 16, ERK1/2 activation was not affected using different agents for cell detachment, suggesting that it was due to loss of cell attachment rather than an artifact of trypsinization (Figure 16). Taken together, these results demonstrated a fundamental difference in ERK1/2 regulation in U251-P and U251-E cells.

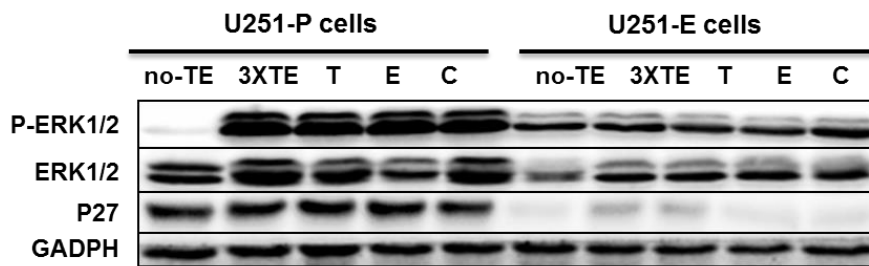
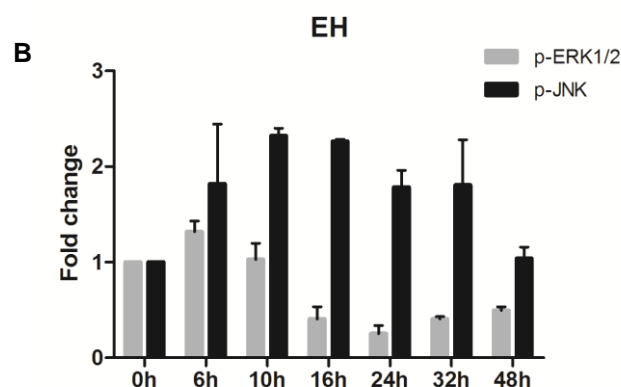
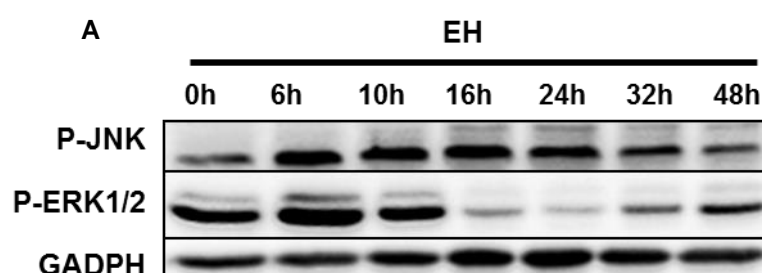


Figure 16. **ERK1/2 activation after cell detachment using different agents in parent cell cultures of U251 cells.** U251-P and U251-E cells were directly scraped from substrate (no-TE) or detached with different agents. The expression of p-ERK1/2, ERK1/2 and p27 was detected by western blots. GAPDH as control. 3xTE: 0.15% trypsin and EDTA; T: 0.25% trypsin; E: 0.06% EDTA; C: 200U/ml Collagenase IV.

3.2.2 The regulation of ERK1/2 and JNK activation

JNKs have been identified to play context-dependent roles in both cell proliferation and apoptosis. To test if JNK was involved in apoptosis in EH cells, JNK activation was detected. Harvesting U251-E cells before re-seeding was referred as 0h. As shown in Figure 17A and 17B, the upregulated expression of activated JNK was inversely related to the decreased ERK1/2 activation in EH cells. However, activation of JNK was prevented by re-plating of starved U251-E cells at high density, accompanied by upregulation of ERK1/2 activation (Figure 17C). The results suggested that increased JNK activation along with decreased ERK1/2 activation was involved in cell apoptosis, which was inverted by upregulation of cell cycle regulator p27.



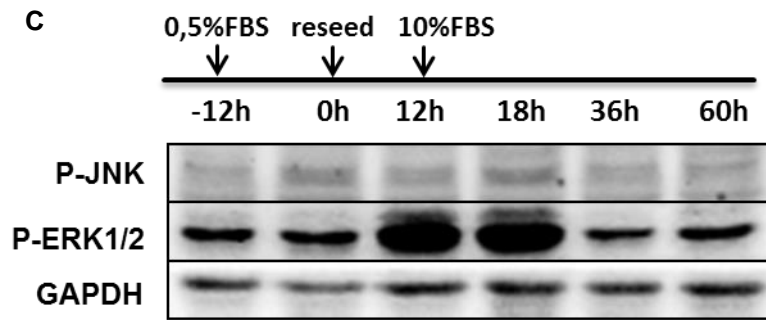


Figure 17. **JNK activation in EH cells.** A. Western blot analysis of p-ERK1/2, p-JNK with GAPDH as control. After re-plating U251-E cells at high density, cells were harvested at different time points. B. Densitometric analysis of the western blot intensity of the indicated proteins shown in Fig.17A, normalized to GAPDH. 0h was used as reference. Results are shown as means \pm SE from two independent experiments. C. Western blot analysis of p-ERK1/2, p-JNK with GAPDH as control. U251-E cells in basal RPMI medium with 0.5%FBS were starved for 12h and re-seeded at high density. After 12h, medium was changed with 10%FBS as 0h and cells were collected at the indicated time points.

Next, JNK and ERK1/2 activation were investigated in U251 parent cultures. U251-E and U251-P cells were exposed to conditioned medium (CM) from detached and attached cells. Western blots showed that U251-P cells had upregulated ERK1/2 activation but not JNK when exposed to CM from detached U251-P cells, while no striking upregulation of ERK1/2 or JNK activation was observed when exposed to CM from attached U251-P cells (Figure 18A, B). In contrast, U251-E cells exposed to CM from detached U251-E cells exhibited downregulation of p-ERK1/2 while expression of JNK activation was upregulated, which was not seen when exposed to CM from attached U251-E cells (Figure 18C, D). The results indicated that a transferrable factor in CM from detached U251-P cells upregulated ERK1/2 activation, while factors in CM from detached U251-E cells inhibited ERK1/2 activation but induced JNK activation resulting in apoptosis.

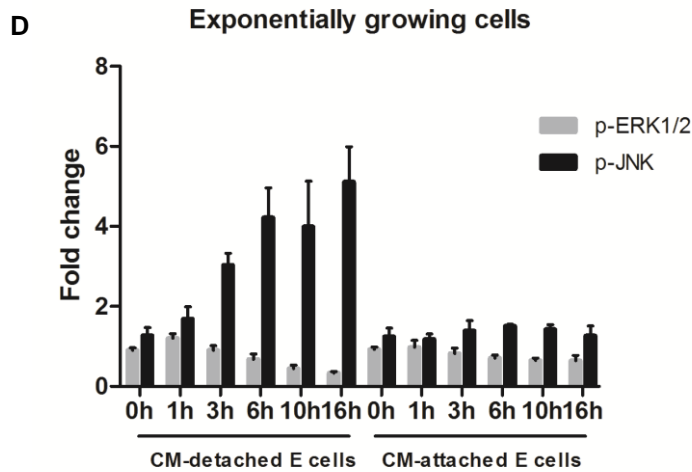
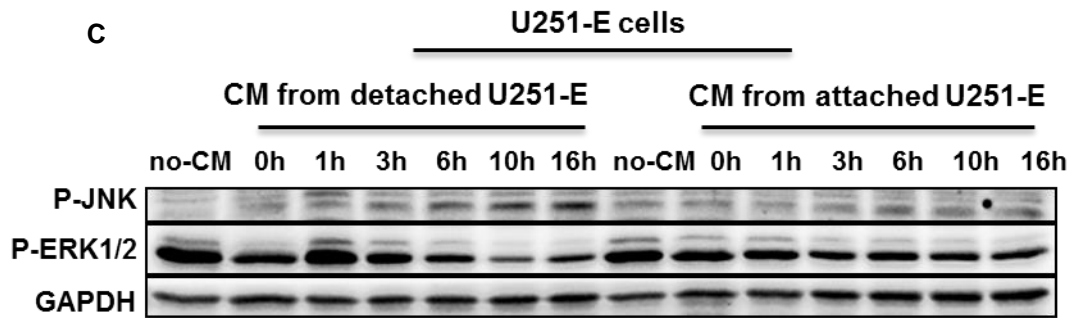
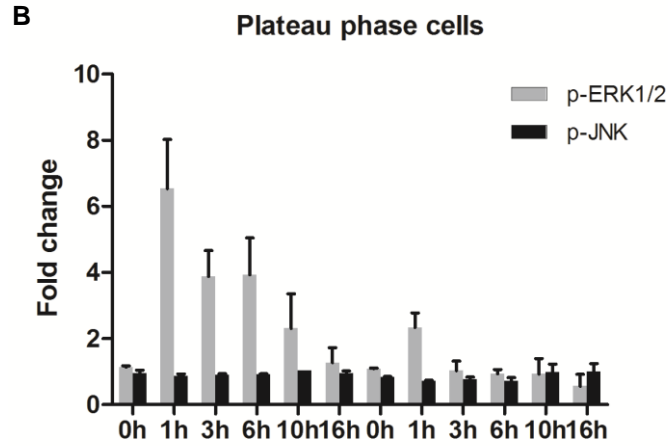
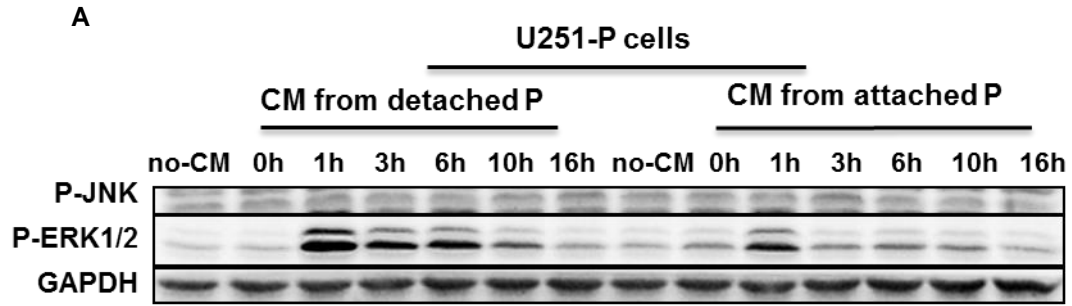


Figure 18. **JNK and ERK1/2 activation in parent cell culture.** A. Western blot analysis of p-JNK and p-ERK1/2 in U251-P cells exposed to conditioned medium from detached U251-P cells and attached U251-P cells at the indicated time points. Cells were harvested by scraping from the plates. no-CM: cells without medium change; 0h: lysates collected after immediately medium change. 1h-16h: cells were harvested after incubation with medium change for indicated time points. B. Densitometric analysis of the western blot intensity of the indicated proteins shown in Fig.18A, normalized to GAPDH. no-CM was used as reference. Results are shown as means \pm SE from two independent experiments. C. Western blot analysis of p-JNK and p-ERK1/2 in U251-E cells exposed to conditioned medium from detached U251-E cells and attached U251-E cells at the indicated time points. D. Densitometric analysis of the western blot intensity of the indicated proteins shown in Fig.18C, normalized to GAPDH. no-CM was used as reference. Results are shown as means \pm SE from three independent experiments.

To further investigate which pathway or transferrable factors might be involved, different inhibitors were applied. U251-P cells were incubated with original medium (no-CM), basal RPMI1640 medium with 1% BSA (BSA) or conditioned medium from detached U251-P cells (CMD). Then 10 μ M MEK inhibitor U0126, 10 μ M EGFR inhibitor Erlotinib and 10 μ M IGF-1R inhibitor AG1024 were added to medium, respectively. Cells were harvested after 1h incubation. 0.1% DMSO was used as control. Western blots showed that CMD-induced ERK1/2 upregulation was abolished by MEK inhibitor U0126 but the other two inhibitors had no effect (Figure 19A, B). These results suggested ERK1/2 activation in detached U251-P cells was mediated via intracellular signaling to MEK and ERK1/2 in an autocrine mechanism rather than EGFR nor IGF-1R signaling pathway.

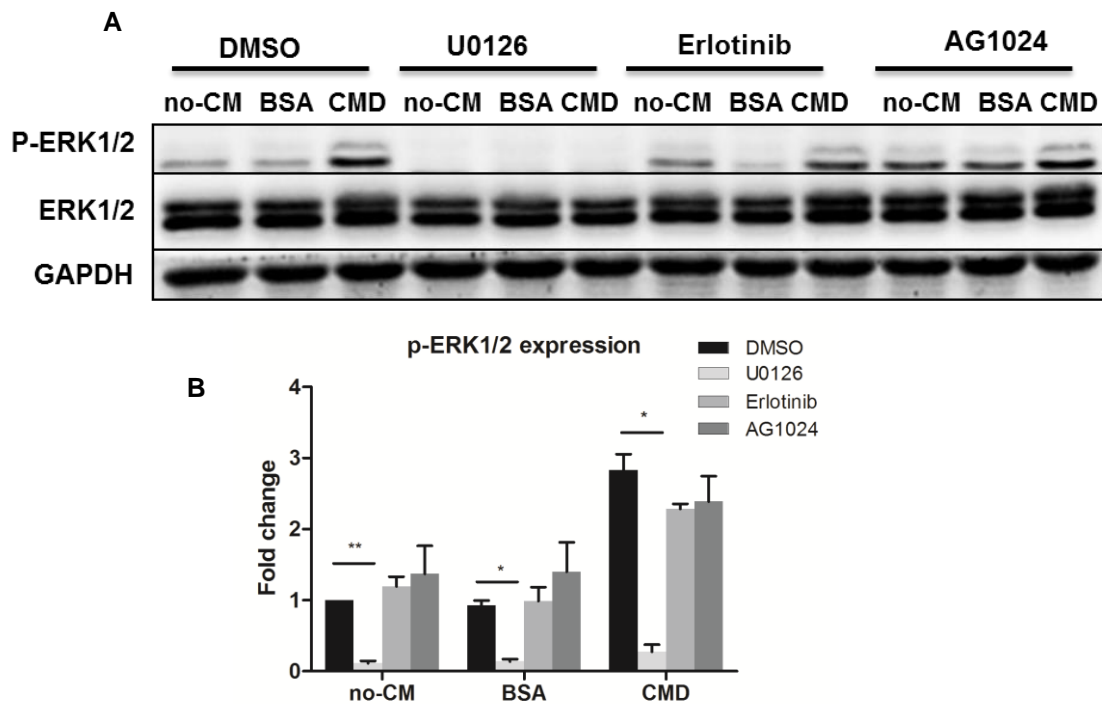


Figure 19. **ERK1/2 activation induced by CMD in plateau phase cells.** A. Western blot analysis of p-ERK and ERK with GAPDH as control. U251-P cells exposed to CMD with or without 10 μ M U0126, Erlotinib and AG1024. 0.1% DMSO was used as control. Cells were harvested by scraping from the plates. no-CM: cells without medium change; BSA: U251-P cells exposed to basal RPMI1640 medium with 1% BSA; CMD: U251-P cells were detached by 3xTE and re-suspended in basal RPMI1640 medium with 1% BSA. Conditioned medium was collected after 1h incubation. B. Densitometric analysis of the western blot intensity of the indicated proteins shown in Fig.19A, normalized to GAPDH. no-CM was used as reference. Results are shown as means \pm SE from three independent experiments. * represents $P < 0.05$; **represents $P < 0.01$.

U251-E cells were incubated with conditioned medium from detached U251-E cells. 10 μ M Erlotinib and AG1024 were added to medium respectively and 0.1% DMSO was used as control. Cells were harvested at different time points. As shown in Figure 20, CM from detached U251-E cells induced increased expression of p-JNK and IGF-1R inhibitor AG1024 significantly inhibited JNK activation ($P < 0.05$). However, EGFR inhibitor Erlotinib had no effect. The results suggested that JNK activation is partially mediated via IGF-1R signaling in exponentially growing cells and may be involved in apoptosis after re-seeded at high density.

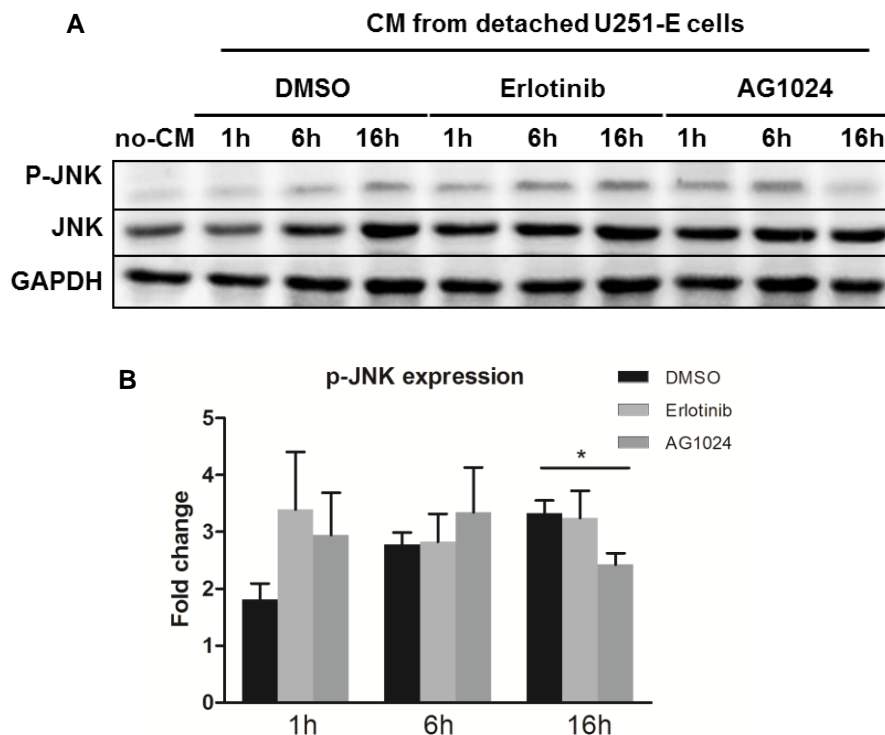


Figure 20. **JNK activation induced by CMD in exponential growth phase cells.** A. Western blot analysis of p-JNK and JNK with GAPDH as control. U251-E cells were exposed to CM with or without 10 μ M Erlotinib and AG1024 for indicated time points. 0.1% DMSO was used as control. no-CM: cells without medium change; CM from detached U251-E: U251-E cells were detached by 3xTE and re-suspended in RPMI1640 medium with 10% FBS. Conditioned medium was collected after 1h incubation. B. Densitometric analysis of the western blot intensity of the indicated proteins shown in Fig.20A, normalized to GAPDH. no-CM was used as reference. Results are shown as means \pm SE from four independent experiments. * represents $P < 0.05$.

3.3 Radiation response of U251 cells from different parent cultures

3.3.1 Clonogenic survival of U251 cells from different parent cultures

The previous data demonstrated different regulation of ERK1/2 and JNK activation after loss of attachment of U251-E and U251-P cells. Thus, it was assumed that such differences had effects on radiation response of U251 cells upon detachment. To characterize the radiation sensitivity of U251 cells from different parent cultures, colony forming assay was performed. As shown in Figure 21A, the clonogenic survival curves were very similar for immediate plating of cells from plateau and exponential growth phase. However, surviving fraction at 2Gy (SF2) in cells from U251-P was significantly higher than that in cells from U251-E (0.76 ± 0.02 vs. 0.66 ± 0.03 , $P < 0.01$), whereas no significance was found regarding surviving fraction at higher doses of 4-8Gy in two groups (Figure 21B, Table 13).

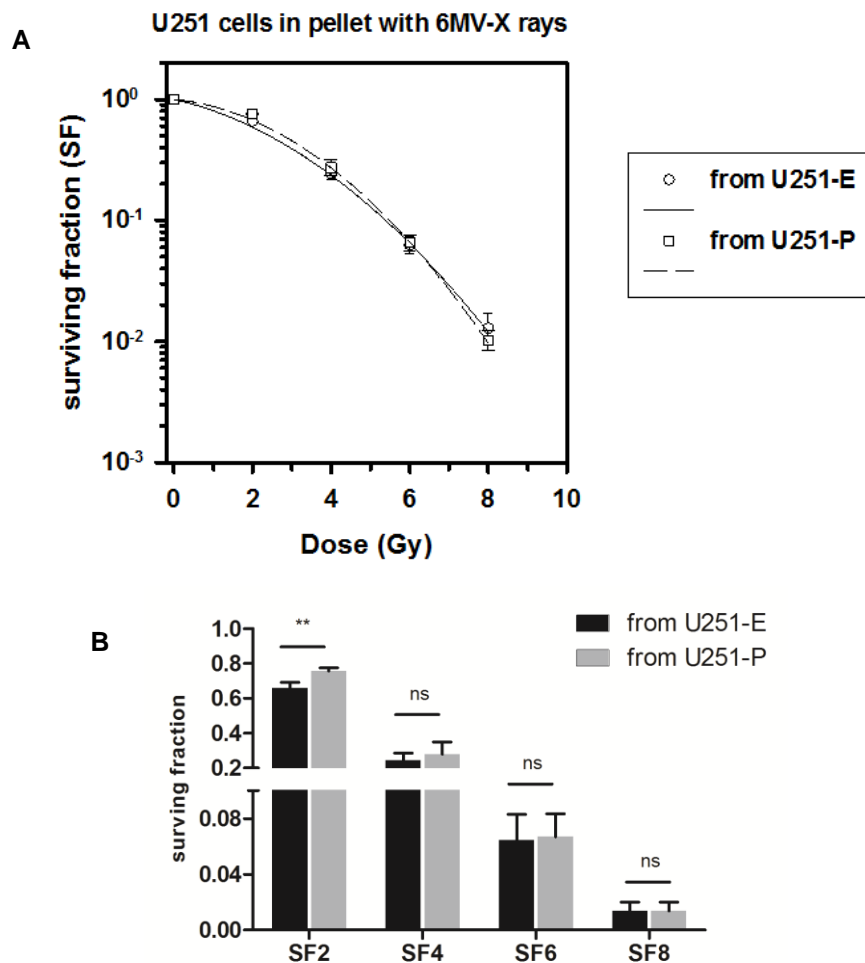


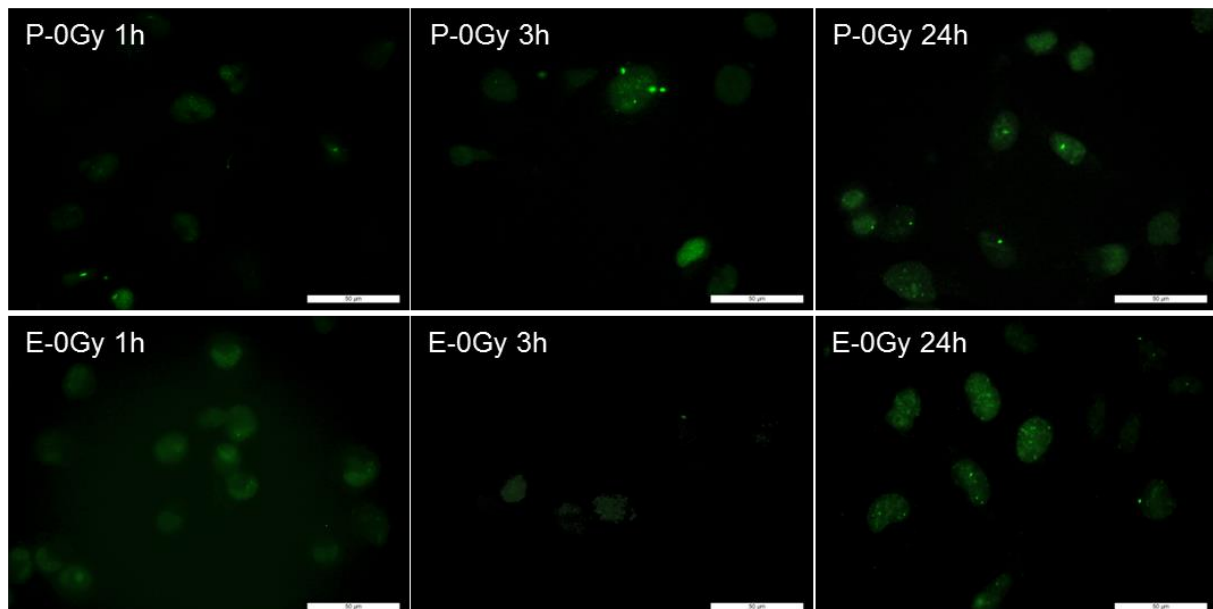
Figure 21. **Clonogenic cell survival curve of U251 cells from different parent cultures.** A. The surviving fraction of colony-forming U251 cells versus dose was fitted by LQ model in three independent experiments. B. Surviving fraction at different doses in both groups. ** represents $P < 0.01$. ns. represents $P > 0.05$. Results are reported as means \pm SD obtained from three independent experiments.

Table 13. Values of the coefficients, α and β , and SF obtained from the LQ model fitted survival curves

	from U251-E	from U251-P
α (Gy^{-1})	0.168 ± 0.038	0.072 ± 0.043
β (Gy^{-2})	0.048 ± 0.005	0.064 ± 0.005
SF(2)	0.66 ± 0.03	0.76 ± 0.02
SF(4)	0.25 ± 0.04	0.28 ± 0.07
SF(6)	0.06 ± 0.02	0.07 ± 0.02
SF(8)	0.01 ± 0.01	0.01 ± 0.00

3.3.2 Induction and decay of DSBs after irradiation

Next, DSBs repair capacity of U251 cells from different cultures was determined by detecting γ H2AX foci formation. The morphology at different time points after different doses of irradiation was shown in Figure 22. Without irradiation, U251 cells from both cultures showed a low background of foci per cell at each time point. Irradiation-induced foci formation was scored by subtracting the background of corresponding non-irradiated cells. The kinetics of induction and decay of γ H2AX foci were similar in each group. The majority of foci were formed 1h post irradiation and most of foci disappeared up to 24h in all groups (Figure 23A). However, the number of γ H2AX foci per cell was significantly higher in cells from U251-P than from U251-E induced at 1h and 3h after 2Gy irradiation (1h: 27.81 ± 2.62 vs. 19.96 ± 0.58 , $P < 0.01$; 3h: 22.52 ± 0.74 vs. 18.15 ± 1.16 , $P < 0.01$, respectively). After 24h, residual foci number did not significantly differ (3.70 ± 1.46 vs. 3.03 ± 0.99 , $P > 0.05$). The results suggested that more DSBs induced by 2Gy irradiation were repaired in cells from U251-P. When cells were exposed to a large dose of 8Gy, no significance of foci number per cell was observed (1h: 61.57 ± 2.89 vs. 58.98 ± 6.52 , $P > 0.05$; 3h: 57.54 ± 3.03 vs. 58.86 ± 6.52 , $P > 0.05$; 24h: 8.32 ± 1.59 vs. 7.24 ± 0.53 , $P > 0.05$, respectively) (Figure 23B).



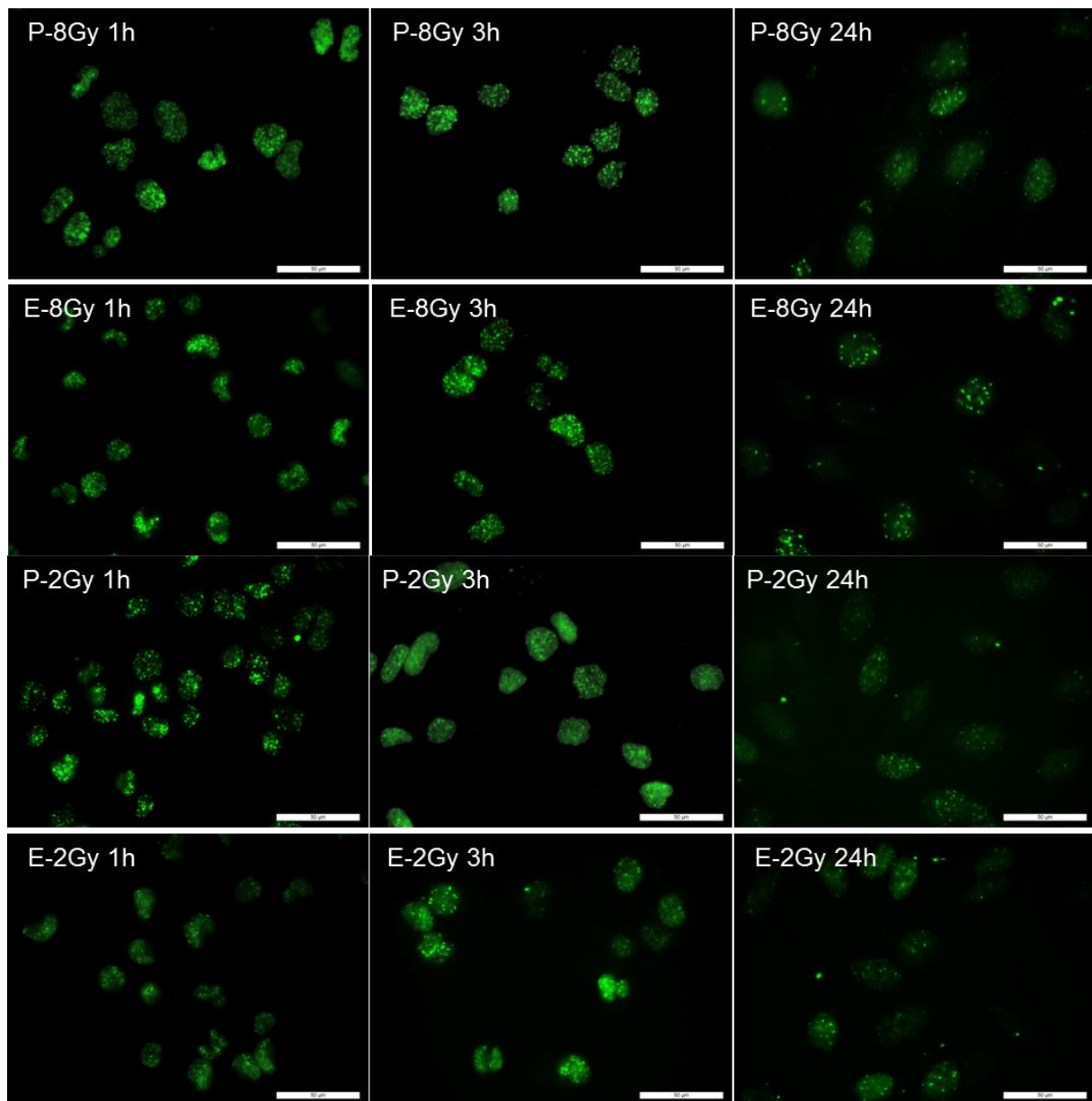


Figure 22. **Images of γ H2AX repair foci in different time points post irradiation in U251 cells from different parent cultures.** U251 cell pellets were exposed to 2Gy and 8Gy 6MV X-rays and seeded in 8 well chambers. Cells were fixed 1h, 3h and 24h after the end of irradiation. Scale bar=50 μ m.

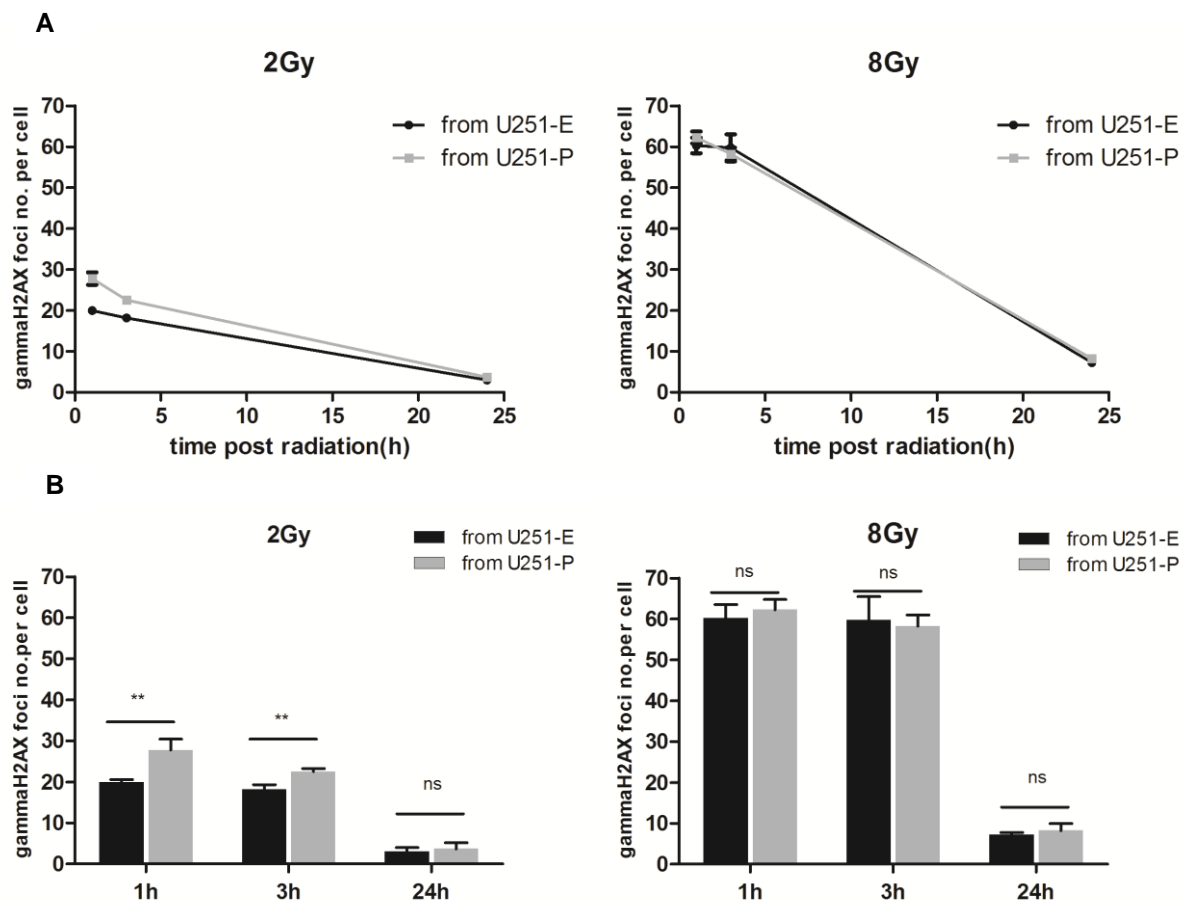
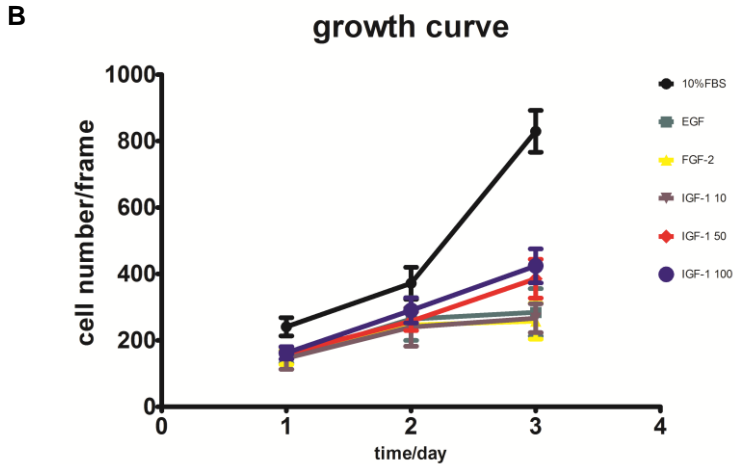
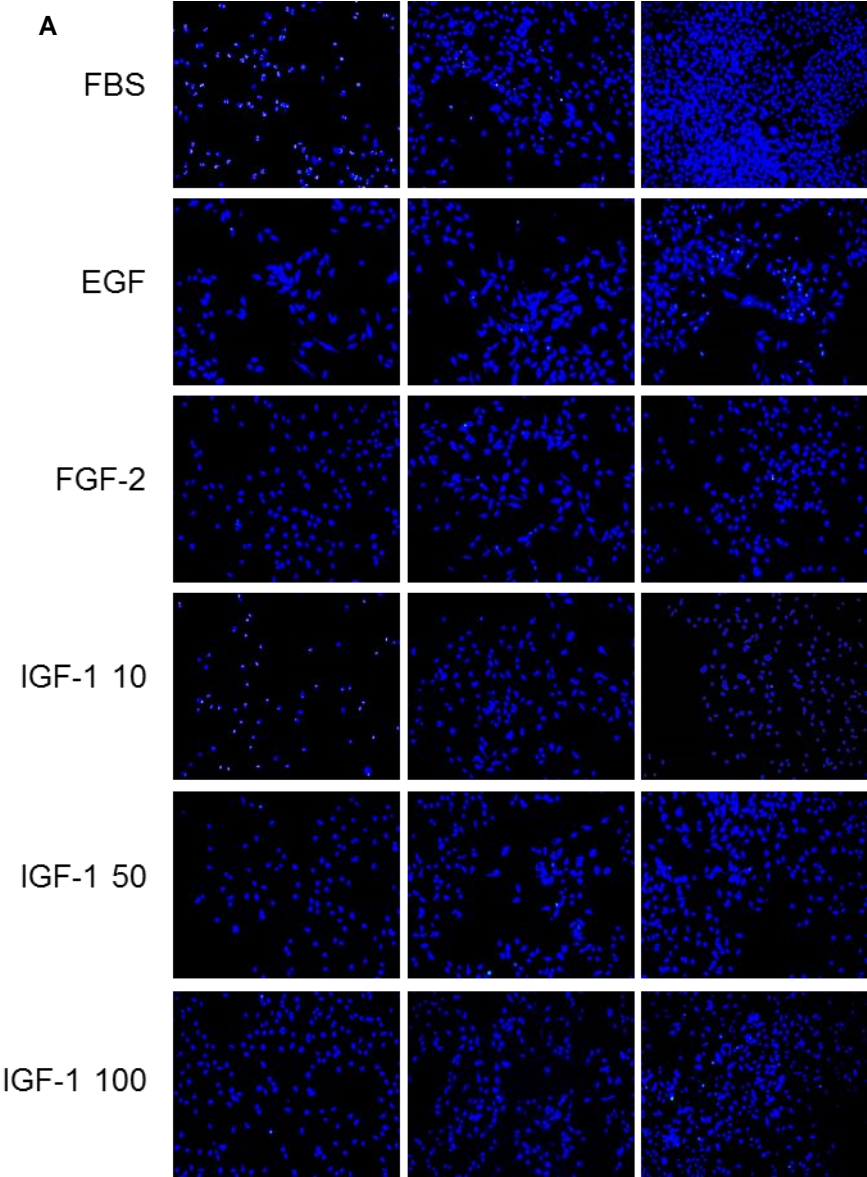


Figure 23. γ H2AX foci number per cell in response to irradiation. A. The kinetics of γ H2AX foci in U251 cells from different cultures exposed to 2Gy and 8Gy with 6MV X-rays. B. Analysis of γ H2AX foci number per cell in U251 cells from different cultures exposed to 2Gy and 8Gy with 6MV X-rays. For each condition in one experiment, 100 cells were scored to detect foci number per cell. Results are shown as means \pm SD from three independent experiments. ** represents $P < 0.01$; ns. represents $P > 0.05$.

3.4 Effect of different growth factors on proliferation of GBM cells *in vitro*

The results presented above and in the previous study by Wang et al. strongly suggest the growth and proliferation of glioblastoma cells are highly regulated processes which depend on growth states of parent cultures. This was further tested by characterizing minimal growth factor requirements of the U251 cells line and NCH644 primary cells.

Exogenous growth factor alone can barely support the proliferation of U251 cells when they were cultured in EGF and FGF-2 at 20ng/ml which is the proper concentration in medium of glioma stem cell, whereas IGF-1 showed dose-dependent stimulation of U251 cells (Figure 24A, B). Combining IGF-1 with FGF-2 resulted in proliferation approaching that seen for FBS in contrast with the combination of EGF and FGF-2 (Figure 24C, D).



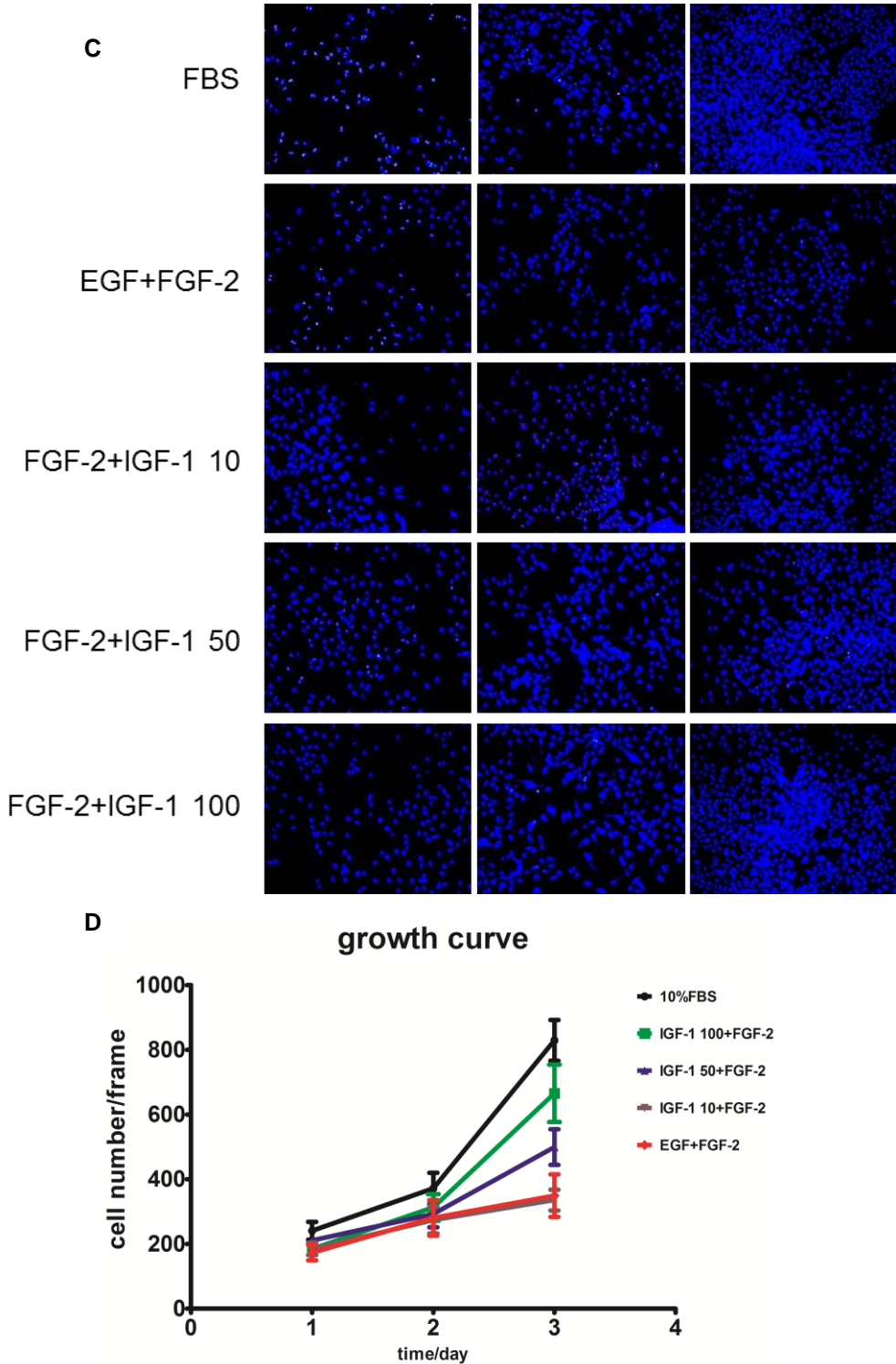
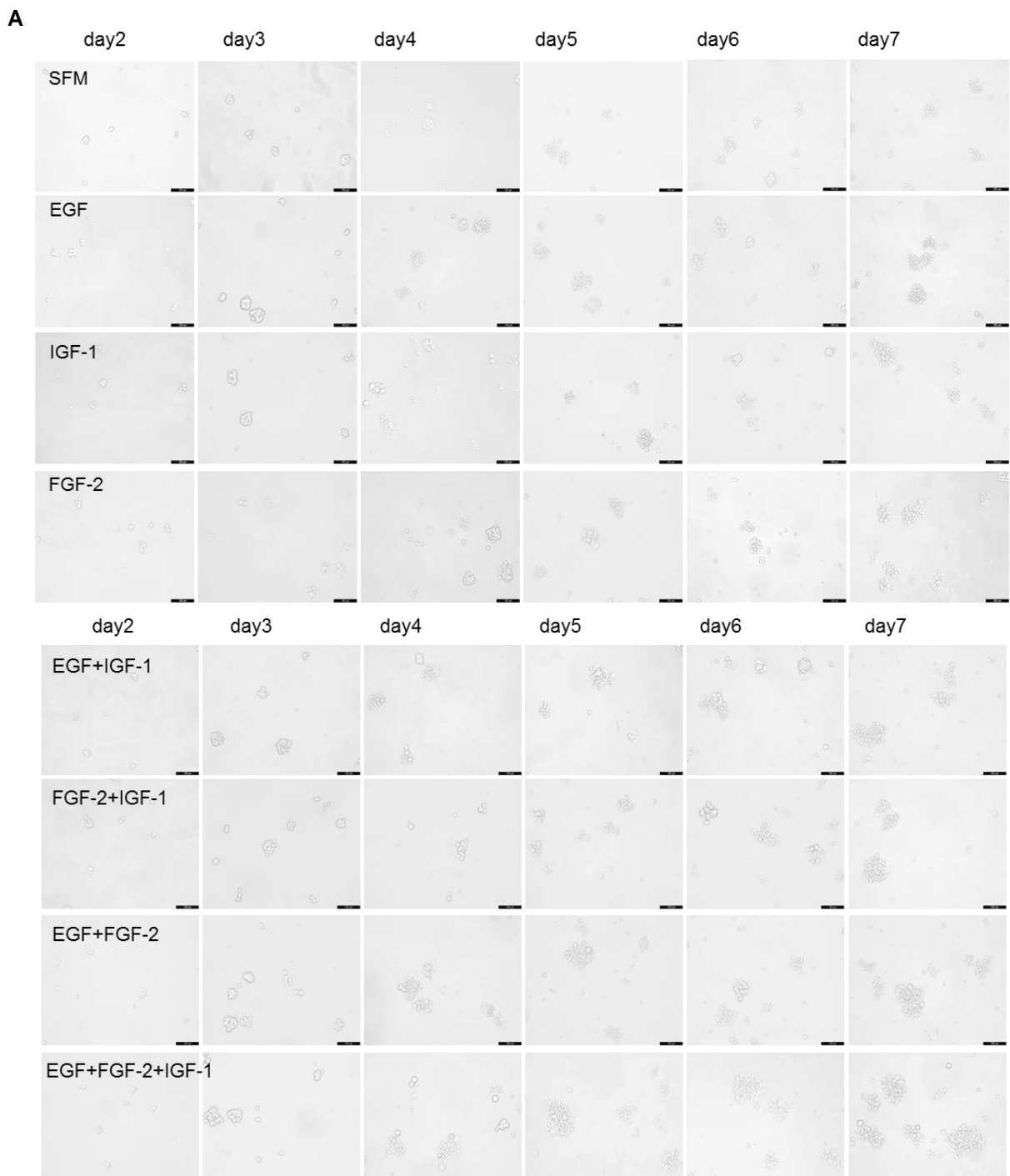


Figure 24. **Effect of different growth factors on proliferation of U251 cells.** A. Images of U251 cells cultured in single growth factors and 10% FBS. Nuclei were stained with DAPI. Scale bar=200µm. B. Growth curve of U251 cells cultured in single growth factors and 10% FBS. C. Representative images of U251 cells in combined growth factors and 10% FBS. Nuclei were stained with DAPI. D. Growth curve of U251 cells stimulated in different combinations of growth factors compared with 10% FBS. Results are shown as means ± SE from three independent experiments.

Results

The human stem cell-like glioma NCH644 cells grew in defined serum-free medium and were passaged by mechanical dissociation. Although single growth factor only supported moderate proliferation, FGF-2 was slightly more effective than EGF and IGF-1 (Figure 25A, B). However, combining all three growth factors supported efficient proliferation while the combination of FGF-2 and EGF was better than other combinations of two growth factors (FGF-2+IGF-1 or EGF+IGF-1: Figure 25C,D). Notably, slow proliferation occurred even in the absence of growth factors in serum-free medium.



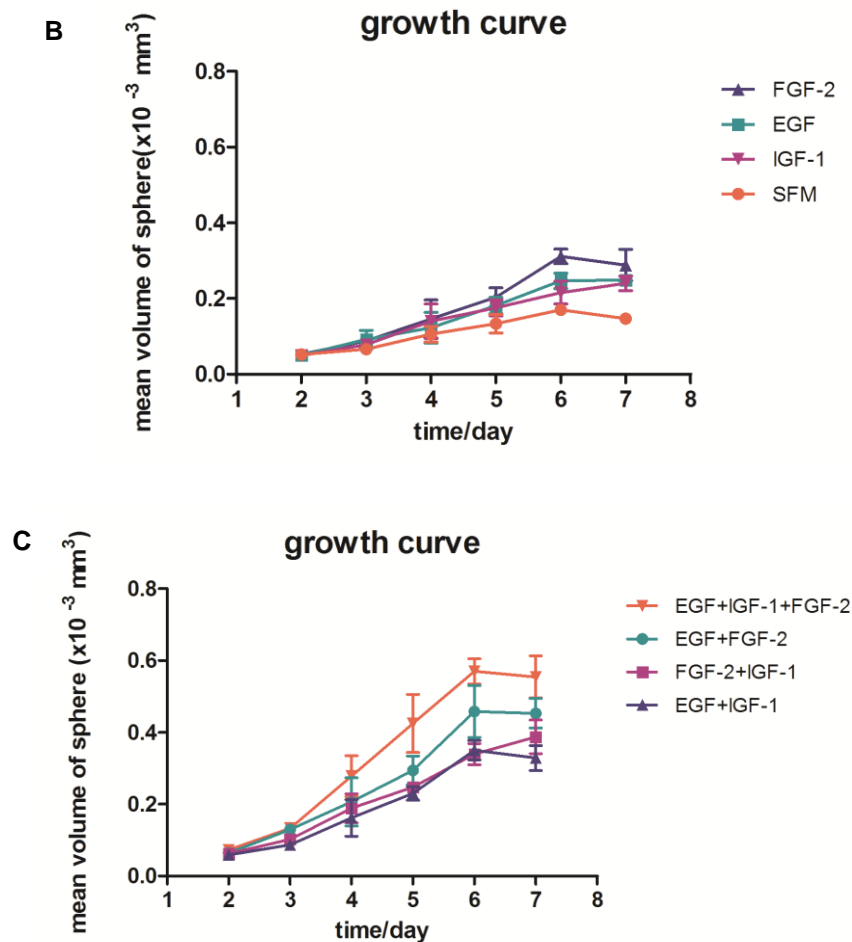


Figure 25. **Effect of different growth factors on proliferation of NCH644 cells.** A. Images of NCH644 cells in different growth factors. Scale bar=100 μ m. B. Growth curve of NCH644 cells cultured in single growth factor. C. The growth curve of NCH644 cells cultured in different combinations of mitogens. Results are shown as means \pm SE from three independent experiments.

3.5 Contact inhibition retained in glioblastoma cells *in vitro*

As shown above cells in plateau phase cultures showed low ERK1/2 activation but high levels of p27 expression (Figure 14). This inverse relationship suggested that some degree of density arrest may remain operative in U251 cells. Low numbers of U251 cells and U87 cells were seeded in clonal cultures, and cultured for several days to form colonies. Cells were stained with proliferative marker Ki67 and nuclear was counterstained with DAPI. In the colonies, Ki67 was expressed mainly in cells at the periphery, supporting the hypothesis that cell-cell contact in the inner part of the colony inhibits cells proliferation. Similar results were obtained with colonies formed by U87 cells (Figure 26).

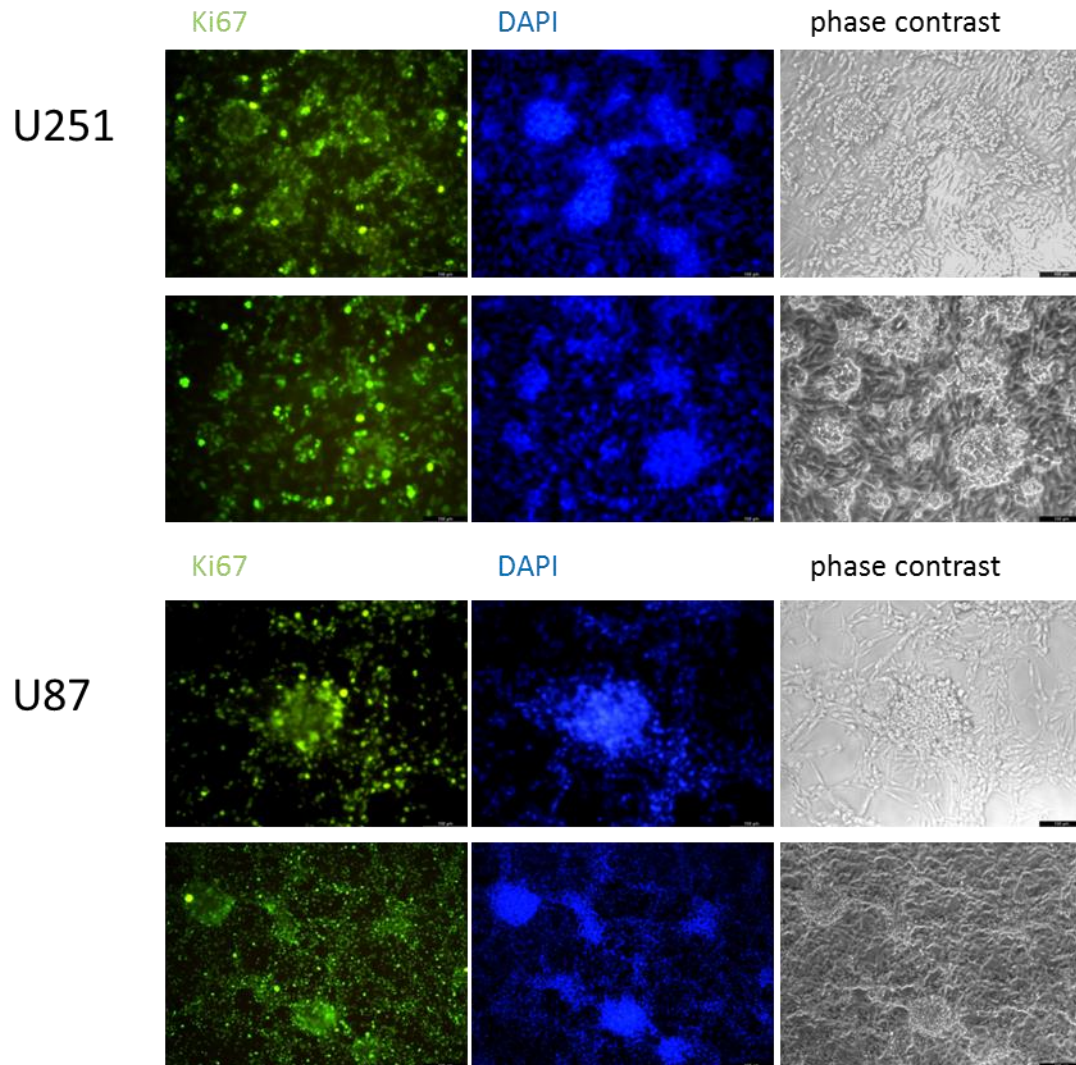
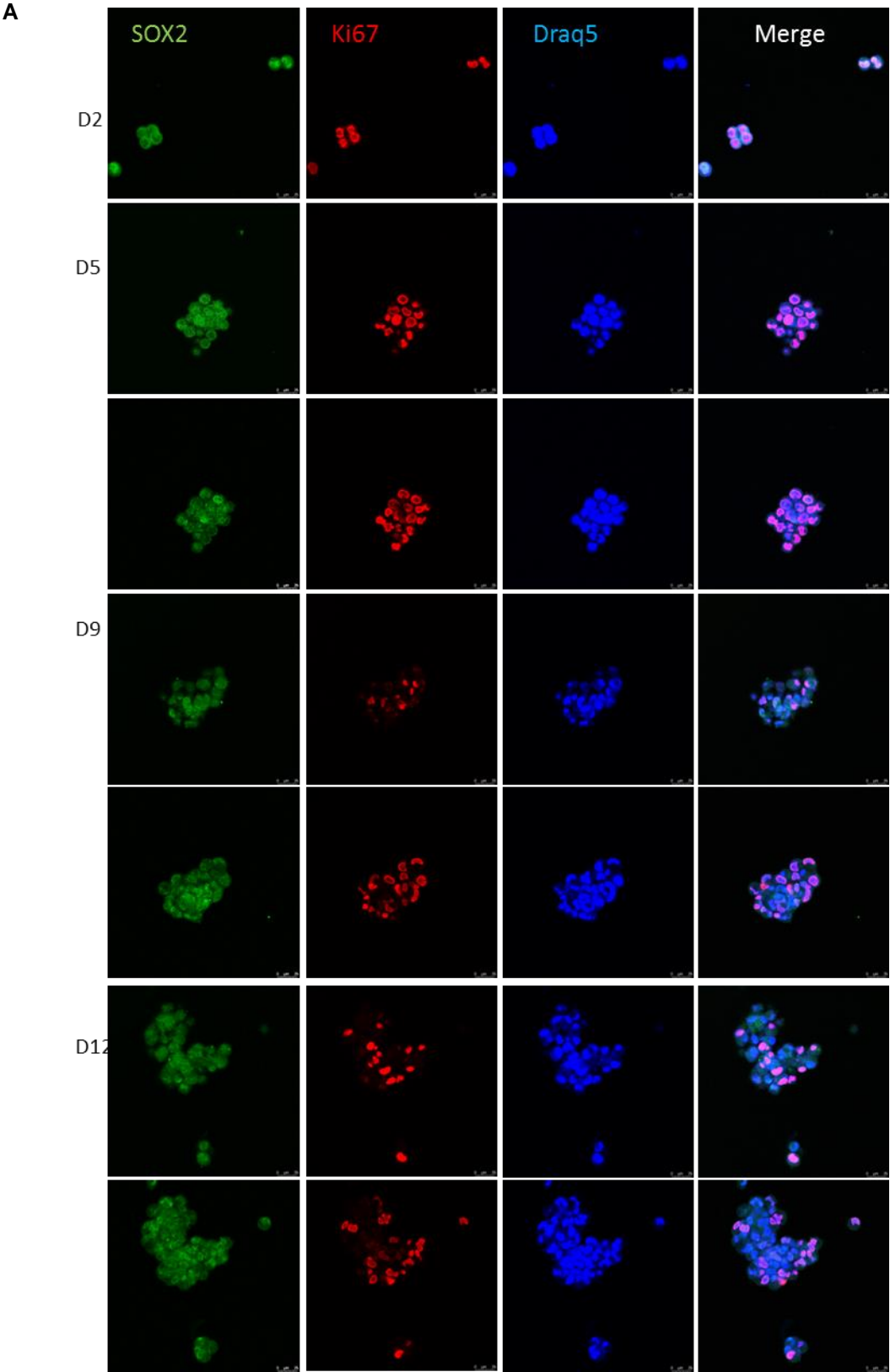


Figure 26. **Immunostaining of U251 and U87 colonies.** Colonies of U251 and U87 cells were stained with Ki67 and nuclei counterstained with DAPI. Scale bar=100 μ m.

Because cells in spheres show more cell-cell contacts growing surrounded by other cells in all directions compared with adherent cell culture, the experiment was also conducted with U251 spheres cultured in defined serum-free medium containing EGF and FGF-2. Single stem-like U251 cells were seeded and cultured as spheres which were harvested at the indicated time points. After 12 days of culture, spheres were split into single cells and re-seeded. Cells were stained with stem cell marker SOX2 and proliferative marker Ki67. On day 2 and day 5, spheres were small and most of cells were Ki67 positive. On day 9 and day 12, the proportion of Ki67 positive cells was decreased in large spheres and Ki67 negative cells were observed mainly in the inner part of spheres. Cells positive for the stem cell marker SOX2 were found in both Ki67 positive and negative cells in the spheres (Figure 27A). However, re-plating of dispersed large spheres at lower density resulted in upregulation of Ki67 in the small

spheres but again Ki67 negative cells were detected in the inner part of large spheres where cells were SOX2 positive (Figure 27B)



B

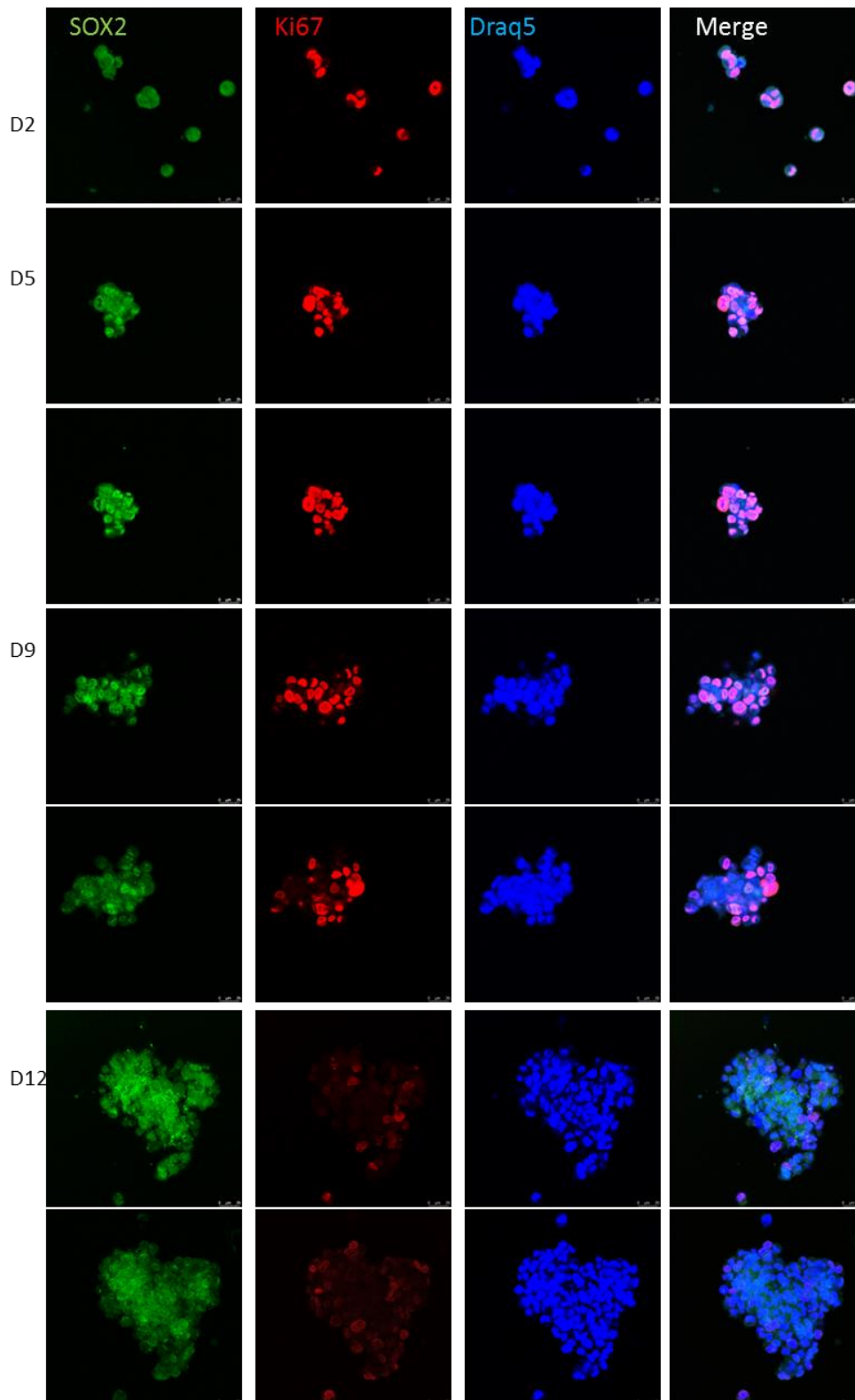
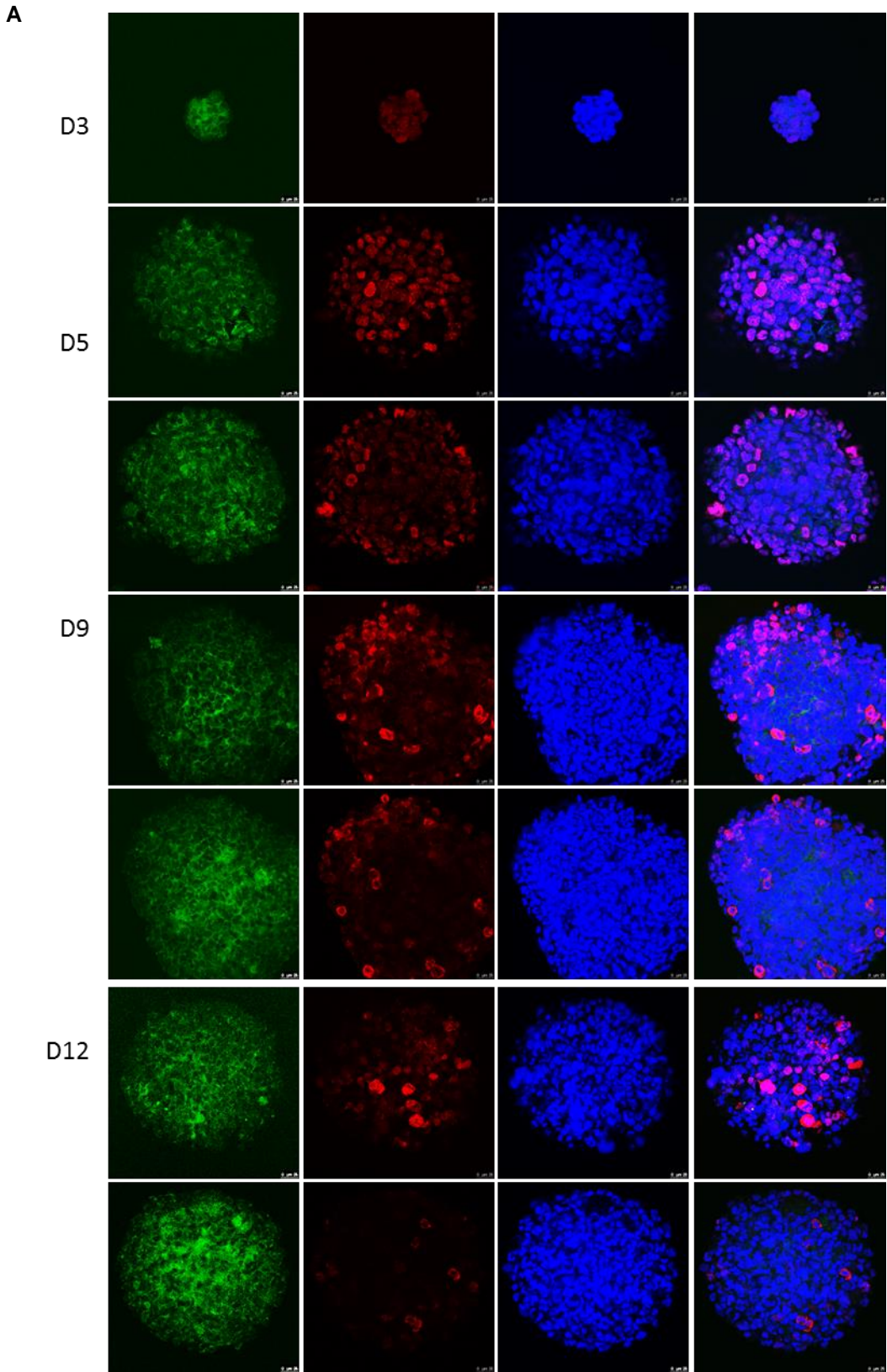


Figure 27. **Immunostaining of U251 spheres.** A. Images of U251 spheres after seeding single cells in defined serum-free medium. Spheres were collected on day 2, day 5, day 9 and day 12 and labelled with SOX2 and Ki67 and nuclei counterstained with Draq5. B. Images of U251 spheres after re-plating single cells from the dissociated spheres. Spheres were collected on day 2, day 5, day 9 and day 12 and labelled with SOX2 and Ki67 and nuclei counterstained with Draq5. Two different layers of the same sphere are displayed. Scale bar=25 μ m.

In order to see this phenomenon in primary glioblastoma, the experiment was repeated with primary NCH644 cells. Single NCH644 cells formed small neurospheres, in which all cells were Ki67 and CD133 positive. After 9 days of culture, Ki-67 positive cells were found predominantly near the surface of big neurospheres of these cells. Similar to SOX2 expression in U251 spheres, the stem cell marker CD133 positive staining did not co-localize with Ki-67 positive cells but was found also inside the neurospheres in areas with low Ki-67 (Figure 28A). After re-seeding neurospheres as single cells, cells in the smaller spheres expressed Ki67 and SOX2 but again CD133 was more pronounced in Ki-67 low areas (Figure 28B).



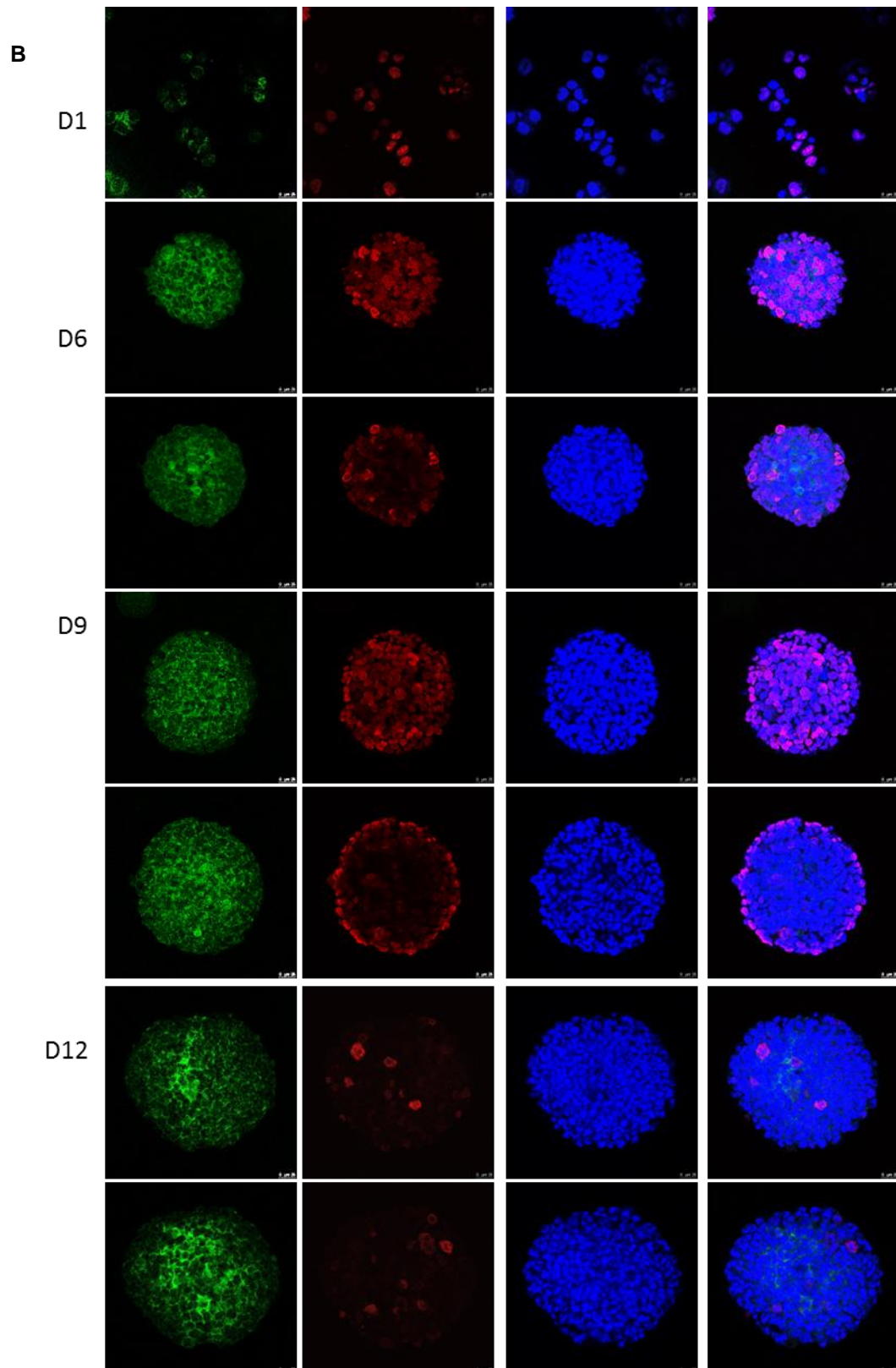


Figure 28. **Immunostaining of NCH644 neurospheres.** A. Images of spheres of primary NCH644 cells after single cells seeded. Spheres were collected on day 3, day 5, day 9 and day 12. Spheres were stained with CD133, Ki67 and Draq5. B. Images of spheres of primary NCH644 cells after re-plating single cells from the dissociated spheres. Spheres were collected on day 1, day 5, day 9 and day 12. Spheres were stained with CD133, Ki67 and Draq5. Two different layers of the same sphere were displayed. Scale bar=25µm.

4 DISCUSSION

GBM cells display the features of apoptosis resistance and aggressiveness due to loss of tumor suppressor genes *PTEN*, *RB* and *p53*, and amplification of growth factor receptors such as EGFR and IGF-1R [166, 167]. In addition, alterations of pro-survival and anti-apoptosis pathways play important roles in gliomagenesis and response to therapies [168]. In a previous study, Wang et al. have shown upregulation of mitogenic signaling when U251 cells were released from density-arrest plateau phase, even when they were re-seeded at high density, while this observation was not seen when exponential growth phase cells were re-seeded at high density. These results suggested ERK1/2 activity was influenced by changes in culture conditions including cell density as well as the growth state of parent culture. In agreement with their findings, a major result of the present study was that the strong mitogenic signaling led to increased proliferation upon re-plating of U251-P cells at high density, whereas ERK1/2 downregulation led to limited proliferation with cell apoptosis when re-plating of U251-E cells at high density. In addition, the mechanisms underlying ERK1/2 activation were investigated further. A fundamental difference of ERK1/2 and JNK regulation was observed in parent cultures, suggesting the balance of these two signaling pathways plays an important part in proliferation and survival of GBM cells. Besides, the present study highlighted the role of functional cycle-dependent kinase inhibitors in growth of GBM cells coordinated with mitogenic signaling.

4.1 Role of FAK in regulating apoptosis

It has been reported migrating glioma cells are less prone to apoptosis, which is attributed to the altered interaction with ECM and modifications of adhesion molecules [169]. The present results showed that re-plating of U251-E cells at high density resulted in limited proliferation accompanied by cell detachment, which was confirmed as apoptosis by caspase activation. The special type of programmed cell death with cell detachment is termed anoikis. Due to the association with cell integrin-ECM interaction, anoikis has been reported to be suppressed by activation of integrin signaling. In primary rat hepatocyte cultures, matrigel abolished spontaneous apoptosis with cell detachment, which was triggered by high density culture [170]. In GBM, integrin inhibition-induced glioma cell death with detachment can be rescued by the addition of recombinant transforming growth factor- β (TGF- β), which promotes

survival downstream of integrin signaling [171]. This cell matrix-dependent regulation of apoptosis may be mediated by FAK activation upon integrin binding to ECM. The importance of FAK signaling in anoikis suppression and cell survival has been documented. Kurenova et al. reported that FAK activation provided a survival signal by binding to the death domain kinase receptor-interacting protein [172]. Besides, Bouchard et al. showed FAK/SRC signaling can promote cell growth in a cell detached condition via activation of PI3K/AKT and MAPK/ERK1/2 signaling pathways [173]. In addition, activation of FAK induced by collagen type I has been reported to contribute to tumor migration, invasion and progression [174, 175]. However, in the present study, increasing FAK expression did not show the hypothesized suppressive effect on apoptosis when exponentially growing U251 cells re-plated at high density. The data suggested the downregulation of FAK was not the cause of apoptosis but the consequence of apoptosis-induced cell detachment. Moreover, downregulation of ERK1/2 was not reversed when cells seeded on ECM coated plates or adding exogenous growth factors, further indicating that FAK dysregulation was not responsible for decreased expression of p-ERK1/2. Although ERK1/2 has been suggested as a downstream effector of FAK signaling [176], the role of FAK regulating ERK1/2 activity still remains controversial. In normal fibroblasts, FAK activation was required for integrin-growth factor synergy pathway to activate ERK1/2 cascade [177]. Besides, enhanced FAK activation was observed to contribute to the adhesion and invasion of pancreatic cancer cells through ERK1/2 signaling pathway, when cells were plated on collagen type IV and stimulated with Interleukin-1 α [178]. In contrast, Barberis et al. proposed that FAK was not necessary for efficient tyrosine phosphorylation of Shc and activation of ERK1/2 upon matrix adhesion in primary fibroblasts [179]. The discrepancy could be attributed to cell type dependency as well as the compensation from other integrin-mediated downstream effectors including Pyk2 and p130Cas [180, 181]. Taken together, despite of some limitations regarding the efficiency of increasing FAK expression, the mechanism in this case is not FAK signaling dependent.

4.2 Role of ERK1/2 and JNK activation in GBM

4.2.1 Regulation of ERK1/2 and JNK

In the previous work, Wang et al. showed different basal levels of ERK1/2 activation after re-plating of U25 cells from plateau and exponential growth phase [91]. Thus,

when ERK1/2 activity was studied in parent cultures of U251 cells, a fundamental difference in ERK1/2 regulation was observed between different parent cultures. U251-P cells with low basal levels of ERK1/2 had strong ERK1/2 activation after loss of attachment and the strong ERK1/2 activation was sustained for several hours in suspension, which provided mitogenic signaling involved in the increased proliferation upon re-plating of U251-P cells at high and low density. Consistent with the present data, Al-Ayoubi et al. found ERK1/2 activation was strongly upregulated after cell detachment from substrate in ovarian cancer cell lines but not in benign ovarian cell lines [182].

Given that trypsin is reported to stimulate MAPK signaling pathway [183], the effect of trypsinization should be taken into account. As the major traditional cell removal method, trypsinization is pointed out to have effects not only on cell morphology but on ECM proteins remaining at cell surface [184]. There is evidence that cold trypsin can be used to quench cell signaling. In a cold trypsin-phosphorylation-specific flow cytometry protocol, the basal pERK1/2 levels remained low using cold trypsin compared with trypsinization at 37°C [185]. In order to test if ERK1/2 activation was an artifact of trypsinization, different agents for cell detachment were compared including collagenase IV which is considered to be relatively gentle to preserve the integrity of cell membrane receptors. Activation of ERK1/2 was not affected in both parent cultures, strongly supporting that activated ERK1/2 in U251-P cells was due to loss of cell attachment rather than trypsinization. This notion was also confirmed by other groups. Zhao et al. showed that Hippo signaling was activated following cell detachment within 10min by either trypsin or EDTA, while direct lysis of the attached cells had no effect [186]. Liu et al. demonstrated cell detachment by different enzymes, calcium depletion and mechanical methods resulted in activation of Notch1 signaling in non-small cell lung cancer cell lines as well as breast cancer MCF7 cells and prostate cancer LnCap cells [187]. These results indicated that numerous signaling pathways are activated after cell detached from ECM. The possible mechanism may be attributed to autocrine activation, cell-matrix interaction leading to the cleavage of receptors, or cytoskeleton organization [188]. The current results demonstrated that a soluble factor produced by detached cells might stimulate intracellular signaling to MEK and ERK1/2 in an autocrine fashion, consistent with the study by Al-Ayoubi et al. [182]. To be noted, blockage of EGFR and IGF-1R did not inhibit ERK1/2 activation, indicating neither pathway plays a dominant role in ERK1/2

regulation upon cell detachment. Several explanations are summarized as followed. First, Wang et al. found IGF-1R was responsible for FBS-induced ERK1/2 activation in U251 cells [91]. However, in this study, ERK1/2 activation was induced by conditioned medium from detached U251-P cells without FBS, in which case IGF-1R might have a minor effect. Thus, it is possible that the IGF-1R pathway mediates ERK1/2 activation in response to FBS, leading to mitogenic effects on U251 cell proliferation. Second, other vital signaling pathways may also be involved. In anoikis-resistant lung tumor cells, elevated Src activity was observed upon cell detachment, which was critical for cell survival in suspension. And Src activation may be mediated via PDGFR signaling [189]. Moreover, the crosstalk and compensatory effects of signaling pathways contribute to the complex ERK1/2 regulation. Therefore, the observation needs to be extended to find involved signaling pathways in ERK1/2 activation.

On the other hand, in the present study, the relative high basal level of p-ERK1/2 remained unchanged following loss of cell attachment but was decreased in suspension in U251-E cells. Although the detailed mechanism of ERK1/2 downregulation is not elucidated by now, lack of ERK1/2 activation in detached U251-E cells may contribute to anoikis after re-plating at high density. The critical role of ERK1/2 activation has been highlighted regarding the survival of cells after detachment. It has been reported that sustained MAPK/ERK1/2 activity was required for EGFR-dependent survival of keratinocytes in suspension culture [190]. In pancreatic cancer cells, enhanced ERK1/2 activity after cell detachment was essential for protecting cells from anoikis via regulating BCL-2 expression [191]. Moreover, since downregulation of activated ERK1/2 preceded activation of caspases 3 and 8, apoptosis may be induced by p-ERK1/2 downregulation causing blockage of cell entry into mitosis.

In contrast with ERK1/2 downregulation, JNK expression was upregulated when U251-E cells were re-seeded at high density, as well as when they were incubated with conditioned medium from detached U251-E cells. It has been shown that JNK is inactive in U251 cells [192]. Given the important role of JNK in stress-induced apoptosis, it was hypothesized that elevated JNK was involved in apoptosis after re-plating of cells at high density, which was further confirmed by the starvation experiment. After starvation, re-plating of U251-E cells at high density did not induce

apoptosis and JNK was not activated, further supporting the essential role of JNK in apoptosis. Next, the present results identified that JNK activation was probably, in part, mediated via IGF-1R pathway. However, the role of IGF-1R/JNK in induction of apoptosis remains controversial. Fan et al. indicated that activated JNK as a downstream growth signal of IGF-1R played a proliferative role in E₂-induced apoptosis in breast cancer cells [193]. Besides, other mechanisms mediating JNK activation have been documented. Yang et al. reported that Sef, a feedback inhibitor of FGFR signaling, activated JNK and apoptosis via TGF- β associated kinase /MKK4/JNK pathway, proving a role of FGFR signaling in JNK activation [194]. Moreover, Yu et al. showed that α -PDGFR signaling played a role in anti-transformation by activating JNK, critical for PDGF-regulation of apoptosis [195]. Other than RTKs, TNF receptor-associated factor 2 has been demonstrated to be involved in JNK mediated apoptosis through apoptosis signal-regulating kinase 1 /MKK/JNK signaling pathway [196]. Thus, it is necessary to further investigate the mechanisms underlying JNK activation.

It has been proposed that JNK and ERK1/2 play distinct roles in the context of apoptosis. Activation of JNK and inhibition of ERK1/2 were reported to be critical for induction of apoptosis, suggesting the balance between these two kinases is important in determining cell fate [197]. Based on the previous finding that IGF-1R was responsible for ERK1/2 activation which has a mitogenic effect, the current study showed that IGF-1R partially mediated JNK activation involving cell apoptosis. In total, the present results implied that the balance between mitogen-activated ERK1/2 and stress-activated JNK pathways mediated via IGF-1R regulated proliferation and survival of U251 glioblastoma cells.

4.2.2 Effect of ERK1/2 on radiation response

The clonogenic survival results showed that radio-sensitivity of cells from U251-P did not significantly differ from that of cells from U251-E. To be noted, cells from U251-P had a significantly higher surviving fraction at 2Gy compared with cells from U251-E (0.76 ± 0.02 vs. 0.66 ± 0.03 , $P < 0.01$), suggesting a more radio-resistant phenotype in cells from U251-P to some extent. The data of immunostaining with γ H2AX revealed higher capacity of DSBs repair in cells from U251-P when exposed to 2Gy. However, at high doses of 8Gy, no differences were found in two groups. One possibility may be the saturation of repair ability at high doses [198].

Cells from U251-P exhibited a relatively more radio-resistant phenotype, which may be the result from enrichment in G0/G1 phase of cell cycle and enhanced ERK1/2 signaling upon release from substrate. Substantial evidence revealed that ERK1/2 signaling plays an important role in regulating response to radio- and chemotherapy. Golding et al. addressed the requirement of EGFR/MEK/ERK1/2 signaling pathway for efficient DNA damage repair induced by irradiation, which contributed significantly to the increased radio-resistance in GBM [199]. In GBM cell line U87 and primary GBM cells, radio-sensitivity was promoted by a decrease of ERK1/2 activation following inhibition of hexokinase 2, while constitutive activation of ERK signaling rescued the increased DNA damage and enhanced radio-resistance [200]. Moreover, Marampon et al. reported that radiation treatment increased MEK/ERK1/2 pathway activation, which in turn contributed to radio-resistance in GBM cells [201]. In addition to radio-resistance, Sato et al. provided the evidence that ERK1/2 pathway mediated MGMT expression, leading to TMZ resistance via MDM2-p53 axis. Consequently, targeting ERK1/2 pathway by MEK inhibitor increased the sensitivity of stem-like glioblastoma cells to TMZ [202].

Concerning translational aspect, cells remaining at the edge of the cavity after tumor debulking can be regarded as cells from plateau phase. The enhanced MAPK/ERK1/2 signaling may contribute to radio-resistance and thus early recurrence. Thus, targeting IGF-1R/ERK1/2 signaling has potential clinical implications to overcome radio-resistance in the treatment of GBM (Figure 29).

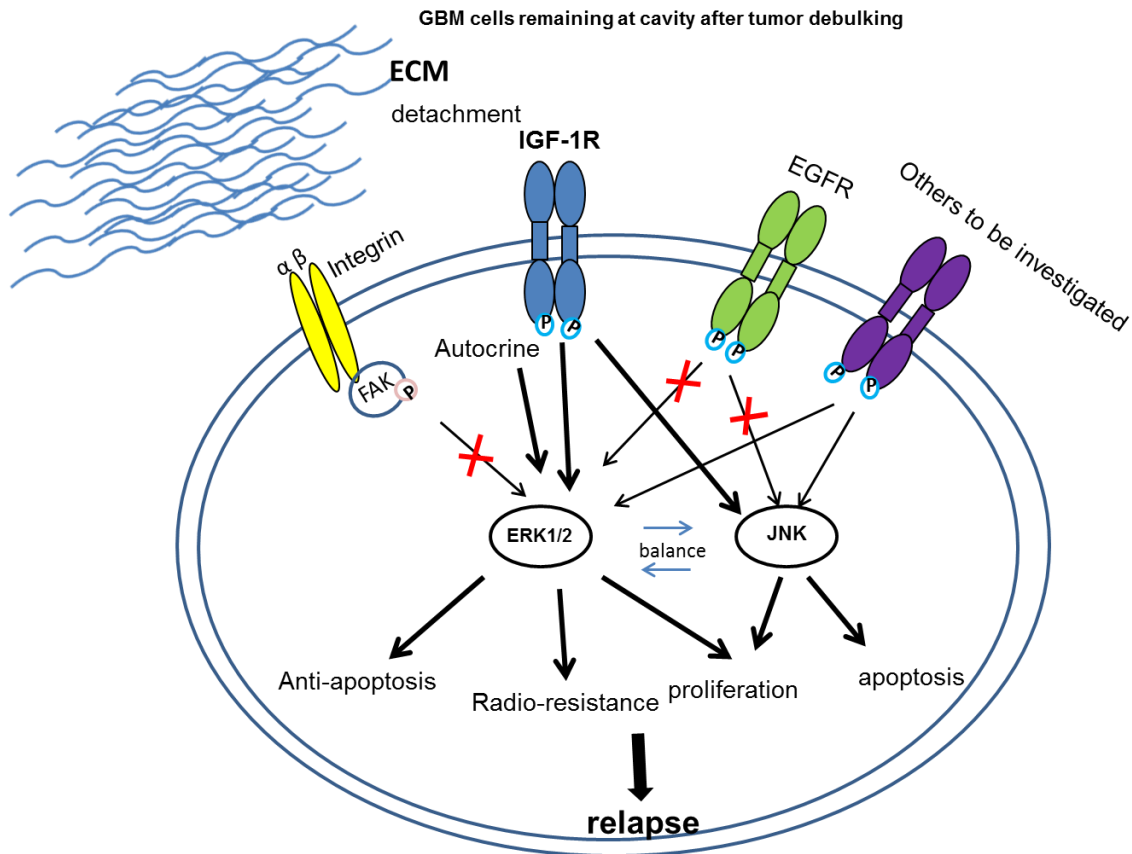


Figure 29. **Schematic illustrations of the balance of ERK1/2 and JNK pathways upon GBM cells detached from ECM.** Plateau phase cells detached from ECM resulted in enhanced ERK1/2 signaling pathway which can be mediated via autocrine mechanism and other RTKs. The balance between ERK1/2 and JNK signaling pathway plays vital roles in anti-apoptosis, radio-resistance and proliferation in GBM cells, leading to tumor relapse.

4.3 Role of cyclin-dependent kinase inhibitor p27

Cyclin-dependent kinase inhibitor p27 controls cell cycle progression through G1 phase. The absence of cell cycle checkpoint is a hallmark of tumor cells, which leads to uncontrolled proliferation [203]. Deregulation of p27 has been implicated in tumorigenesis and malignant progression in many cancers, and loss of p27 protein is frequently observed in various types of tumors [204, 205]. The current results implied the significant role of p27 as a cell cycle regulator in the regulation of GBM cells. The expression of p27 was elevated in U251-P cells but absent in U251-E cells. This contrasts with the findings by Fuse et al., in which U251 cells lacked the capacity of p27 induction [155]. However, another study assessed 12 established GBM cell lines including U251 cell line and found p27 expression was increased in all cell lines under the conditions of confluence or serum deprivation [206]. The expression of p27 can be also influenced by other unfavorable changes in microenvironment. In an

immunohistochemical analysis of human GBM, high levels of p27 expression were maintained in hypoxic areas present within the tumor [207].

Regarding the clinical value, it has been reported that low p27 expression was associated with poor prognosis and short survival in GBM patients [208], especially linked to cytoplasmic expression of p27 [209]. Therefore, restoring p27 expression has become a promising approach for GBM gene therapy. Komata et al. reported that overexpression of p27 by using recombinant adenoviral vectors suppressed cell growth in several GBM cell lines *in vitro* [210]. *In vivo*, Schiappacassi et al. showed that induction of p27 by adenoviral system inhibited GBM cell growth as well as local invasion and tumor induced neoangiogenesis [211]. When tumor suppressor gene *p27* was upregulated, GBM cell proliferation was inhibited *in vivo* and *in vitro* [212].

In addition to the tumor suppressive role, it has also been demonstrated that the absence of this cell cycle regulator has impacts on induction of apoptosis. In fibroblast, loss of p27 led to apoptosis and functional p27 expression was able to protect cells from apoptosis [213]. Therefore, in the current study, the cause of apoptosis might be associated with the absence of p27 in U251-E cells, causing uncontrolled cell cycle progression. Additionally, the necessity of functional p27 was also confirmed by the fact that induction of p27 by starvation of U251-E cells abolished apoptosis. A similar protective function of p27 was observed in other reports. Masuda et al. demonstrated that induction of p27 enabled small cell lung cancer cells to escape from apoptosis and supported cell survival under unfavorable culture conditions for cell growth [214]. In T98G GBM cells, downregulation of p27 expression induced apoptosis when S-phase kinase associated protein 2 was synergistically inactivated under conditions of growth factors deprivation [215]. These data revealed that the functional p27 is essential for cell survival not only in normal cells but also in GBM cells.

The presence of functional p27 in U251-P cells, and the large proportion of cells arrested in G1 with low-Ki67 expression in PH cells on day 3, suggested that GBM cells preserve a certain degree of contact inhibition. Therefore, the present data showed that cells in colonies or spheres had low Ki67 expressions while still kept their stem-like potential. This contact inhibition was reversible since cells re-proliferated after re-plating, which is in line with a recent study by Compos et al. [216]. By using label retention techniques in glioblastoma stem cells, they found

labelled cells with Ki67-low expression reacquired the ability to proliferate and form new colonies after re-plating. Moreover, quiescence of these labelled cells was mostly controlled by cell-cell contact inhibition. The underlying mechanisms of growth regulation may be mediated via several pathways. Notch signaling is reported to play a role in the control of contact inhibition in neuron [217]. Hippo-YAP signaling pathway as well as mTOR signaling pathway participated in regulation of reversible cell density arrest [218]. In addition, macrophage migration inhibitory factor was shown to mediate contact inhibition in GBM cells *in vitro*, providing a new insight into growth processes in GBM cells [219]. These findings supported that GBM cell proliferation is under proper regulation by functional cyclin-dependent kinase inhibitors.

4.4 Role of exogenous growth factors

The previous data by Wang et al. illustrated the important role of IGF-1R in the mitogenic signaling of U251 cells [91]. Thus, the requirement of growth factors including IGF-1 as essential components *in vitro* culture medium was further investigated. The present results demonstrated that single exogenous growth factors can barely support the growth of U251 cells when they were cultivated in the presence of EGF or FGF-2 alone. IGF-1 showed dose-dependent stimulation of U251 cell proliferation. Of note, the combination of IGF-1 and FGF-2 provided a growth advantage approaching that stimulated by FBS. These results further confirmed an essential role of IGF-1 in growth of GBM cells compared with EGF and FGF-2. In several *in vitro* studies, IGFs system plays important roles in the progression of GBM. Friend et al. pointed out that the addition of exogenous IGF-1 can stimulate the growth of several glioma cell lines including U251 cells which were not capable of endogenous IGF-I or IGF-II production [220]. Similarly, Schlenska-Lange et al. showed administration of IGF-1 but not IGF-2 enhanced proliferation and migration of other three glioma cell lines [221].

As another important mitogen, increased FGF-2 has been found in glioma compared with normal brain [69]. Loilome et al. showed FGF-2 had a growth stimulatory effect in 8 out of 10 GBM and GBM stem-like cell lines in concentration-dependent manner [222]. However, 100 ng/ml of FGF-2 resulted in a growth inhibitory effect in some GBM cell lines [222]. Combining FGF-2 with IGF-1 supported growth of U251 cells. This can be explained by the fact that FGF-2 interacts with the IGF pathway by

increasing IGF-1R expression, thus enhancing activity of IGF-1 ligand [223]. Moreover, it has been found that FGF-2 coordinated with IGF-1 to enhance proliferation of primary oligodendrocyte progenitors by synergistically regulating cell cycle progression past G1/S transition [224]. In NCH644 glioma stem-like cells, FGF-2 was slightly more effective than EGF and IGF-1. The critical role of FGF-2 has been implicated in GSC. It is well established that FGF-2, along with EGF, is a necessary supplement in culture medium of GSC *in vitro* [72]. Besides, of the two exogenous mitogens used in cell culture, FGF-2 had a stronger influence on growth of GSC than EGF [225, 226]. The insufficient effect of EGF on growth of GSC may result from loss of EGFR expression in the presence of EGF *in vitro* [226]. Furthermore, the addition of IGF-1 enhanced growth of NCH644 cells, indicating the stimulatory effect of IGF-1 on GSC. Arsenijevic et al. demonstrated that IGF-1 was essential for EGF/FGF-2 to promote proliferation of neural stem cells [81]. Aberg et al. showed that IGF-1 and FGF-2 were required for maximal proliferation and IGF-1 had impacts on generation of new neurons in adult hippocampus [227]. Substantial evidence revealed that FGF-2 and IGF-1 have cooperative effects on regulation and proliferation of stem cells *in vitro* [228, 229]. Therefore, the importance of IGF-1 should be taken into consideration when cultivating patient-derived glioblastoma cells *in vitro*.

In conclusion, U251 cell proliferation was influenced by culture conditions including cell density as well as growth factors. The limited proliferation with cell apoptosis was seen when exponentially growing U251 cells were re-seeded at high density, which was associated with decreased p-ERK1/2, increased p-JNK and low p27 expression. The strong activation of ERK1/2 in plateau phase U251 cells upon release from substrate contributed to increased proliferation after re-seeding at high density, and a more radio-resistant phenotype to some extent. Moreover, a reversible contact inhibition was detected in GBM cells, suggesting cyclin-dependent kinase inhibitors remain some functionality. Besides, the addition of IGF-1 with FGF-2 and/or EGF provided a growth advantage in GBM cells *in vitro*, suggesting the important role of IGF-1R signaling pathway in GBM proliferation. The findings of the present work indicated the balance between mitogen activated ERK1/2 and stress activated JNK signaling pathways mediated via IGF-1R signaling, as well as functional cyclin-dependent kinase inhibitors might play important roles in proliferation and survival of GBM cells.

5 SUMMARY

GBM cells are characterized by uncontrolled proliferation and resistance to apoptosis, which leads to undesirable clinical outcome, specifically poor prognosis in patients. A previous study by our group showed that passage of exponentially growing U251 cells (U251-E) and re-seeding at high density resulted in complete downregulation of ERK1/2 phosphorylation, whereas ERK1/2 activation was more strongly upregulated when U251 cells were harvested from plateau phase (U251-P). This suggested that releasing cells from density arrest provided a strong mitogenic signal which had an effect on GBM cell proliferation.

In the present work, the impacts of the dysregulated ERK1/2 activity induced by changes in culture conditions including cell density were studied in U251 cells. A major result was that ERK1/2 activation suggested increased proliferation upon re-plating of U251-P at high density, while ERK1/2 downregulation led to limited proliferation with cell apoptosis when re-plating of U251-E at high density (EH). The limited proliferation was associated with G2 accumulation (35%) and dysregulation of cell cycle proteins including p27, cyclin D1 and PLK-1. Upregulation of p27 in U251-E cells upon starvation enabled the cells to survive and continue to proliferate with no obvious detachment after re-seeding at high density, thus supporting a role for uncontrolled cell cycle progression in inducing apoptosis. Although FAK activation was suppressed, EH cells were not rescued from apoptosis by the induction of FAK expression. The results suggested that the downregulation of FAK signaling pathway was not responsible for the decreased ERK1/2 activation and that cell apoptosis in this case did not depend on FAK.

To explore the underlying mechanisms of ERK1/2 downregulation in EH cells, ERK1/2 activation in parent cultures was further studied. The results showed a fundamental difference of ERK1/2 and JNK regulation in parent cultures. ERK1/2 activation in U251-P cells was strongly upregulated upon loss of attachment. MEK inhibitor U0126 significantly inhibited ERK1/2 activation which was induced by conditioned medium from detached U251-P cells ($P < 0.05$), indicating a role of autocrine signaling. Furthermore, conditioned medium from detached U251-E cells increased JNK activation, which was significantly reduced by IGF-1R inhibitor AG1024 ($P < 0.05$). The results suggested the increased JNK activation, partially

mediated via IGF-1R signaling in U251-E cells, contributed to apoptosis after re-seeded at high density. To characterize the radiation sensitivity of U251 cells from different parent cultures, colony forming assay was performed. Although the clonogenic survival curves were very similar for immediate plating of cells from both phases, surviving fraction at 2Gy was significantly higher in cells from U251-P than from U251-E (0.76 ± 0.02 vs. 0.66 ± 0.03 , $P < 0.01$). Immunostaining with γ H2AX showed a significantly higher foci number at 1h and 3h after 2Gy irradiation in cells from U251-P (1h: 27.81 ± 2.62 vs. 19.96 ± 0.58 , $P < 0.01$; 3h: 22.52 ± 0.74 vs. 18.15 ± 1.16 , $P < 0.01$, respectively). The results indicated that re-seeded U251-P cells exhibited a relatively more radio-resistant phenotype to some extent.

In addition, a reversible contact inhibition was detected in U251 cells as well as NCH644 glioma stem-like cells. Ki67 positive cells were mainly at the periphery of spheres while cells in the inner part with low Ki67 expression showed density arrest by cell-cell contact, which was reversible by release from contact inhibition. Besides, the combination of IGF-1 and FGF-2 provided a growth advantage approaching that stimulated by FBS in U251 cells. In NCH644 cells, FGF-2 was slightly more effective than EGF and IGF-1 and the addition of IGF-1 with EGF and FGF-2 enhanced growth of NCH644 cells.

Taken together, these results highlight certain molecular regulations preserved in GBM cells, specifically, (a) that a balance between mitogen activated ERK1/2 and stress activated JNK pathways mediated via IGF-1R pathway regulate GBM cell proliferation and survival, (b) that cyclin-dependent kinase inhibitors remain some functionality in GBM cells, which guarantees the proper cell cycle progression coordinated with mitogenic signaling, (c) and that these regulatory mechanisms contributed to cellular homeostasis and can provide a better understanding of the aggressiveness in GBM.

6 REFERENCE

1. Louis, D.N., et al., *The 2016 World Health Organization Classification of Tumors of the Central Nervous System: a summary*. Acta Neuropathologica, 2016. **131**(6): p. 803-820.
2. Ostrom, Q.T., et al., *CBTRUS Statistical Report: Primary Brain and Other Central Nervous System Tumors Diagnosed in the United States in 2009-2013*. Neuro Oncol, 2016. **18**(suppl_5): p. v1-v75.
3. Thakkar, J.P., et al., *Epidemiologic and molecular prognostic review of glioblastoma*. Cancer Epidemiol Biomarkers Prev, 2014. **23**(10): p. 1985-96.
4. Stupp, R., et al., *Radiotherapy plus concomitant and adjuvant temozolomide for glioblastoma*. N Engl J Med, 2005. **352**(10): p. 987-96.
5. Stupp, R., et al., *Effects of radiotherapy with concomitant and adjuvant temozolomide versus radiotherapy alone on survival in glioblastoma in a randomised phase III study: 5-year analysis of the EORTC-NCIC trial*. Lancet Oncol, 2009. **10**(5): p. 459-66.
6. Lamborn, K.R., S.M. Chang, and M.D. Prados, *Prognostic factors for survival of patients with glioblastoma: recursive partitioning analysis*. Neuro Oncol, 2004. **6**(3): p. 227-35.
7. Walid, M.S., *Prognostic factors for long-term survival after glioblastoma*. Perm J, 2008. **12**(4): p. 45-8.
8. Grabowski, M.M., et al., *Residual tumor volume versus extent of resection: predictors of survival after surgery for glioblastoma*. J Neurosurg, 2014. **121**(5): p. 1115-23.
9. Urbanska, K., et al., *Glioblastoma multiforme - an overview*. Contemp Oncol (Pozn), 2014. **18**(5): p. 307-12.
10. Kondo, N., et al., *DNA damage induced by alkylating agents and repair pathways*. J Nucleic Acids, 2010. **2010**: p. 543531.
11. Qian, X.C. and T.P. Brent, *Methylation hot spots in the 5' flanking region denote silencing of the O6-methylguanine-DNA methyltransferase gene*. Cancer Res, 1997. **57**(17): p. 3672-7.
12. Hegi, M.E., et al., *MGMT gene silencing and benefit from temozolomide in glioblastoma*. N Engl J Med, 2005. **352**(10): p. 997-1003.
13. Paz, M.F., et al., *CpG island hypermethylation of the DNA repair enzyme methyltransferase predicts response to temozolomide in primary gliomas*. Clin Cancer Res, 2004. **10**(15): p. 4933-8.
14. Laperriere, N., L. Zuraw, and G. Cairncross, *Radiotherapy for newly diagnosed malignant glioma in adults: a systematic review*. Radiother Oncol, 2002. **64**(3): p. 259-73.
15. Ramirez, Y.P., et al., *Glioblastoma multiforme therapy and mechanisms of resistance*. Pharmaceuticals (Basel), 2013. **6**(12): p. 1475-506.
16. Kelley, K., et al., *Radioresistance of Brain Tumors*. Cancers (Basel), 2016. **8**(4): p. 42.
17. Barker, H.E., et al., *The tumour microenvironment after radiotherapy: mechanisms of resistance and recurrence*. Nat Rev Cancer, 2015. **15**(7): p. 409-25.
18. Bao, S., et al., *Glioma stem cells promote radioresistance by preferential activation of the DNA damage response*. Nature, 2006. **444**(7120): p. 756-760.

19. Beier, D., J.B. Schulz, and C.P. Beier, *Chemoresistance of glioblastoma cancer stem cells--much more complex than expected*. *Mol Cancer*, 2011. **10**: p. 128.
20. Bansal, K., M.L. Liang, and J.T. Rutka, *Molecular biology of human gliomas*. *Technol Cancer Res Treat*, 2006. **5**(3): p. 185-94.
21. Hanahan, D. and R.A. Weinberg, *Hallmarks of cancer: the next generation*. *Cell*, 2011. **144**(5): p. 646-74.
22. Nakada, M., et al., *Aberrant signaling pathways in glioma*. *Cancers (Basel)*, 2011. **3**(3): p. 3242-78.
23. Nurse, P., *A long twentieth century of the cell cycle and beyond*. *Cell*, 2000. **100**(1): p. 71-8.
24. Lim, S. and P. Kaldis, *Cdks, cyclins and CKIs: roles beyond cell cycle regulation*. *Development*, 2013. **140**(15): p. 3079-93.
25. Suryadinata, R., M. Sadowski, and B. Sarcevic, *Control of cell cycle progression by phosphorylation of cyclin-dependent kinase (CDK) substrates*. *Biosci Rep*, 2010. **30**(4): p. 243-55.
26. Barnum, K.J. and M.J. O'Connell, *Cell cycle regulation by checkpoints*. *Methods Mol Biol*, 2014. **1170**: p. 29-40.
27. Foster, D.A., et al., *Regulation of G1 Cell Cycle Progression: Distinguishing the Restriction Point from a Nutrient-Sensing Cell Growth Checkpoint(s)*. *Genes Cancer*, 2010. **1**(11): p. 1124-31.
28. Dai, Y. and S. Grant, *Cyclin-dependent kinase inhibitors*. *Curr Opin Pharmacol*, 2003. **3**(4): p. 362-70.
29. Vazquez, A., et al., *The genetics of the p53 pathway, apoptosis and cancer therapy*. *Nature reviews Drug discovery*, 2008. **7**(12): p. 979.
30. Abbas, T. and A. Dutta, *p21 in cancer: intricate networks and multiple activities*. *Nat Rev Cancer*, 2009. **9**(6): p. 400-14.
31. Biernat, W., et al., *Alterations of cell cycle regulatory genes in primary (de novo) and secondary glioblastomas*. *Acta Neuropathol*, 1997. **94**(4): p. 303-9.
32. Furnari, F.B., et al., *Malignant astrocytic glioma: genetics, biology, and paths to treatment*. *Genes Dev*, 2007. **21**(21): p. 2683-710.
33. Mao, H., et al., *Deregulated Signaling Pathways in Glioblastoma Multiforme: Molecular Mechanisms and Therapeutic Targets*. *Cancer investigation*, 2012. **30**(1): p. 48-56.
34. Cancer Genome Atlas Research, N., *Comprehensive genomic characterization defines human glioblastoma genes and core pathways*. *Nature*, 2008. **455**(7216): p. 1061-8.
35. Brennan, C.W., et al., *The somatic genomic landscape of glioblastoma*. *Cell*, 2013. **155**(2): p. 462-77.
36. Ohgaki, H. and P. Kleihues, *Genetic pathways to primary and secondary glioblastoma*. *Am J Pathol*, 2007. **170**(5): p. 1445-53.
37. Agarwal, M.L., et al., *p53 controls both the G2/M and the G1 cell cycle checkpoints and mediates reversible growth arrest in human fibroblasts*. *Proc Natl Acad Sci U S A*, 1995. **92**(18): p. 8493-7.
38. Hirose, Y., M.S. Berger, and R.O. Pieper, *p53 effects both the duration of G2/M arrest and the fate of temozolomide-treated human glioblastoma cells*. *Cancer Res*, 2001. **61**(5): p. 1957-63.
39. Blough, M.D., et al., *Effect of aberrant p53 function on temozolomide sensitivity of glioma cell lines and brain tumor initiating cells from glioblastoma*. *J Neurooncol*, 2011. **102**(1): p. 1-7.

40. Elmore, S., *Apoptosis: a review of programmed cell death*. Toxicol Pathol, 2007. **35**(4): p. 495-516.
41. Jin, Z. and W.S. El-Deiry, *Overview of cell death signaling pathways*. Cancer Biol Ther, 2005. **4**(2): p. 139-63.
42. Norohe, D.S., H.S. Poulsen, and U. Lassen, *Hallmarks of glioblastoma: a systematic review*. ESMO Open, 2016. **1**(6): p. e000144.
43. Krakstad, C. and M. Chekenya, *Survival signalling and apoptosis resistance in glioblastomas: opportunities for targeted therapeutics*. Mol Cancer, 2010. **9**: p. 135.
44. Strik, H., et al., *BCL-2 family protein expression in initial and recurrent glioblastomas: modulation by radiochemotherapy*. J Neurol Neurosurg Psychiatry, 1999. **67**(6): p. 763-8.
45. Kang, M.H. and C.P. Reynolds, *Bcl-2 inhibitors: targeting mitochondrial apoptotic pathways in cancer therapy*. Clin Cancer Res, 2009. **15**(4): p. 1126-32.
46. Eisele, G. and M. Weller, *Targeting apoptosis pathways in glioblastoma*. Cancer Lett, 2013. **332**(2): p. 335-45.
47. Petrecca, K., et al., *Failure pattern following complete resection plus radiotherapy and temozolomide is at the resection margin in patients with glioblastoma*. J Neurooncol, 2013. **111**(1): p. 19-23.
48. Nakada, M., et al., *Molecular targets of glioma invasion*. Cell Mol Life Sci, 2007. **64**(4): p. 458-78.
49. Onishi, M., et al., *Angiogenesis and invasion in glioma*. Brain Tumor Pathol, 2011. **28**(1): p. 13-24.
50. Alfonso, J.C.L., et al., *The biology and mathematical modelling of glioma invasion: a review*. J R Soc Interface, 2017. **14**(136).
51. Juliano, R.L. and S. Haskill, *Signal transduction from the extracellular matrix*. J Cell Biol, 1993. **120**(3): p. 577-85.
52. Xiao, W., A. Sohrabi, and S.K. Seidlits, *Integrating the glioblastoma microenvironment into engineered experimental models*. Future Sci OA, 2017. **3**(3): p. Fso189.
53. Zagzag, D., et al., *Molecular events implicated in brain tumor angiogenesis and invasion*. Pediatr Neurosurg, 2000. **33**(1): p. 49-55.
54. Konnecke, H. and I. Bechmann, *The role of microglia and matrix metalloproteinases involvement in neuroinflammation and gliomas*. Clin Dev Immunol, 2013. **2013**: p. 914104.
55. Carrasco-Garcia, E., M. Saceda, and I. Martinez-Lacaci, *Role of receptor tyrosine kinases and their ligands in glioblastoma*. Cells, 2014. **3**(2): p. 199-235.
56. Martin, G.S., *Cell signaling and cancer*. Cancer Cell, 2003. **4**(3): p. 167-74.
57. Witsch, E., M. Sela, and Y. Yarden, *Roles for growth factors in cancer progression*. Physiology (Bethesda), 2010. **25**(2): p. 85-101.
58. Lindsey, S. and S.A. Langhans, *Epidermal growth factor signaling in transformed cells*. Int Rev Cell Mol Biol, 2015. **314**: p. 1-41.
59. Hatanpaa, K.J., et al., *Epidermal growth factor receptor in glioma: signal transduction, neuropathology, imaging, and radioresistance*. Neoplasia, 2010. **12**(9): p. 675-84.
60. Lund-Johansen, M., et al., *Effect of epidermal growth factor on glioma cell growth, migration, and invasion in vitro*. Cancer Res, 1990. **50**(18): p. 6039-44.

61. Chen, X.C., et al., *EGF stimulates glioblastoma metastasis by induction of matrix metalloproteinase-9 in an EGFR-dependent mechanism*. *Oncotarget*, 2017. **8**(39): p. 65969-65982.
62. Dunn, I.F., O. Heese, and P.M. Black, *Growth factors in glioma angiogenesis: FGFs, PDGF, EGF, and TGFs*. *J Neurooncol*, 2000. **50**(1-2): p. 121-37.
63. Keller, S. and M.H.H. Schmidt, *EGFR and EGFRvIII Promote Angiogenesis and Cell Invasion in Glioblastoma: Combination Therapies for an Effective Treatment*. *Int J Mol Sci*, 2017. **18**(6).
64. Zheng, Y., et al., *Epidermal growth factor (EGF)-enhanced vascular cell adhesion molecule-1 (VCAM-1) expression promotes macrophage and glioblastoma cell interaction and tumor cell invasion*. *J Biol Chem*, 2013. **288**(44): p. 31488-95.
65. Soeda, A., et al., *Epidermal growth factor plays a crucial role in mitogenic regulation of human brain tumor stem cells*. *J Biol Chem*, 2008. **283**(16): p. 10958-66.
66. Yun, Y.R., et al., *Fibroblast growth factors: biology, function, and application for tissue regeneration*. *J Tissue Eng*, 2010. **2010**: p. 218142.
67. Morrison, R.S., et al., *Fibroblast growth factor receptor gene expression and immunoreactivity are elevated in human glioblastoma multiforme*. *Cancer Res*, 1994. **54**(10): p. 2794-9.
68. Shim, J.W., et al., *Expression of bFGF and VEGF in brain astrocytoma*. *J Korean Med Sci*, 1996. **11**(2): p. 149-57.
69. Stefanik, D.F., et al., *Acidic and basic fibroblast growth factors are present in glioblastoma multiforme*. *Cancer Res*, 1991. **51**(20): p. 5760-5.
70. Cuevas, P., et al., *Antiglioma effects of a new, low molecular mass, inhibitor of fibroblast growth factor*. *Neurosci Lett*, 2011. **491**(1): p. 1-7.
71. Toyoda, K., et al., *Initial contact of glioblastoma cells with existing normal brain endothelial cells strengthen the barrier function via fibroblast growth factor 2 secretion: a new in vitro blood-brain barrier model*. *Cell Mol Neurobiol*, 2013. **33**(4): p. 489-501.
72. Lee, J., et al., *Tumor stem cells derived from glioblastomas cultured in bFGF and EGF more closely mirror the phenotype and genotype of primary tumors than do serum-cultured cell lines*. *Cancer cell*, 2006. **9**(5): p. 391-403.
73. Chang, K.W., et al., *Fibroblast growth factor-2 up-regulates the expression of nestin through the Ras-Raf-ERK-Sp1 signaling axis in C6 glioma cells*. *Biochem Biophys Res Commun*, 2013. **434**(4): p. 854-60.
74. Lathia, J.D., et al., *Distribution of CD133 reveals glioma stem cells self-renew through symmetric and asymmetric cell divisions*. *Cell Death & Disease*, 2011. **2**: p. e200.
75. Kelly, J.J., et al., *Proliferation of human glioblastoma stem cells occurs independently of exogenous mitogens*. *Stem Cells*, 2009. **27**(8): p. 1722-33.
76. Li, G., et al., *Autocrine factors sustain glioblastoma stem cell self-renewal*. *Oncol Rep*, 2009. **21**(2): p. 419-24.
77. Haley, E.M. and Y. Kim, *The role of basic fibroblast growth factor in glioblastoma multiforme and glioblastoma stem cells and in their in vitro culture*. *Cancer Lett*, 2014. **346**(1): p. 1-5.
78. Kurmasheva, R.T. and P.J. Houghton, *IGF-I mediated survival pathways in normal and malignant cells*. *Biochim Biophys Acta*, 2006. **1766**(1): p. 1-22.
79. Sandberg-Nordqvist, A.C., et al., *Characterization of insulin-like growth factor 1 in human primary brain tumors*. *Cancer Res*, 1993. **53**(11): p. 2475-8.

80. Ho, K.H., et al., *Identification of IGF-1-enhanced cytokine expressions targeted by miR-181d in glioblastomas via an integrative miRNA/mRNA regulatory network analysis*. Sci Rep, 2017. **7**(1): p. 732.
81. Arsenijevic, Y., et al., *Insulin-like growth factor-I is necessary for neural stem cell proliferation and demonstrates distinct actions of epidermal growth factor and fibroblast growth factor-2*. J Neurosci, 2001. **21**(18): p. 7194-202.
82. Hubbard, S.R. and W.T. Miller, *Receptor tyrosine kinases: mechanisms of activation and signaling*. Curr Opin Cell Biol, 2007. **19**(2): p. 117-23.
83. Hynes, N.E. and H.A. Lane, *ERBB receptors and cancer: the complexity of targeted inhibitors*. Nat Rev Cancer, 2005. **5**(5): p. 341-54.
84. Huang, P.H., A.M. Xu, and F.M. White, *Oncogenic EGFR signaling networks in glioma*. Sci Signal, 2009. **2**(87): p. re6.
85. Gan, H.K., A.H. Kaye, and R.B. Luwor, *The EGFRvIII variant in glioblastoma multiforme*. J Clin Neurosci, 2009. **16**(6): p. 748-54.
86. Montano, N., et al., *Expression of EGFRvIII in glioblastoma: prognostic significance revisited*. Neoplasia, 2011. **13**(12): p. 1113-21.
87. Shinojima, N., et al., *Prognostic value of epidermal growth factor receptor in patients with glioblastoma multiforme*. Cancer Res, 2003. **63**(20): p. 6962-70.
88. Quan, A.L., et al., *Epidermal growth factor receptor amplification does not have prognostic significance in patients with glioblastoma multiforme*. Int J Radiat Oncol Biol Phys, 2005. **63**(3): p. 695-703.
89. Brand, T.M., et al., *The nuclear epidermal growth factor receptor signaling network and its role in cancer*. Discov Med, 2011. **12**(66): p. 419-32.
90. Pandita, A., et al., *Contrasting in vivo and in vitro fates of glioblastoma cell subpopulations with amplified EGFR*. Genes Chromosomes Cancer, 2004. **39**(1): p. 29-36.
91. Wang, M., et al., *Mitogenic signalling in the absence of epidermal growth factor receptor activation in a human glioblastoma cell line*. J Neurooncol, 2013. **115**(3): p. 323-31.
92. Denley, A., et al., *Molecular interactions of the IGF system*. Cytokine Growth Factor Rev, 2005. **16**(4-5): p. 421-39.
93. Denduluri, S.K., et al., *Insulin-like growth factor (IGF) signaling in tumorigenesis and the development of cancer drug resistance*. Genes & Diseases, 2015. **2**(1): p. 13-25.
94. Maris, C., et al., *IGF-IR: a new prognostic biomarker for human glioblastoma*. Br J Cancer, 2015. **113**(5): p. 729-37.
95. Osuka, S., et al., *IGF1 receptor signaling regulates adaptive radioprotection in glioma stem cells*. Stem Cells, 2013. **31**(4): p. 627-40.
96. Zamykal, M., et al., *Inhibition of intracerebral glioblastoma growth by targeting the insulin-like growth factor 1 receptor involves different context-dependent mechanisms*. Neuro Oncol, 2015. **17**(8): p. 1076-85.
97. Aldape, K., et al., *Glioblastoma: pathology, molecular mechanisms and markers*. Acta Neuropathol, 2015. **129**(6): p. 829-48.
98. Porta, C., C. Paglino, and A. Mosca, *Targeting PI3K/Akt/mTOR Signaling in Cancer*. Front Oncol, 2014. **4**: p. 64.
99. Cantley, L.C., *The phosphoinositide 3-kinase pathway*. Science, 2002. **296**(5573): p. 1655-7.
100. Maehama, T. and J.E. Dixon, *The tumor suppressor, PTEN/MMAC1, dephosphorylates the lipid second messenger, phosphatidylinositol 3,4,5-trisphosphate*. J Biol Chem, 1998. **273**(22): p. 13375-8.

101. Sarbassov, D.D., S.M. Ali, and D.M. Sabatini, *Growing roles for the mTOR pathway*. *Curr Opin Cell Biol*, 2005. **17**(6): p. 596-603.
102. Song, G., G. Ouyang, and S. Bao, *The activation of Akt/PKB signaling pathway and cell survival*. *J Cell Mol Med*, 2005. **9**(1): p. 59-71.
103. Mullany, L.K., et al., *Akt-mediated liver growth promotes induction of cyclin E through a novel translational mechanism and a p21-mediated cell cycle arrest*. *J Biol Chem*, 2007. **282**(29): p. 21244-52.
104. Dunn, G.P., et al., *Emerging insights into the molecular and cellular basis of glioblastoma*. *Genes Dev*, 2012. **26**(8): p. 756-84.
105. Kita, D., et al., *PIK3CA alterations in primary (de novo) and secondary glioblastomas*. *Acta Neuropathol*, 2007. **113**(3): p. 295-302.
106. Georgescu, M.M., *PTEN Tumor Suppressor Network in PI3K-Akt Pathway Control*. *Genes Cancer*, 2010. **1**(12): p. 1170-7.
107. Song, M.S., L. Salmena, and P.P. Pandolfi, *The functions and regulation of the PTEN tumour suppressor*. *Nat Rev Mol Cell Biol*, 2012. **13**(5): p. 283-96.
108. Koul, D., *PTEN signaling pathways in glioblastoma*. *Cancer Biol Ther*, 2008. **7**(9): p. 1321-5.
109. Ghosh, M.K., et al., *PI3K-AKT pathway negatively controls EGFR-dependent DNA-binding activity of Stat3 in glioblastoma multiforme cells*. *Oncogene*, 2005. **24**(49): p. 7290-300.
110. Suzuki, Y., et al., *Higher pAkt expression predicts a significant worse prognosis in glioblastomas*. *J Radiat Res*, 2010. **51**(3): p. 343-8.
111. Li, H.-F., J.-S. Kim, and T. Waldman, *Radiation-induced Akt activation modulates radioresistance in human glioblastoma cells*. *Radiation Oncology*, 2009. **4**(1): p. 43.
112. Narayan, R.S., et al., *Targeting the Akt-pathway to improve radiosensitivity in glioblastoma*. *Curr Pharm Des*, 2013. **19**(5): p. 951-7.
113. Mehta, M., et al., *Radiosensitization of Primary Human Glioblastoma Stem-like Cells with Low-Dose AKT Inhibition*. *Mol Cancer Ther*, 2015. **14**(5): p. 1171-80.
114. Roberts, P.J. and C.J. Der, *Targeting the Raf-MEK-ERK mitogen-activated protein kinase cascade for the treatment of cancer*. *Oncogene*, 2007. **26**(22): p. 3291-310.
115. Pearson, G., et al., *Mitogen-activated protein (MAP) kinase pathways: regulation and physiological functions*. *Endocr Rev*, 2001. **22**(2): p. 153-83.
116. Chang, L. and M. Karin, *Mammalian MAP kinase signalling cascades*. *Nature*, 2001. **410**(6824): p. 37-40.
117. Yunoue, S., et al., *Neurofibromatosis type 1 tumor suppressor neurofibromin regulates neuronal differentiation via its GTPase-activating protein function toward Ras*. *J Biol Chem*, 2003. **278**(29): p. 26958-69.
118. Dhillon, A.S., et al., *MAP kinase signalling pathways in cancer*. *Oncogene*, 2007. **26**(22): p. 3279-90.
119. Pelloski, C.E., et al., *Prognostic associations of activated mitogen-activated protein kinase and Akt pathways in glioblastoma*. *Clin Cancer Res*, 2006. **12**(13): p. 3935-41.
120. Patil, C.G., et al., *High levels of phosphorylated MAP kinase are associated with poor survival among patients with glioblastoma during the temozolomide era*. *Neuro Oncol*, 2013. **15**(1): p. 104-11.
121. Bhaskara, V.K., et al., *Comparative status of activated ERK1/2 and PARP cleavage in human gliomas*. *Neuropathology*, 2005. **25**(1): p. 48-53.

122. Glassmann, A., et al., *Pharmacological targeting of the constitutively activated MEK/MAPK-dependent signaling pathway in glioma cells inhibits cell proliferation and migration*. *Int J Oncol*, 2011. **39**(6): p. 1567-75.
123. Shannon, S., et al., *Inhibition of glioblastoma dispersal by the MEK inhibitor PD0325901*. *BMC Cancer*, 2017. **17**(1): p. 121.
124. Lopez-Gines, C., et al., *The activation of ERK1/2 MAP kinases in glioblastoma pathobiology and its relationship with EGFR amplification*. *Neuropathology*, 2008. **28**(5): p. 507-15.
125. Antonelli, M., et al., *Expression of pERK and pAKT in pediatric high grade astrocytomas: correlation with YKL40 and prognostic significance*. *Neuropathology*, 2012. **32**(2): p. 133-8.
126. Chen, D., et al., *Glioma cell proliferation controlled by ERK activity-dependent surface expression of PDGFRA*. *PLoS One*, 2014. **9**(1): p. e87281.
127. Kyriakis, J.M., et al., *The stress-activated protein kinase subfamily of c-Jun kinases*. *Nature*, 1994. **369**(6476): p. 156-60.
128. Bogoyevitch, M.A. and B. Kobe, *Uses for JNK: the many and varied substrates of the c-Jun N-terminal kinases*. *Microbiol Mol Biol Rev*, 2006. **70**(4): p. 1061-95.
129. Plotnikov, A., et al., *The MAPK cascades: signaling components, nuclear roles and mechanisms of nuclear translocation*. *Biochim Biophys Acta*, 2011. **1813**(9): p. 1619-33.
130. Dhanasekaran, D.N. and E.P. Reddy, *JNK signaling in apoptosis*. *Oncogene*, 2008. **27**(48): p. 6245-51.
131. Antonyak, M.A., et al., *Elevated JNK activation contributes to the pathogenesis of human brain tumors*. *Oncogene*, 2002. **21**(33): p. 5038-46.
132. Wu, C.J., X. Qian, and D.M. O'Rourke, *Sustained mitogen-activated protein kinase activation is induced by transforming erbB receptor complexes*. *DNA Cell Biol*, 1999. **18**(10): p. 731-41.
133. Cui, J., et al., *c-Jun NH(2)-terminal kinase 2alpha2 promotes the tumorigenicity of human glioblastoma cells*. *Cancer Res*, 2006. **66**(20): p. 10024-31.
134. Trejo-Solis, C., et al., *Copper compound induces autophagy and apoptosis of glioma cells by reactive oxygen species and JNK activation*. *BMC Cancer*, 2012. **12**: p. 156.
135. Yoo, Y.D., et al., *Glioma-derived cancer stem cells are hypersensitive to proteasomal inhibition*. *EMBO Rep*, 2017. **18**(9): p. 1671.
136. Tomicic, M.T., et al., *Apoptosis induced by temozolomide and nimustine in glioblastoma cells is supported by JNK/c-Jun-mediated induction of the BH3-only protein BIM*. *Oncotarget*, 2015. **6**(32): p. 33755-68.
137. Chen, Y.R., et al., *The role of c-Jun N-terminal kinase (JNK) in apoptosis induced by ultraviolet C and gamma radiation. Duration of JNK activation may determine cell death and proliferation*. *J Biol Chem*, 1996. **271**(50): p. 31929-36.
138. Gérard, C. and A. Goldbeter, *The balance between cell cycle arrest and cell proliferation: control by the extracellular matrix and by contact inhibition*. *Interface Focus*, 2014. **4**(3): p. 20130075.
139. Warchol, M.E., *Cell density and N-cadherin interactions regulate cell proliferation in the sensory epithelia of the inner ear*. *J Neurosci*, 2002. **22**(7): p. 2607-16.
140. Xu, F. and Z.J. Zhao, *Cell density regulates tyrosine phosphorylation and localization of focal adhesion kinase*. *Exp Cell Res*, 2001. **262**(1): p. 49-58.

141. McLean, G.W., et al., *The role of focal-adhesion kinase in cancer - a new therapeutic opportunity*. Nat Rev Cancer, 2005. **5**(7): p. 505-15.
142. Mitra, S.K. and D.D. Schlaepfer, *Integrin-regulated FAK-Src signaling in normal and cancer cells*. Curr Opin Cell Biol, 2006. **18**(5): p. 516-23.
143. Cox, B.D., et al., *New concepts regarding focal adhesion kinase promotion of cell migration and proliferation*. J Cell Biochem, 2006. **99**(1): p. 35-52.
144. Jones, G., et al., *PTEN-independent induction of caspase-mediated cell death and reduced invasion by the focal adhesion targeting domain (FAT) in human astrocytic brain tumors which highly express focal adhesion kinase (FAK)*. Cancer Res, 2001. **61**(15): p. 5688-91.
145. Hecker, T.P., et al., *Focal adhesion kinase enhances signaling through the Shc/extracellular signal-regulated kinase pathway in anaplastic astrocytoma tumor biopsy samples*. Cancer Res, 2002. **62**(9): p. 2699-707.
146. Hecker, T.P., et al., *Overexpression of FAK promotes Ras activity through the formation of a FAK/p120RasGAP complex in malignant astrocytoma cells*. Oncogene, 2004. **23**(22): p. 3962-71.
147. Natarajan, M., T.P. Hecker, and C.L. Gladson, *FAK signaling in anaplastic astrocytoma and glioblastoma tumors*. Cancer J, 2003. **9**(2): p. 126-33.
148. Batt, D.B. and T.M. Roberts, *Cell density modulates protein-tyrosine phosphorylation*. J Biol Chem, 1998. **273**(6): p. 3408-14.
149. Azzalin, A., et al., *Cell density modulates SHC3 expression and survival of human glioblastoma cells through Fak activation*. J Neurooncol, 2014. **120**(2): p. 245-56.
150. Yee, K.L., V.M. Weaver, and D.A. Hammer, *Integrin-mediated signalling through the MAP-kinase pathway*. IET Syst Biol, 2008. **2**(1): p. 8-15.
151. Zhang, L., M. Bewick, and R.M. Lafrenie, *Role of Raf-1 and FAK in cell density-dependent regulation of integrin-dependent activation of MAP kinase*. Carcinogenesis, 2002. **23**(7): p. 1251-8.
152. Liu, W., et al., *FAK and IGF-IR interact to provide survival signals in human pancreatic adenocarcinoma cells*. Carcinogenesis, 2008. **29**(6): p. 1096-107.
153. Swat, A., et al., *Cell density-dependent inhibition of epidermal growth factor receptor signaling by p38alpha mitogen-activated protein kinase via Sprouty2 downregulation*. Mol Cell Biol, 2009. **29**(12): p. 3332-43.
154. Seluanov, A., et al., *Hypersensitivity to contact inhibition provides a clue to cancer resistance of naked mole-rat*. Proc Natl Acad Sci U S A, 2009. **106**(46): p. 19352-7.
155. Fuse, T., et al., *p27Kip1 expression by contact inhibition as a prognostic index of human glioma*. J Neurochem, 2000. **74**(4): p. 1393-9.
156. Gumbiner, B.M. and N.G. Kim, *The Hippo-YAP signaling pathway and contact inhibition of growth*. J Cell Sci, 2014. **127**(Pt 4): p. 709-17.
157. Faust, D., et al., *p38alpha MAPK is required for contact inhibition*. Oncogene, 2005. **24**(53): p. 7941-5.
158. Guerrero, P.A., et al., *Oncogenic role of Merlin/NF2 in glioblastoma*. Oncogene, 2015. **34**(20): p. 2621-30.
159. Teng, J., et al., *Dissecting inherent intratumor heterogeneity in patient-derived glioblastoma culture models*. Neuro Oncol, 2017. **19**(6): p. 820-32.
160. Urruticoechea, A., I.E. Smith, and M. Dowsett, *Proliferation marker Ki-67 in early breast cancer*. J Clin Oncol, 2005. **23**(28): p. 7212-20.
161. Krishan, A., *Rapid DNA content analysis by the propidium iodide-hypotonic citrate method*. Methods Cell Biol, 1990. **33**: p. 121-5.

162. Chacon, M.R. and P. Fazzari, *FAK: dynamic integration of guidance signals at the growth cone*. Cell Adh Migr, 2011. **5**(1): p. 52-5.
163. Kim, S.H., J. Turnbull, and S. Guimond, *Extracellular matrix and cell signalling: the dynamic cooperation of integrin, proteoglycan and growth factor receptor*. J Endocrinol, 2011. **209**(2): p. 139-51.
164. Hanks, S.K., et al., *Focal adhesion protein-tyrosine kinase phosphorylated in response to cell attachment to fibronectin*. Proc Natl Acad Sci U S A, 1992. **89**(18): p. 8487-91.
165. Masson-Pevet, M., H.J. Jongsma, and J. De Bruijne, *Collagenase- and trypsin-dissociated heart cells: a comparative ultrastructural study*. J Mol Cell Cardiol, 1976. **8**(10): p. 747-57.
166. Pearson, J.R.D. and T. Regad, *Targeting cellular pathways in glioblastoma multiforme*. Signal Transduct Target Ther, 2017. **2**: p. 17040.
167. Network, T.C., *Corrigendum: Comprehensive genomic characterization defines human glioblastoma genes and core pathways*. Nature, 2013. **494**(7438): p. 506.
168. Ziegler, D.S., A.L. Kung, and M.W. Kieran, *Anti-apoptosis mechanisms in malignant gliomas*. J Clin Oncol, 2008. **26**(3): p. 493-500.
169. Lefranc, F., J. Brotchi, and R. Kiss, *Possible future issues in the treatment of glioblastomas: special emphasis on cell migration and the resistance of migrating glioblastoma cells to apoptosis*. J Clin Oncol, 2005. **23**(10): p. 2411-22.
170. Qiao, L. and G.C. Farrell, *The effects of cell density, attachment substratum and dexamethasone on spontaneous apoptosis of rat hepatocytes in primary culture*. In Vitro Cell Dev Biol Anim, 1999. **35**(7): p. 417-24.
171. Silginer, M., et al., *Integrin inhibition promotes atypical anoikis in glioma cells*. Cell Death Dis, 2014. **5**: p. e1012.
172. Kurenova, E., et al., *Focal adhesion kinase suppresses apoptosis by binding to the death domain of receptor-interacting protein*. Mol Cell Biol, 2004. **24**(10): p. 4361-71.
173. Bouchard, V., et al., *Fak/Src signaling in human intestinal epithelial cell survival and anoikis: differentiation state-specific uncoupling with the PI3-K/Akt-1 and MEK/Erk pathways*. J Cell Physiol, 2007. **212**(3): p. 717-28.
174. Koenig, A., et al., *Collagen type I induces disruption of E-cadherin-mediated cell-cell contacts and promotes proliferation of pancreatic carcinoma cells*. Cancer Res, 2006. **66**(9): p. 4662-71.
175. Li, A., et al., *Collagen type I regulates beta-catenin tyrosine phosphorylation and nuclear translocation to promote migration and proliferation of gastric carcinoma cells*. Oncol Rep, 2010. **23**(5): p. 1247-55.
176. Hayashida, T., et al., *MAP-kinase activity necessary for TGFbeta1-stimulated mesangial cell type I collagen expression requires adhesion-dependent phosphorylation of FAK tyrosine 397*. J Cell Sci, 2007. **120**(Pt 23): p. 4230-40.
177. Renshaw, M.W., X.D. Ren, and M.A. Schwartz, *Growth factor activation of MAP kinase requires cell adhesion*. EMBO J, 1997. **16**(18): p. 5592-9.
178. Sawai, H., et al., *Activation of focal adhesion kinase enhances the adhesion and invasion of pancreatic cancer cells via extracellular signal-regulated kinase-1/2 signaling pathway activation*. Mol Cancer, 2005. **4**: p. 37.
179. Barberis, L., et al., *Distinct roles of the adaptor protein Shc and focal adhesion kinase in integrin signaling to ERK*. J Biol Chem, 2000. **275**(47): p. 36532-40.
180. Wozniak, M.A., et al., *Focal adhesion regulation of cell behavior*. Biochim Biophys Acta, 2004. **1692**(2-3): p. 103-19.

181. Sieg, D.J., et al., *Pyk2 and Src-family protein-tyrosine kinases compensate for the loss of FAK in fibronectin-stimulated signaling events but Pyk2 does not fully function to enhance FAK- cell migration*. *Embo j*, 1998. **17**(20): p. 5933-47.
182. Al-Ayoubi, A., et al., *ERK activation and nuclear signaling induced by the loss of cell/matrix adhesion stimulates anchorage-independent growth of ovarian cancer cells*. *J Cell Biochem*, 2008. **105**(3): p. 875-84.
183. Dery, O., et al., *Proteinase-activated receptors: novel mechanisms of signaling by serine proteases*. *Am J Physiol*, 1998. **274**(6 Pt 1): p. C1429-52.
184. Canavan, H.E., et al., *Cell sheet detachment affects the extracellular matrix: a surface science study comparing thermal liftoff, enzymatic, and mechanical methods*. *J Biomed Mater Res A*, 2005. **75**(1): p. 1-13.
185. Abrahamsen, I. and J.B. Lorens, *Evaluating extracellular matrix influence on adherent cell signaling by cold trypsin phosphorylation-specific flow cytometry*. *BMC Cell Biol*, 2013. **14**: p. 36.
186. Zhao, B., et al., *Cell detachment activates the Hippo pathway via cytoskeleton reorganization to induce anoikis*. *Genes Dev*, 2012. **26**(1): p. 54-68.
187. Liu, W., K.M. Morgan, and S.R. Pine, *Activation of the Notch1 Stem Cell Signaling Pathway during Routine Cell Line Subculture*. *Front Oncol*, 2014. **4**: p. 211.
188. Shi, J., et al., *Distinct roles for ROCK1 and ROCK2 in the regulation of cell detachment*. *Cell Death Dis*, 2013. **4**: p. e483.
189. Wei, L., et al., *Altered regulation of Src upon cell detachment protects human lung adenocarcinoma cells from anoikis*. *Oncogene*, 2004. **23**(56): p. 9052-61.
190. Jost, M., et al., *Matrix-independent survival of human keratinocytes through an EGF receptor/MAPK-kinase-dependent pathway*. *Mol Biol Cell*, 2001. **12**(5): p. 1519-27.
191. Galante, J.M., et al., *ERK/BCL-2 pathway in the resistance of pancreatic cancer to anoikis*. *J Surg Res*, 2009. **152**(1): p. 18-25.
192. Li, J.Y., et al., *SP600125, a JNK inhibitor, suppresses growth of JNK-inactive glioblastoma cells through cell-cycle G2/M phase arrest*. *Pharmazie*, 2012. **67**(11): p. 942-6.
193. Fan, P., et al., *Integration of Downstream Signals of Insulin-like Growth Factor-1 Receptor by Endoplasmic Reticulum Stress for Estrogen-Induced Growth or Apoptosis in Breast Cancer Cells*. *Mol Cancer Res*, 2015. **13**(10): p. 1367-76.
194. Yang, X., et al., *Sef interacts with TAK1 and mediates JNK activation and apoptosis*. *J Biol Chem*, 2004. **279**(37): p. 38099-102.
195. Yu, J., C. Ustach, and H.R. Kim, *Platelet-derived growth factor signaling and human cancer*. *J Biochem Mol Biol*, 2003. **36**(1): p. 49-59.
196. Dhanasekaran, D.N. and E.P. Reddy, *JNK signaling in apoptosis*. *Oncogene*, 2008. **27**: p. 6245.
197. Xia, Z., et al., *Opposing effects of ERK and JNK-p38 MAP kinases on apoptosis*. *Science*, 1995. **270**(5240): p. 1326-31.
198. Herskind, C., et al., *Biology of high single doses of IORT: RBE, 5 R's, and other biological aspects*. *Radiat Oncol*, 2017. **12**(1): p. 24.
199. Golding, S.E., et al., *Pro-survival AKT and ERK signaling from EGFR and mutant EGFRvIII enhances DNA double-strand break repair in human glioma cells*. *Cancer Biol Ther*, 2009. **8**(8): p. 730-8.
200. Vartanian, A., et al., *Targeting hexokinase 2 enhances response to radio-chemotherapy in glioblastoma*. *Oncotarget*, 2016. **7**(43): p. 69518-69535.

201. Marampon, F., et al., *Hypoxia sustains glioblastoma radioresistance through ERKs/DNA-PKcs/HIF-1alpha functional interplay*. *Int J Oncol*, 2014. **44**(6): p. 2121-31.
202. Sato, A., et al., *MEK-ERK signaling dictates DNA-repair gene MGMT expression and temozolomide resistance of stem-like glioblastoma cells via the MDM2-p53 axis*. *Stem Cells*, 2011. **29**(12): p. 1942-51.
203. Sandal, T., *Molecular aspects of the mammalian cell cycle and cancer*. *The oncologist*, 2002. **7**(1): p. 73-81.
204. Slingerland, J. and M. Pagano, *Regulation of the cdk inhibitor p27 and its deregulation in cancer*. *J Cell Physiol*, 2000. **183**(1): p. 10-7.
205. Alkarain, A. and J. Slingerland, *Deregulation of p27 by oncogenic signaling and its prognostic significance in breast cancer*. *Breast Cancer Res*, 2004. **6**(1): p. 13-21.
206. Naumann, U., et al., *p27 modulates cell cycle progression and chemosensitivity in human malignant glioma*. *Biochem Biophys Res Commun*, 1999. **261**(3): p. 890-6.
207. Zagzag, D., et al., *Expression of p27KIP1 in human gliomas: relationship between tumor grade, proliferation index, and patient survival*. *Hum Pathol*, 2003. **34**(1): p. 48-53.
208. Kirla, R.M., et al., *Low expression of p27 indicates a poor prognosis in patients with high-grade astrocytomas*. *Cancer*, 2003. **97**(3): p. 644-8.
209. Hidaka, T., et al., *The combination of low cytoplasmic and high nuclear expression of p27 predicts a better prognosis in high-grade astrocytoma*. *Anticancer Res*, 2009. **29**(2): p. 597-603.
210. Komata, T., et al., *Antitumour effect of cyclin-dependent kinase inhibitors (p16(INK4A), p18(INK4C), p19(INK4D), p21(WAF1/CIP1) and p27(KIP1)) on malignant glioma cells*. *Br J Cancer*, 2003. **88**(8): p. 1277-80.
211. Schiappacassi, M., et al., *p27Kip1 expression inhibits glioblastoma growth, invasion, and tumor-induced neoangiogenesis*. *Mol Cancer Ther*, 2008. **7**(5): p. 1164-75.
212. Zhang, C., et al., *Co-suppression of miR-221/222 cluster suppresses human glioma cell growth by targeting p27kip1 in vitro and in vivo*. *Int J Oncol*, 2009. **34**(6): p. 1653-60.
213. Hiromura, K., et al., *Modulation of apoptosis by the cyclin-dependent kinase inhibitor p27(Kip1)*. *J Clin Invest*, 1999. **103**(5): p. 597-604.
214. Masuda, A., et al., *Protective function of p27(KIP1) against apoptosis in small cell lung cancer cells in unfavorable microenvironments*. *Am J Pathol*, 2001. **158**(1): p. 87-96.
215. Lee, S.H. and F. McCormick, *Downregulation of Skp2 and p27/Kip1 synergistically induces apoptosis in T98G glioblastoma cells*. *J Mol Med (Berl)*, 2005. **83**(4): p. 296-307.
216. Campos, B., et al., *Aberrant self-renewal and quiescence contribute to the aggressiveness of glioblastoma*. *J Pathol*, 2014. **234**(1): p. 23-33.
217. Sestan, N., S. Artavanis-Tsakonas, and P. Rakic, *Contact-dependent inhibition of cortical neurite growth mediated by notch signaling*. *Science*, 1999. **286**(5440): p. 741-6.
218. Leontieva, O.V., Z.N. Demidenko, and M.V. Blagosklonny, *Contact inhibition and high cell density deactivate the mammalian target of rapamycin pathway, thus suppressing the senescence program*. *Proc Natl Acad Sci U S A*, 2014. **111**(24): p. 8832-7.

219. Schrader, J., et al., *Restoration of contact inhibition in human glioblastoma cell lines after MIF knockdown*. BMC Cancer, 2009. **9**: p. 464.
220. Friend, K.E., et al., *Growth hormone and insulin-like growth factor-I: effects on the growth of glioma cell lines*. Growth Horm IGF Res, 2001. **11**(2): p. 84-91.
221. Schlenska-Lange, A., et al., *Cell proliferation and migration in glioblastoma multiforme cell lines are influenced by insulin-like growth factor I in vitro*. Anticancer Res, 2008. **28**(2A): p. 1055-60.
222. Loilome, W., et al., *Glioblastoma cell growth is suppressed by disruption of Fibroblast Growth Factor pathway signaling*. J Neurooncol, 2009. **94**(3): p. 359-66.
223. Hernandez-Sanchez, C., et al., *Differential regulation of insulin-like growth factor-I (IGF-I) receptor gene expression by IGF-I and basic fibroblastic growth factor*. J Biol Chem, 1997. **272**(8): p. 4663-70.
224. Frederick, T.J. and T.L. Wood, *IGF-I and FGF-2 coordinately enhance cyclin D1 and cyclin E-cdk2 association and activity to promote G1 progression in oligodendrocyte progenitor cells*. Mol Cell Neurosci, 2004. **25**(3): p. 480-92.
225. Bajetto, A., et al., *Differential role of EGF and bFGF in human GBM-TIC proliferation: relationship to EGFR-tyrosine kinase inhibitor sensibility*. J Biol Regul Homeost Agents, 2013. **27**(1): p. 143-54.
226. Podergajs, N., et al., *Expansive growth of two glioblastoma stem-like cell lines is mediated by bFGF and not by EGF*. Radiol Oncol, 2013. **47**(4): p. 330-7.
227. Aberg, M.A., et al., *IGF-I has a direct proliferative effect in adult hippocampal progenitor cells*. Mol Cell Neurosci, 2003. **24**(1): p. 23-40.
228. Bendall, S.C., et al., *IGF and FGF cooperatively establish the regulatory stem cell niche of pluripotent human cells in vitro*. Nature, 2007. **448**(7157): p. 1015-21.
229. Park, S.B., et al., *bFGF enhances the IGFs-mediated pluripotent and differentiation potentials in multipotent stem cells*. Growth Factors, 2009. **27**(6): p. 425-37.

7 LIST OF FIGURES AND TABLES

7.1 List of figures

Figure 1. Schematic illustration of PI3K/AKT/mTOR pathway

Figure 2. Schematic illustrations of MAPK pathways

Figure 3. Culture of U251 cells with different growth factors in 12 well plates

Figure 4. Culture of NCH644 cells with different growth factors

Figure 5. Proliferation of U251 cells from different culture conditions

Figure 6. Caspase assay in U251 cells from different culture conditions

Figure 7. Caspase assay in GBM46 and GBM48 cells from different culture conditions

Figure 8. Effect of different culture conditions on cell cycle distribution of U251 cells

Figure 9. Western blot analysis of cell cycle proteins of U251 cells

Figure 10. Western blot analysis of cell cycle proteins of GBM46 and GBM48 cells

Figure 11. FAK expression in different culture conditions in U251 cells

Figure 12. Effect of increasing FAK on cell apoptosis

Figure 13. Effect of P27 upregulation on cell apoptosis

Figure 14. ERK1/2 activation after cell detachment by trypsinization in parent cell cultures of U251 cells

Figure 15. ERK1/2 activation in suspension after detachment in parent cell cultures of U251 cells

Figure 16. ERK1/2 activation after cell detachment using different agents in parent cell cultures of U251 cells

Figure 17. JNK activation in EH cells

Figure 18. JNK and ERK1/2 activation in parent cell culture

Figure 19. ERK1/2 activation induced by CMD in plateau phase cells.

Figure 20. JNK activation induced by CMD in exponential growth phase cells

Figure 21. Clonogenic cell survival curve of U251 cells from different parent cultures

Figure 22. Images of γ H2AX repair foci in different time points post irradiation in U251 cells from different parent cultures

Figure 23. γ H2AX foci number per cell in response to irradiation

Figure 24. Effect of different growth factors on proliferation of U251 cells

Figure 25. Effect of different growth factors on proliferation of NCH644 cells

Figure 26. Immunostaining of U251 and U87 colonies

Figure 27. Immunostaining of U251 spheres

Figure 28. Immunostaining of NCH644 neurospheres

Figure 29. Schematic illustrations of the balance of ERK1/2 and JNK pathways upon GBM cells detached from ECM

7.2 List of tables

Table 1. Chemicals and reagents

Table 2. Growth factors

Table 3. Inhibitors

Table 4. Buffer

Table 5. Antibodies

Table 6. Cell culture materials

Table 7. Apparatus and software

Table 8. Parent culture of U251 cells in exponential growth and plateau phase

Table 9. Re-seeding culture of U251 cells in 12-well plates

Table 10. Separating and stacking gels

Table 11. Reaction scheme for 96 well plate microassay method

Table 12. The cell number seeded in T25 flask with different doses

Table 13. Values of the coefficients, α and β , and SF obtained from the LQ model fitted survival curve

8 CURRICULUM VITAE

Personal information

Name: Yun Liu
Date of birth: 1989-06-08
Place of birth: Pingding shan, China
Nationality: Chinese
Marital Status: Happily married
Email: Yun.Liu@medma.uni-heidelberg.de; yunliu0608@126.com

Education

10/2014-present Ph.D. student (Dr.sc.hum.), Ruprecht-Karls-University Heidelberg
Ph.D. project: Regulation of glioblastoma cell proliferation in dependence of cell density and growth factors *in vitro*
09/2012-06/2014 Master of Medicine, Zhengzhou University
Thesis: Clinical observation of Endostar combined with chemoradiotherapy for patients with locally advanced oesophageal carcinoma
09/2007-06/2012 Bachelor of Medicine, Zhengzhou University

Scholarship

Ph.D. scholarship from China Scholarship Council

Abstract

Yun Liu, Frank A. Giordano, Frederik Wenz, and Carsten Herskind. Upregulation of mitogenic signaling and proliferation upon detachment of plateau phase U251 glioblastoma cells *in vitro*. 21st Annual Meeting of the Society for Biological Radiation Research (GBS), 09/2018, Frankfurt, Germany (submitted).

9 ACKNOWLEDGEMENT

Firstly of all, I would like to thank my doctor father, Prof. Dr. med. Frederik Wenz for providing me with the precious opportunity of study in radiobiology laboratory in Mannheim Medical Faculty of Heidelberg University.

I would like to express my sincere appreciation to my supervisor PD. Dr. med. Frank A. Giordano for the continuous support of my PhD study and related research. His valuable guidance and encouragement accompanied me through the hardship and frustration during my study. I was deeply inspired by his serious scientific attitude which helped me accomplish my PhD research.

My sincere thanks also go to PD Dr. Carsten Herskind who gave me unrelenting support during the whole period of PhD study. His immense knowledge and insightful comments helped me overcome the difficulties. I benefit a lot from him during my four years of study here. Without his patience and precise suggestions, I would not have completed my PhD thesis.

I am also deeply grateful for the help and kindness from Prof. Marlon Veldwijk. His professional skill and valuable advice helped me when I encountered problems. In particular, I would like to thank Miriam and Adriana for their excellent experimental techniques and kind help during my research. I owe my thanks to all my colleagues in our lab as well: Kaga, Barbara, Marianne, Julianne, Xiaolei, Junqi, who are super nice and warm-hearted. We shared an unforgettable memory working together.

Most importantly, I want to show extensive gratitude and love to my parents whose support and belief make me strong and powerful no matter where I am. My final appreciation and love goes to my husband, Xiaodong. Thank you for everything!